

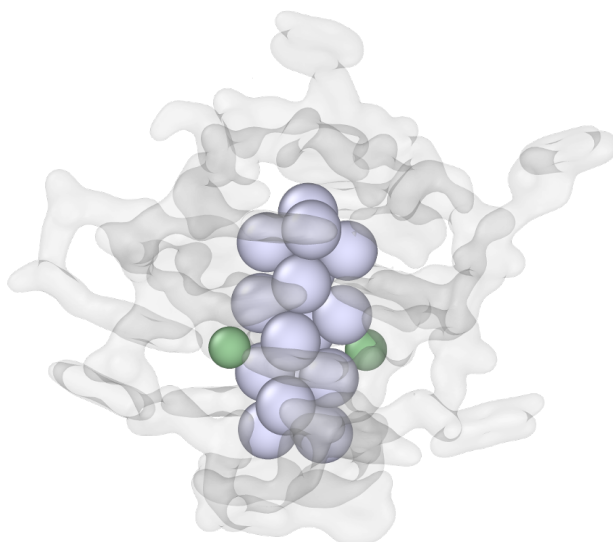
## PDF meets DNA: Pushing the limits of solution-state characterisation

Adam F. Sapnik,\* Giacomo Romolini, Cecilia Cerretani, Tom Vosch,\* and Kirsten M. Ø. Jensen\*

Department of Chemistry, University of Copenhagen, Denmark  
afs@chem.ku.dk

We demonstrate the power of synchrotron X-ray total scattering and pair distribution function (PDF) analysis to resolve the first solution-state structure of a complex, dynamic, nanoscale system: a DNA-stabilised silver nanocluster (DNA-AgNC).<sup>[1]</sup> These nanoclusters exhibit tuneable photophysical properties, making them attractive for sensing, imaging, and quantum applications, yet their atomic structures remain largely unknown.<sup>[2]</sup> While a handful of DNA-AgNCs have been characterised by single-crystal X-ray diffraction, the vast majority have been inaccessible in crystalline form. Here, we isolate atomic correlations from an 18-atom  $\text{Ag}_{16}\text{Cl}_2$  core embedded within a highly disordered DNA matrix in solution. PDF refinement reveals displacive and rotational distortions relative to the known crystalline form, alongside new insights into the conformational dynamics of the DNA scaffold.<sup>[3]</sup> We develop a statistical ensemble refinement approach—drawing inspiration from reverse Monte Carlo methods—to quantify structural heterogeneity and assess model uniqueness. This work showcases how modern synchrotron PDF methods can resolve sub-nanometre structural differences in complex, solvated nanoclusters at low concentrations, allowing for *in situ* structure–function studies across soft matter, biomolecular, and cluster chemistry domains.

- [1] A. F. Sapnik *et al.*, *Angew. Chem. Int. Ed.*, e202422432 (2025).
- [2] A. González-Rosell *et al.*, *Nanoscale Adv.*, **3**, 1230-1260 (2021).
- [3] C. Cerretani *et al.*, *Angew. Chem. Int. Ed.*, **58**, 17153–17157 (2019).



# «Mapping orientation variations of nanocrystals in bone near cement line using texture tomography approach»

A. Sadetskaia<sup>1</sup>, M. Stammer<sup>2</sup>, M. Frewein<sup>2</sup>, T. Grünewald<sup>2</sup>, H. Birkedal<sup>1</sup>

asad@inano.au.dk, <sup>1</sup>Dept. of Chemistry and iNANO, Aarhus University, Aarhus, Denmark, <sup>2</sup>Institut Fresnel, CNRS, Aix-Marseille University, Marseille, France

The hierarchical structure of bone spans across many length scales from angstrom to centimeters, where each organizational unit contributes to its mechanical performance. At the nanoscale, coaligned collagen fibers and hydroxyapatite (HAP) crystals assemble into layered structures of different patterns with varied orientations [1, 2]. The spatial organization of these patterns and heterogeneity of the mineralized matrix are a result of a constant bone remodeling process – they define the mechanical behavior of bone on larger length scales [3]. Bone remodeling also leads to formation of structural features, for example, cement lines - highly mineralized borderlines between parts of altered bone structure arrangements, namely old and newly laid-down matrix [4]. Previous results from SAXS/WAXS tensor tomography [1] showed strongly varied 3D orientational organization and spatial changes in mineral properties, when comparing regions surrounding the cement lines with the lamellar bone. While these results give invaluable insight into matrix spatial arrangement, we still need to (1) characterize the region at the submicron scale to reach the desired resolution, which is achievable with recent advances in synchrotron technology, and (2) be able to describe the distribution of different orientation near cement line and its alignment with mineral properties, which is possible with the development of texture tomography approaches (TextOM) [5].

For the purpose of the study, a piece of femoral bone was cut to obtain a sample of  $\sim 70 \times 90 \times 100 \mu\text{m}^3$  containing the cement line and glued to PMMA. Prior to that, the lab absorption tomography was done to later align the TextOM results with the absorption tomogram. The sample was scanned at the ID13 beamline, ESRF, France at X-Ray energy of 15 keV and 750 nm step size. A total of 262 projections were collected for 10 tilt angles between 0 and 45°. For TextOM reconstructions the algorithm of Frewein et.al [5] was implemented both with one (002) HAP diffraction peak (tensor tomography approach) and multiple peaks (TextOM approach).

We have successfully achieved submicron step size and performed TextOM reconstructions to get texture information. The preliminary results show the presence of different orientational domains on each side of the cement line. The extracted local misorientations relative to neighboring voxels in mineral texture match the cement line border from absorption tomography. In addition to the cement line, it was also possible to obtain orientational information around several lacunae spaces – voids in matrix that store bone cells. The XRD-CT data provides valuable information on HAP mineral properties to align with absorption and texture tomography results. Thus, we have managed to characterize at a submicron scale the distribution of orientations by identifying the orientational domains. While it gives us a preview of texture surrounding cement lines, in order to properly access texture information inside the cement line, our next experiment will be done on a smaller sample at much higher resolution.

## References

- [1] – T. A. Grünewald, et al. *IUCrJ* **10**(2), 189-198 (2023).
- [2] – A. Rodriguez-Palomo, et al. *Adv. Funct. Mater.* **34**, 2307026 (2023)
- [3] – T. A. Grünewald et al. *Sci. Adv.* **6**, eaba4171 (2020).
- [4] – M. Langer et al. *PLoS One* **7**(8), e35691 (2012)
- [5] – M. P. K. Frewein, et al. *IUCrJ* **11**(5), 809-820 (2024).

# The solvothermal formation mechanism of Pd-containing bimetals

A. B. Borup<sup>1\*</sup>, M. Kløve<sup>1</sup>, A. D. Bertelsen<sup>1</sup>, B. B. Iversen<sup>1</sup>

<sup>1</sup>Center for Integrated Materials Research, Department of Chemistry, Aarhus University, Langelandsgade 140, 8000 Aarhus, Denmark

\*Contact: andersborup@chem.au.dk

Pd is commonly used as a catalyst in a variety of fields including alcohol oxidation [1], selective hydrogenation/dehydrogenation [2, 3], and direct synthesis of H<sub>2</sub>O<sub>2</sub> [4]. To improve the catalytic performance and abilities of the Pd catalyst, alloying Pd with another element is commonly used since alloying can give rise to three effects; the element can change the electronic nature of the catalytic active atom, it can block neighboring catalytic sites, which alters the bond to poisonous intermediates, and lastly, the metal can catalyze the reaction by itself [5].

However, there exists no general theory for how bimetallic nanoparticles are formed under solvothermal conditions, although they are commonly believed to form as a result of a co-reduction, which among others are the case for Pt<sub>3</sub>Gd [6] and PbPt [7]. Recently, we unveiled a more complex multistep formation mechanism for the Pb<sub>x</sub>Pd<sub>y</sub> system (Figure 1), where Pd particles are formed first followed by an adsorption and diffusion of Pb into the Pd structure [8]. Using *in situ* X-ray diffraction, it is revealed that this complex mechanism is of a more general character for Pd-containing bimetals, since Pd<sub>x</sub>Ga<sub>y</sub>, Pd<sub>x</sub>Ge<sub>y</sub>, Sn<sub>x</sub>Pd<sub>y</sub>, and In<sub>x</sub>Pd<sub>y</sub> are found to obey the same mechanism. Even though both the counterion of the precursor salt as well as the solvent have been shown to affect the phase outcome for solvothermal synthesis with 3d metals [9, 10], the mechanism for the formation of the Pd-containing bimetals is found to be the same when changing the solvent and utilizing precursors with different counter ions.

The amount of the secondary element incorporated into the Pd-structure can be controlled by temperature, which was shown for the Pb<sub>x</sub>Pd<sub>y</sub> case [8]. In addition to this, the solvent can also be used to control the amount of the secondary element incorporated into the Pd-structure, with, at least for the Sn<sub>x</sub>Pd<sub>y</sub> case, ethanol giving a significantly more Pd-poor phase at the end of the *in situ* experiment compared with ethylene glycol.

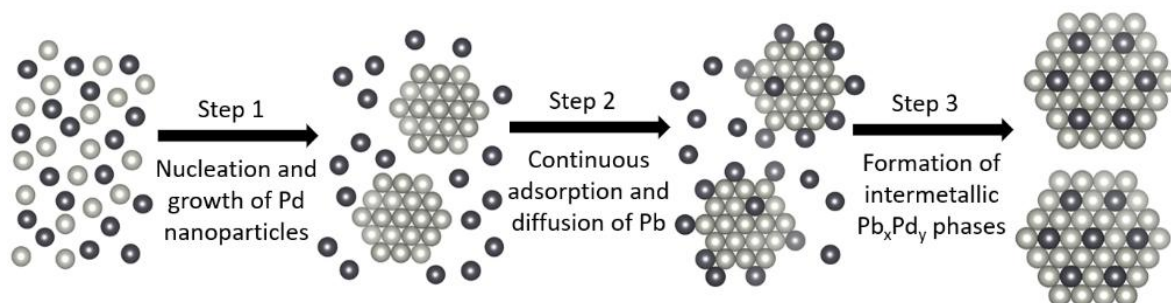


**Figure 1.** Illustration of the proposed mechanism for the formation of intermetallic Pb<sub>x</sub>Pd<sub>y</sub> nanoparticles. The light grey atoms are Pd, while the dark grey atoms are Pb. For simplicity, ions and atoms are shown by the same symbols, and counter ions are omitted. Reproduced from Borup *et al.* [8]

- [1] P. Xin, J. Li, Y. Xiong, X. Wu, J. Dong, W. Chen, Y. Wang, L. Gu, J. Luo, H. Rong, C. Chen, Q. Peng, D. Wang & Y. Li. (2018). *Angew. Chem. Int. Ed.* **57**, 4642-4646.
- [2] Y. Izawa, D. Pun, & S. S. Stahl. (2011). *Science*. **333**, 209-213.
- [3] S. Kidambi, J. Dai, J. Li & M. L. Bruening. (2004). *J. Am. Chem. Soc.* **126**, 2658-2659.
- [4] Q. Liu, J. C. Bauer, R. E. Schaak, & J. H. Lundsford. (2008). *Angew. Chem. Int. Ed.* **47**, 6221-6224.
- [5] S. Mondal, V. S. K. Choutipalli, B. K. Jena, V. Subramanian & C. R. Raj. (2020). *J. Phys. Chem C*. **124**, 9631-9643.
- [6] D. Saha, E. D. Bøjesen, K. M. Ø. Jensen, A.-C. Dippel & B. B. Iversen. (2015). *J. Phys. Chem. C*. **119**, 13357-13362.
- [7] D. Saha, E. D. Bøjesen, A. H. Mamakhel, M. Bremholm & B. B. Iversen (2017). *ChemNanoMat*. **3**, 472-478.
- [8] A. B. Borup, A. D. Bertelsen, M. Kløve, R. S. Christensen, N. L. N. Broge, A.-C. Dippel, M. R. V. Jørgensen & B. B. Iversen. (2023). *Nanoscale*. **15**, 18481-18488.
- [9] N. L. N. Broge, A. D. Bertelsen, I. G. Nielsen, M. Kløve, M. Roelsgaard, A.-C. Dippel, M. R. V. Jørgensen & B. B. Iversen. (2024). *Phys. Chem. Chem. Phys.* **26**, 12121-12132.
- [10] N. L. N. Broge, F. Søndergaard-Pedersen, M. Roelsgaard, X. Hassing-Hansen & B. B. Iversen. *Nanoscale*. **12**, 8511-8518.

# Teaching neutron scattering through virtual experiments and digital instrument twins – lessons from the COVID period

Anders Bærentzen<sup>1</sup> Petroula Karakosta<sup>1,2</sup>, Kristine M. L. Krighaar<sup>1</sup>, Jesper Bruun<sup>2</sup>, Peter Willendrup<sup>4,5</sup>, Kim Lefmann<sup>1</sup>

<sup>1</sup> Niels Bohr Institute, University of Copenhagen, Denmark

<sup>2</sup> School of Engineering, The University of Edinburgh, Edinburgh, UK

<sup>3</sup> Department of Science Education, University of Copenhagen, Denmark

<sup>4</sup> European Spallation Source, Data Management and Software Center, Denmark

<sup>5</sup> Department of Physics, Technical University of Denmark, Denmark

The Copenhagen Neutron Scattering Course is held for around 15 M.Sc. Students annually within Physics, Chemistry, and Nanoscience. The course has run since 2005 and is taught by standard textbook theory [1], e-learning- and computer resources supported by the PANOSC program [2] and the ESS DMSC [3], virtual experiments through McStas simulations [4], and actual experiments, mostly carried out at SINQ. The Nordic/Baltic Neutron School for starting Ph.D. students has run since 2017 and contains many of the same elements. It is our experience that the e-learning and virtual experiments are highly efficient teaching tools.

During the times of COVID, access to hands-on beam time was very limited. For this reason, we developed a virtual experiment consisting of a sample unknown for the students, plus a digital twin of a generic triple-axis spectrometer with a McStas interface reminiscent of an instrument control program.

We present our teaching resources, the latest developments with the digital twins, and discuss pros and cons of replacing hands-on experiments with virtual ones.

[1] K. Lefmann et al, Neutron Scattering in Theory, Experiment, and Simulation, CRC Press (expected 2026)

[2] [https://pan-training.eu/content\\_providers/pan-training](https://pan-training.eu/content_providers/pan-training)

[3] <https://europeanspallationsource.se/data-management-software-centre>

[4] P. K. Willendrup and K. Lefmann, McStas (i): Introduction, use, and basic principles for ray-tracing simulations, Journal of Neutron Research **22**, 1-16 (2020)



# EasyScience Framework for Data Analysis at ESS

Andrew Sazonov, Piotr Rozyczko, Christian Vedel, Henrik Jacobsen, Ales Kutsepau

*European Spallation Source ERIC, Data Management and Software Center, P.O. Box 176, SE-221 00 Lund, Sweden*

*andrew.sazonov@ess.eu*

EasyScience is a data analysis framework initiated by the European Spallation Source (ESS) to unify and streamline workflows across neutron scattering techniques. Developed in Python and QML, it facilitates the transition from data acquisition to publication by offering intuitive graphical interfaces for newcomers and Jupyter notebook integration for advanced users.

The framework comprises two core components: EasyApp (front-end) and EasyScience (back-end). EasyApp provides a shared library of graphical interface elements for building user-friendly applications, while the back-end supports model-based analysis through integration with widely used scientific engines.

Successful implementations include EasyDiffraction and EasyReflectometry, which support powder diffraction and reflectometry, respectively. These applications simplify data processing and model refinement by providing a consistent interface and unified analysis logic. Both tools are under active development, with new features planned as the projects evolve. Building on this foundation, additional tools such as EasyImaging (for Bragg edge imaging) and EasyDynamics (for quasielastic neutron scattering) are underway.

A complementary initiative, EasyTexture, is being developed in collaboration with Forschungszentrum Jülich and the University of Göttingen. It focuses on data reduction workflows and broadens the framework's scope within the neutron community.

Another ongoing project aims to develop a graphical interface for Shapesspyer, a tool for setting up and running molecular dynamics (MD) simulations. Created in collaboration with the UK Science and Technology Facilities Council (STFC/UKRI) and Chalmers University, this effort seeks to make Shapesspyer more accessible to a wider range of researchers.

We envision EasyScience as a community-driven, open-source ecosystem supported by a diverse network of contributors. This contribution provides an overview of the framework and highlights its current applications and future potential for neutron and X-ray scattering data analysis.

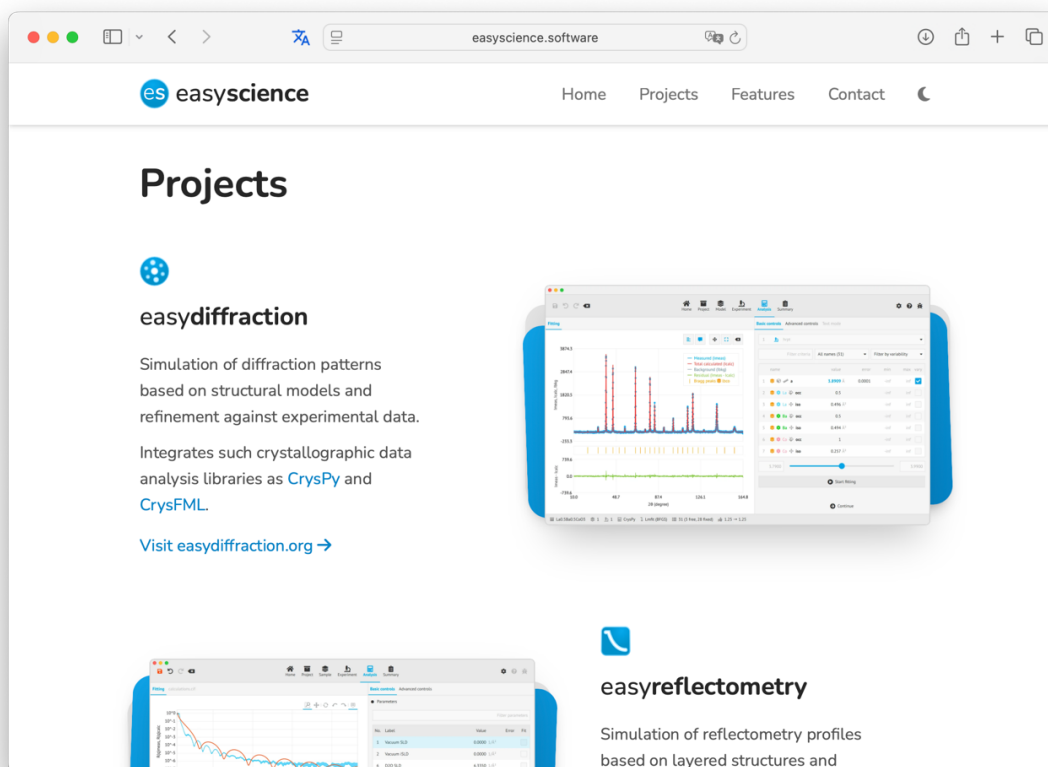


**Figure.** EasyScience web page <https://easyscience.software>.

## **Spatial heterogeneity of bone nanocrystals revealed by position resolved X-ray powder diffraction and X-ray fluorescence with ~100 nm sized X-ray beams.**

Anne Marie Møller Faaborg<sup>1</sup>, J. Palle<sup>1</sup>, T.E.K. Christensen<sup>1</sup>, N.K. Wittig<sup>1</sup>, A. Brüel<sup>2</sup>, T.L. Andersen<sup>3,4</sup>, T.A. Grünewald<sup>5</sup>, H. Birkedal<sup>1,6</sup>

<sup>1</sup>Interdisciplinary Nanoscience Center, Aarhus University, Aarhus, Denmark, <sup>2</sup>Department of Biomedicine, Aarhus University, Aarhus, Denmark,

<sup>3</sup>Department of Clinical Research, University of Southern Denmark, Odense, Denmark,

<sup>4</sup>Department of Forensic Medicine, Aarhus University, Aarhus, Denmark

<sup>5</sup>Institute Fresnel, Aix Marseille University, Marseille, France

<sup>6</sup>Department of Chemistry, Aarhus University, Aarhus, Denmark

Bone as a material is both strong, flexible, and lightweight. Its properties are a result of its hierarchical structure spanning from the cm, whole organ, scale to the nm scale of collagen fibers and hydroxyapatite (HAP) nanocrystals – the two main components of the mineralized bone matrix<sup>[1]</sup>. Spatially resolved X-ray powder diffraction (XRD) and fluorescence (XRF) are powerful tools to investigate the mineralized matrix, as they allow for comparisons between key structural elements and spatial variations in the HAP crystals or elemental composition<sup>[2]</sup>. One key structure is the osteocyte lacuna, a void in the bone matrix housing bone cells - osteocytes. Osteocytes control vital functions in bone biology<sup>[3]</sup>, suggesting that the matrix closest to the lacunae differs from the surrounding matrix<sup>[2, 4]</sup>. The goal of this project is to investigate the elemental distribution and HAP mineral properties as a function of distance to the lacunar surface. For this purpose, healthy bone samples from 5 individuals were investigated using 2D scanning nanobeam XRD/XRF at synchrotron facilities ID13 (ESRF), NanoMAX (MAX IV), and P06 (Petra-III), with step sizes between 75-500 nm. The obtained diffraction data were azimuthally integrated and Rietveld refined to determine the HAP crystallite properties. Fluorescence spectra were fitted to obtain maps of the relative calcium and zinc content. The obtained properties were evaluated as a function of distance from lacunae, which showed that the Zn content depends on distance from the lacunar surface, while the mean crystallite properties remain constant. The results are promising for a further analysis of azimuthally resolved HAP crystallite properties in the region.

[1] N. Reznikov, *et al.* Acta Biomater. 2014, 10, 3815-3826.

[2] N.K. Wittig, *et al.* ACS Nano. 2019, 13, 12949-12956.

[3] A.G. Robling, L.F. Bonewald, Annu. Rev. Physiol. 2020, 82, 485-506.

[4] B. Hesse, *et al.* JBMR. 2015, 30, 346-356.

# Structural and dynamical properties of PS-PNIPAM block copolymer micelles in concentrated samples

B. Rosi<sup>1,\*</sup>, R. Biehl<sup>1</sup>, J. Allgaier<sup>1</sup>, K. Schwärzer<sup>1</sup>, W. Pyckhout-Hintzen<sup>1</sup>, O. Czakkel<sup>2</sup>, S. Prevost<sup>2</sup>, N. R. de Souza<sup>3</sup>, O. Holderer<sup>4</sup>, S. Förster<sup>1</sup>, M. Kruteva<sup>1</sup>

<sup>1</sup>Jülich Centre for Neutron Science, Forschungszentrum Jülich, 52425 Jülich, Germany

<sup>2</sup>Institut Laue-Langevin, 71 Av. des Martyrs, 38000 Grenoble, France

<sup>3</sup>Australian Nuclear Science and Technology Organisation, New Illawarra Road, Lucas Heights, NSW 2234, Australia

<sup>4</sup>Jülich Centre for Neutron Science at MLZ, Lichtenbergstraße 1, 85748 Garching, Germany

\* Current address: European Spallation Source ERIC, Partikelgatan 2, 224 84 Lund, Sweden

Corresponding author: [benedetta.rosi@ess.eu](mailto:benedetta.rosi@ess.eu)

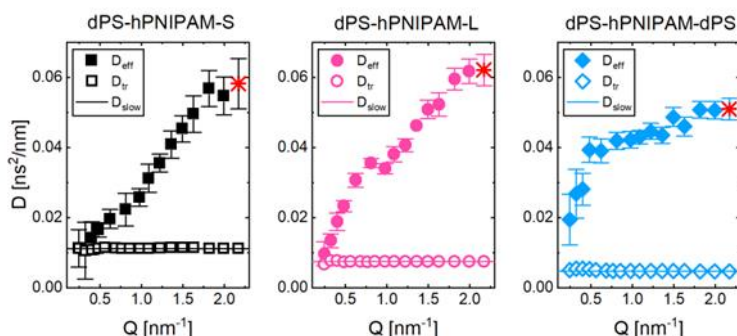


Fig.1: Full symbols: effective diffusion coefficient from NSE. Open symbols: translational diffusion coefficient, corrected of structure factor effects. Solid line: diffusion coefficient of the core as observed on NBS.

Concentrated solutions and gels of block copolymer micelles demonstrate both the cohesive strength of solids and the diffusive transport characteristics of liquids, and are subject of theoretical and technological interest [1]. Special attention is devoted to polymers containing a stimuli-responsive "switching" block that imparts the system the ability to undergo sharp, reversible changes in response to variation of external control parameters (e.g. temperature)[2]. In this work we investigate the behaviour of diblock and triblock copolymers containing thermoresponsive poly-N-isopropyl acrylamide (PNIPAM) and persistently hydrophobic polystyrene (PS) blocks, in concentrated water solution [3]. The polymers form spherical micelles in water, whose structural parameters have been determined by small-angle neutron scattering (SANS). At high concentration, the micellar samples show a completely different rheological behaviour depending on block size and, most importantly, architecture. In particular, a "soft" gel is formed in triblock-containing samples as the triblocks form junctions bridging different micellar cores. At the microscopic level, the PNIPAM chain mobility is influenced by the size and architecture of the polymer as well as topological constraints induced by the grafting on the PS core (Fig.1). Neutron spin echo (NSE) data shows how the single-chain dynamics is at best described by Zimm with one end fixed and additional internal friction between monomers. Moreover, the data clearly show an additional slow diffusion contribution that results from static correlation between on the micellar core grafted chains. Additional information is provided on the analysis of PNIPAM dynamics on shorter time and length scales by neutron backscattering (NBS). The evaluation confirms that backbone dynamics is mostly frozen on the nanosecond time scale due to internal friction, whereas side chains are mobile on the scale of hundreds of picoseconds.

## References

- [1] R. Ganguly *et al.*, *J. J. Mol. Liq.* **2020**, 314, 113591. R. Tamate *et al.*, *Adv. Mat.* **2018**, 30, 1802792.
- [2] A. Nykänen *et al.*, *Macromolecules* **2007**, 40(16), 5827–5834. S. P. Sridhar *et al.*, *Surfaces and Interfaces* **2020**, 21, 100800. S. Kirkland *et al.*, *Biomacromolecules* **2008**, 9, 481–486.
- [3] J. Adelsberger *et al.*, *Colloid Polym Sci* **2011**, 289, 711–720. J. Adelsberger *et al.*, *Macromolecules* **2010**, 43, 2490–2501.

# Characterization of thin film mirrors for a neutron condenser based on Wolter type I optics

Brandur Bárðarson Varup<sup>1</sup>, Luise Theil Kuhn<sup>2</sup>, Sonny Massahi<sup>3,4</sup>, Finn Christensen<sup>3</sup>, Kim Lefmann<sup>1</sup>, Cæcilie Lundahl Andersen<sup>3</sup>, and Nolann Ravinet<sup>3</sup>

<sup>1</sup>Niels Bohr Institute, University of Copenhagen, 2100 København Ø, Denmark.

<sup>2</sup>DTU Energy, Technical University of Denmark, 2800 Kgs. Lyngby, Denmark

<sup>3</sup>CHEXS, 2800 Kgs. Lyngby, Denmark

<sup>4</sup>DTU Space, Technical University of Denmark, 2800 Kgs. Lyngby, Denmark.

A major drawback in neutron imaging is the low flux, along with it being expensive to run neutron sources. These factors have kept neutron imaging as a relatively niche, though highly effective, method.

Combating this issue is one of the greater challenges of today's neutron imaging world. In 2011 researchers from National Institute of Standards and Technology (NIST)[1] experimented with grazing incidence reflective optics in the form of Wolter type I optics. These were also used for the NuSTAR telescope, for which the mirrors were designed as a condenser for x-rays. Using them to reflect and focus neutrons, yielded positive results, leading to a greater experimental investigation of the viability of Wolter optics in neutron imaging.

In this project CHEXS produces multi-layered thin-film NiTi mirrors, specifically for neutrons. X-ray characterization of the mirrors have already been made, showing reflection at up to  $3\theta_{c, \text{Ni}}$ [2]. However, the mirrors were produced for neutrons, not x-rays. X-rays are more susceptible to micro-roughness, which may lead to a lower intensity. Simulations using the ODIN instrument at ESS (European Spallation Source) show  $\sim 80\%$  reflectivity up to  $3\theta_{c, \text{Ni}}$  at a roughness RMS of 1.5nm[2].

Using AMOR (Apparatus for Multioptional Reflectometry) at the Paul Scherrer Institute we will make reflectometric measurements<sup>1</sup> with the aim of reproducing the simulated reflectivity of the mirrors.

## References

<sup>1</sup>D. Mildner and M. Gubarev, “Neutron optics for neutron focusing”, Nucl. Instrum. Methods Phys. Res. A **634**, 7–11 (2011).

<sup>2</sup>C. L. Andersen, “Coating development of thin film x-ray optics and neutron optics applications”, MA thesis (Technical University of Denmark, 2025).

---

<sup>1</sup>PSI Beam time proposal pending

# Modern applications of polarized neutron imaging

Cédric Qvistgaard<sup>1</sup>, Søren Schmidt<sup>2</sup>, Alexander Wolfertz<sup>3</sup>, Vahid Karimi<sup>4</sup>, Shuang Ma Andersen<sup>4</sup>, Estrid Naver<sup>1</sup>, Takenao Shinohara<sup>5</sup>, Tetsuya Kai<sup>5</sup>, Joeseeph D. Parker<sup>6</sup>, Hirotoishi Hayashida<sup>6</sup>, Luise Theil Kuhn<sup>1</sup>

<sup>1</sup>DTU Energy, Technical University of Denmark, Denmark

<sup>2</sup>ESS Eric, DMSE, Denmark

<sup>3</sup>FRM II, Technical University Munich, Germany

<sup>4</sup>Department of Green Technology (IGT), University of Southern Denmark, Denmark

<sup>5</sup>RADEN, J-PARC, J-PARC Center, JAEA, Japan

<sup>6</sup>RADEN, J-PARC, Neutron Science and Technology Center, CROSS, Japan

Polarized neutron imaging(PNI) is an emerging technique in the field of neutron imaging, capable of imaging the integrated magnetic field along the neutron flight path. We present results from two recent experiments conducted at RADEN@J-PARC, representing two new approaches to the application of the technique.

In the first experiment polarized neutron imaging was used as a tool to measure current distributions in energy devices, instead of magnetic domains as is otherwise the norm. PNI was used to measure the induced magnetic field from a 2D current distribution passing through an in-operando electrolyzer cell. From the magnetic field, the current density distribution in the cell was subsequently reconstructed and compared to the structure of the cell, as well as information on gas production in the cell, measured via other experiments.

In the second experiment we show how time-of-flight based 3D polarimetric neutron tomography [1], is used in conjunction with a novel iterative reconstruction technique for PNI experiments, to retrieve the full magnetic field information of a piece of the Martian meteorite NWA7034, the results of which can be seen in Fig.1.

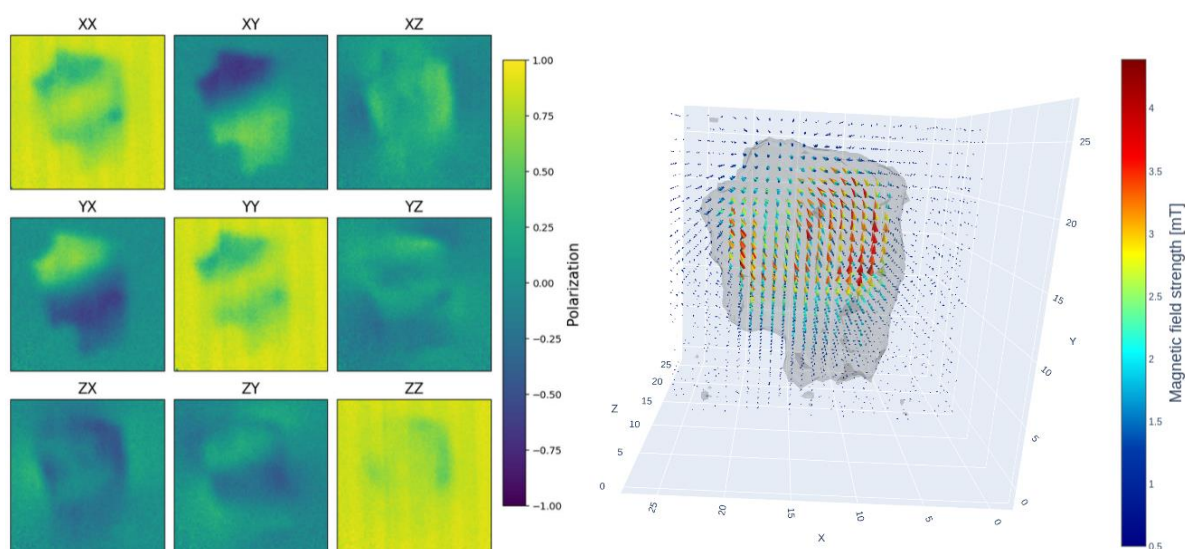


**Figure 1 Left:** Example of polarimetric measurements here acquired with the meteorite facing the detector.

**Right:** Final 3D reconstruction of magnetic field inside the meteorite sample, derived from iterative reconstruction of the 3D polarimetric tomography.

[1] Sales, M, et. Al. (2018). Three Dimensional Polarimetric Neutron Tomography of Magnetic Fields. Scientific Reports, 8(1). <https://doi.org/10.1038/s41598-018-20461-7>

## **Hydrophobicity-Driven Water Dynamics in Silica-Stabilized Microbubbles: Insights from Multi-Scale Neutron Spectroscopy**

Understanding interfacial dynamics of water in colloidal systems is essential for enhancing the design of encapsulation and release platforms. However, obtaining this information is not straightforward. Here we show that by examining the vibrational and relaxational dynamics of water confined in silica-stabilized microbubbles with adjusted surface wettability from the femtosecond to nanosecond timescales it was possible to explain how hydrophobicity affects water confinement and mobility.

Our results reveal that increasing hydrophobicity enhances water vibrational freedom and mechanical rigidity, as shown by blue-shifted librational bands, increased mean-square displacements, and higher Boson Peak energies. Conversely, hydrophilic systems demonstrate strong confinement, restricted mobility, and increased structural disorder—reflecting tightly bound hydration shells. These behaviors are influenced by enthalpy–entropy trade-offs at the silica–water interface, which significantly affect the structural relaxation landscape and molecular packing of the hydrated shell.

From a practical perspective, the enhanced mobility and rigidity observed in more hydrophobic systems are directly associated with higher stability during storage or thermal processing, important parameters for drug delivery vehicles and food-grade controlled release systems. This study provides a molecular-level basis for designing particle-stabilized encapsulation systems, promoting the use of tailored hydrophobic interfaces in bioactive compound delivery.

# Novel Precursor for Synthesis of Hexaferrite Magnets

Christian Lund Rasmussen<sup>1</sup>, Parvathy Namangalam Subrahmanian<sup>1</sup>, and Mogens Christensen<sup>1,2</sup>

<sup>1</sup>*Department of Chemistry, Aarhus University, Aarhus, Denmark,* <sup>2</sup>*Interdisciplinary Nanoscience Center, Aarhus, Denmark*

Magnets play a crucial role in most green energy technologies and energy conversion systems. As the transition to green energy proceeds, an increase in magnet production is therefore inevitable. Although the production of iron-based magnets is a well-developed field of industry, it involves multiple complex steps and requires substantial amounts of energy.<sup>[1]</sup> Using an optimal precursor of the magnetic material as a starting reactant can significantly reduce the complexity of the production process and lower energy consumption.

This study utilizes a novel precursor for the synthesis of hexaferrite magnets. The morphology and magnetic properties of this precursor makes it possible to use a new synthesis route, which yields magnets with a high degree of crystallite alignment. The magnetic performance of the resulting materials has been optimized to a level that is very close to that of grade Y35 magnets, which is some of the highest quality of hexaferrite magnets commercially available for purchase in large quantities.<sup>[2]</sup> Table 1 shows a comparison of the relevant magnetic properties.

Unlike commercially available magnets, which typically incorporate a variety of additives to enhance magnetic and structural characteristics, the magnets produced in this study contain only a single additive, which is used to control grain growth.<sup>[3]</sup> It is anticipated that the magnetic properties can be further improved through the incorporation of additional additives.

Magnet	$BH_{\max} \left[ \frac{\text{kJ}}{\text{m}^3} \right]$	$M_s \left[ \frac{\text{Am}^2}{\text{kg}} \right]$	$M_r/M_s$	$H_c \left[ \frac{\text{kA}}{\text{m}} \right]$
Commercial Y35	35	73.0	0.93	219
This Study Y34-Y35	33	72.8	0.92	200

Table 1: Comparison of the properties of a commercial Y35 hexaferrite magnet and the magnets prepared in the present study. All porperties have been measured using the same instrument. Data treatment and demagnetization correction have been performed uniformly on both samples.

## References

[1] SDM Magnetics. (2017, June 23). *Manufacturing Process of Ferrite Magnet*. Retrieved May 15, 2025, from <https://www.magnet-sdm.com/2017/06/23/1186/>

[2] e-Magnets UK. *Grades of Ferrite*. Retrieved May 15, 2025, from <https://e-magnetsuk.com/ferrite-magnets/grades-of-ferrite/>

[3] Matran, W. M., Mustapha, M., & Nor, M. F. (2024). The influences of additives in M-type (Ba and Sr) hexaferrites' microstructure, sintering and magnetic properties: A review. *ScienceDirect*, 96, 78–83.



# Investigation of the effect of reductive annealing on spin fluctuations in superconducting electron-doped $\text{Nd}_{1.85}\text{Ce}_{0.15}\text{CuO}_{4-\delta}$

Kristine M. L. Krighaar,<sup>1</sup> Jeppe J. Cederholm,<sup>1</sup> Ellen M. S. Schriver,<sup>1</sup> Christine P. Lauritzen,<sup>1</sup> Cédric H. Qvistgaard,<sup>1, 2</sup> Ursula B. Hansen,<sup>3</sup> Ahmed Alshemi,<sup>4</sup> Dongjoon Song,<sup>5</sup> Anton Stampfl,<sup>6</sup> Jean-Claude Grivel,<sup>2</sup> Kim Lefmann,<sup>1</sup> and Machteld E. Kamminga<sup>7</sup>

<sup>1</sup>Nanoscience Center, Niels Bohr Institute, University of Copenhagen, 2100 Copenhagen, Denmark \*

<sup>2</sup>Department of Energy Conversion and Storage, Technical University of Denmark, 2800 Kgs. Lyngby, Denmark

<sup>3</sup>Institut Laue-Langevin (ILL), Grenoble, France

<sup>4</sup>Division of Synchrotron Radiation Research, Department of Physics, Lund University, SE-22100 Lund, Sweden

<sup>5</sup>Department of Physics and Astronomy, University of British Columbia, Vancouver BC V6T 1Z1, Canada

<sup>6</sup>Australian Nuclear Science and Technology Organisation, Lucas Heights, NSW 2234, Australia

<sup>7</sup>Condensed Matter and Interfaces, Debye Institute for Nanomaterials Science, Utrecht University, 3508 TA Utrecht, The Netherlands

The insulating cuprate  $\text{Nd}_{2-x}\text{Ce}_x\text{CuO}_{4-\delta}$  (NCCO) becomes superconducting upon reductive post-synthesis annealing. However, the exact nature of the effect of reductive annealing remains a matter of debate. For example, adding additional electrons, by increasing the Ce content, does not produce superconductivity in non-annealed samples. To elucidate the annealing effect, we study the effect of annealing on the magnetic fluctuations. While some other neutron spectroscopy studies have focused on annealed samples, the as-grown samples as yet remain unreported.

In this study, we have grown a large single crystal NCCO, split it in two, and annealed one of the pieces. Growing one crystal and then splitting it allows us to study only the effect of annealing and not other factors such as composition. We measured our data on the thermal triple axis spectrometers TAIPAN (ANSTO) and the IN20 instrument at ILL. We studied the spin wave spectrum in the annealed and as-grown samples below and above  $T_c$  (26 K). The data shows a large spin pseudo-gap in the as-grown sample below 26 K, with a smaller spin pseudo-gap in the superconducting sample.

The closing of the spin pseudo-gap by annealing suggest a connection between the size of the spin pseudo-gap and the observed superconductivity. Here we hypothesise that the spin pseudogap present in as-grown NCCO can be explained by disorder present in the system. By reductively annealing and therefore providing more pristine  $\text{CuO}_2$  sheets, we significantly reduce the size of the spin pseudo-gap, allowing for spin pairing. As a result, we argue that the low-energy spin fluctuations are a necessary attribute to superconductivity in electron-doped cuprates, and reductive annealing is necessary to obtain these in the NCCO system. Our study helps to elucidate the interplay between magnetism, superconductivity, and crystal structure in the intriguing NCCO system.



# Simulating neutron diffraction from deformed mosaic crystals in McStas

Daniel Lomholt Christensen<sup>1</sup>, Sandra Cabeza<sup>2</sup>, Thilo Pirling<sup>2</sup>, Kim Lefmann<sup>1</sup>, and Jan Saroun<sup>3</sup>

<sup>1</sup>Niels Bohr Institute, University of Copenhagen, DK-2100 Copenhagen Ø , Denmark

<sup>2</sup>Institut Laue-Langevin, F-38000 Grenoble, France

<sup>3</sup>Nuclear Physics Institute CAS, Rez 25068, Czech Republic

January 6, 2025

McStas plays an important part in the development and optimization of neutron instrumentation. In the McStas package there is a specific need for a component that simulates bent single crystals. These crystals grant a high resolution and high peak reflectivity in specific focusing conditions, at the cost of lower integrated reflectivity, and a heavy dependence on the diffraction geometry. These crystals therefore give great power to the experiment, but also great responsibility to the instrument setup. These crystals are therefore often used for engineering diffractometers and triple-axis spectrometers.

The current crystal components in McStas either implement a very simplified model of a crystal (infinitely thin), or a very detailed model of a crystal (NCrystal), neither of which supports the case of a bent single crystal of finite thickness. This work therefore implements a new component in the McStas library called `Monochromator_Bent`. The component is based upon the crystal component in the SIMRES software package. The component simulates neutron diffraction in a crystal of finite thickness, which can be bent or mosaic, and any combination of these.

We then define showcase configurations, that highlights the capabilities of the component. In these configurations, we compare the component to its sister in the SIMRES software, and the NCrystal component in McStas. Finally we also simulate the SALSA instrument at the ILL, and compare the results to data taken from SALSA. The results from these comparisons show that the component is able to simulate the effects of a bending mosaic/non-mosaic crystal with a finite thickness. The added features to McStas from this component is then both diffraction off of bent single crystals as well as a more realistic crystal simulation than the current monochromators, whilst still being faster than the NCrystal component.

# Status of the LINAC-driven MAX IV Short Pulse Facility FemtoMAX beamline

D. Kroon<sup>1</sup>, J. C. Ekström<sup>1</sup>, B. Ahn<sup>1</sup>, A. Jurgilaitis<sup>1</sup>, J. Larsson<sup>1,2</sup>

<sup>1</sup> MAX IV Laboratory, Lund University, P.O. Box 118, SE-221 00 Lund, Sweden

<sup>2</sup> Department of Physics, Lund University, P.O. Box 118, SE-221 00 Lund, Sweden

The FemtoMAX beamline is a LINAC-driven time-resolved laser pump/x-ray probe beamline dedicated to study solids and liquids. The beamline is designed to explore dynamics in materials at time scales ranging from femtoseconds to microseconds [1,2]. The sub-50 fs x-ray pulses are generated in two in-vacuum undulators, with a photon energy tuneable between 1.8 – 15 keV at a repetition rate of 10 Hz. The femtosecond laser excitation source spans wavelengths of 400 nm-1.6  $\mu$ m. THz pulses, generated from optical rectification in DAST and DSTMS crystals (2.1 THz), are also available as a pump source.

A Pilatus time-over-threshold single photon counting detector and a collection of sCMOS detectors are employed to capture SAXS/WAXS and diffraction signals. In addition, ultrashort x-ray pulses in combination with fast detectors can be used to study x-ray time resolved fluorescence from fast scintillators, nanofilms and organic materials.

Here, we present the current beamline status, development plans and a few scientific use cases to exemplify the beamline capabilities.

## References

1. Enquist, H., Jurgilaitis, A., Jarnac, A., Bengtsson, A.U. J., Burza, M., Curbis, F., Disch, C., Ekstrom, J. C., Harb, M., Isaksson, L., Kotur, M., Kroon, D., Lindau, F., Mansten, E., Nygaard, J., Persson, A. I. H., Pham, V. T., Rissi, M., Thorin, S., Tu, C.-M., Wallen, E., Wang, X., Werin, S. & Larsson, J. (2018). *J. Synchrotron Rad.* 25, 570-579
2. Gonzalez, A., Krojer, T., Nan, J., Bjelcic, M., Aggarwal, S., Gorgisyan, I., Milas, M., Eguiraun, M., Casadei, C., Chenchiliyan, M., Jurgilaitis, A., Kroon, D., Ahn, B., Ekstrom, J. C., Aurelius, O., Lang, D., Ursby, T. & Thunnissen, M. M. G. M. (2025). *J. Synchrotron Rad.* 32.

# Fragment Based Active Site Exploration of Thermoset Plastic Degrading Enzymes for Structure-guided Protein Engineering

Deniz Bicer, Aarhus University

## Abstract

Thermoset plastic is crosslinked polymer which are widely used in adhesive and coating application, and they are extremely resistant to environmental factors which make them also very hard to be recycled by standard chemical processing. However, most of the thermoset plastics such as Polyurethane, contain biodegradable bonds including amide, ester and carbamate in which can be targeted by enzymes. Novel enzymes that are discovered in nature has great potential for biocatalytic recycling of thermoset plastics through directed evolution and protein engineering. For structure-guided protein engineering, it is key to characterize active site of enzymes along with plastic fragments which provide valuable insights into transition state stabilization, substrate binding and so on. Therefore, we aim to characterize active site of plastic degrading enzymes by using short-soluble fragment of plastic which mimics substrate, transition state and product respectively. Crystallographic studies of fragment-enzyme structure will rationalize our effort to target hot-spots on active site to boost the catalytic activity of novel enzymes. So far, we solved crystal structures of several enzyme from amidase family that are discovered from plastic waste and metagenomic analysis with and without various fragment bound states. Structural details of ligand interactions and conformational changes upon ligand binding are investigated and possible mutations are suggested for kinetic test.

# Electrochemical Performance and Structural Insights into IrRuO<sub>x</sub> Electrocatalysts via PDF Analysis

Ebrahim Sadeghi<sup>1</sup>, Martin Aaskov Karlsen<sup>2</sup>, Raghunandan Sharma<sup>1</sup>, and Shuang Ma Andersen<sup>1</sup>

<sup>1</sup> Department of Green Technology, University of Southern Denmark, Campusvej 55, DK-5230 Odense M, Denmark

<sup>2</sup> Deutsches Elektronen-Synchrotron (DESY), Notkestraße 85, 22607 Hamburg, Germany

The commercialization of proton exchange membrane (PEM) electrolyzers for water splitting critically depends on the development of efficient, durable, and cost-effective Iridium (Ir) and Ruthenium (Ru)-based electrocatalysts for the oxygen evolution reaction (OER) in acidic media. In this study, we synthesized IrRuO<sub>x</sub> catalysts via a molten-salt route using ammonium hexachloroiridate(IV) and ammonium hexachlororuthenate(IV) as precursors. A wide range of compositions and thermal treatment conditions were explored to tailor the structure and performance. Structural characterization was carried out using in-house X-ray Powder Diffraction (PXRD), Scanning Transmission Electron Microscopy (STEM), X-ray Photoelectron Spectroscopy (XPS), and synchrotron-based total scattering experiments combined with Pair Distribution Function (PDF) analysis at beamline P02.1 (PETRA III, DESY, Hamburg).

In-house PXRD revealed significant peak broadening, suggesting nanoscale crystallite domains. Synchrotron PXRD confirmed this observation with higher resolution and extended reciprocal space coverage, showing persistent broadening despite reduced instrumental effects. These findings indicated the presence of highly disordered or amorphous domains, which limited the structural insights extractable from conventional Rietveld analysis. Total scattering and PDF analysis provided complementary and critical information, allowing direct evaluation of short- and medium-range order. Local structural motifs such as nearest-neighbor distances, atomic coordinates, and coherent domain sizes were determined by modeling and refining the PDF.

The best-performing catalyst, Ir<sub>0.25</sub>Ru<sub>0.75</sub>O<sub>x</sub>-500, showed a disordered, nanoscale structure correlating with superior electrochemical activity, achieving a mass-specific OER performance of 480 A g<sub>metal</sub><sup>-1</sup> at 1.65 V—significantly outperforming the commercial IrRuO<sub>x</sub> catalyst (158 A g<sub>metal</sub><sup>-1</sup>). These results highlight the importance of combining synchrotron-based structural analysis with electrochemical evaluation to reveal structure–property relationships in complex, nanostructured electrocatalysts. The use of PDF analysis, especially in cases where traditional diffraction fails, proves essential in deciphering the active structure of amorphous and nanoscale OER materials.

# Time-resolved structural amorphisation of LaMO<sub>3</sub> perovskites by acid leaching

Emma Solé Chaos<sup>1</sup>, Guilherme B. Strapasson<sup>1,2,3</sup>, Adrian Sanz Arjona<sup>1</sup>, Kirsten M. Ø. Jensen<sup>1</sup>

<sup>1</sup>Department of Chemistry and Nano-Science Centre, University of Copenhagen, Copenhagen, Denmark, <sup>2</sup>Institute of Chemistry, University of Campinas, Campinas, Brazil, <sup>3</sup>Brazilian Synchrotron Light Laboratory, CNPEM, Campinas, Brazil

esc@chem.ku.dk

Perovskites have been in the spotlight for the last decade due to the potential as energy materials [1]. Even though their scalability has been limited by their rather poor stability, specially under acidic conditions, we can further induce the perovskites collapse to form amorphous materials. Specifically, amorphous first-row transition metal oxides have recently stood out as promising materials for multiple applications, for which the enhanced properties are often related to their short-range structural features, describing a direct synthesis-structure-properties dependence. However, synthesising these materials is challenging, and thus the amorphisation synthesis is proposed as an easy and approachable one-step process, which takes place at room temperature, and it is supported only by sonication [3,4]. Here, when acidifying an aqueous suspension of perovskite type LaMO<sub>3</sub>, the bigger cation (La) has been described to leach out, causing the structure to collapse into an amorphous MO<sub>x</sub>.

Additionally, detailed structural analysis of the amorphisation process by standard X-rays measurements is deficient, and often samples are simply described to be amorphous if no defined Bragg peaks are observed. Thus, if we aim to map structure-synthesis relations, it is required to apply more advanced structural characterisation techniques, being total scattering and pair distribution function (PDF) analysis of great interest, due to their possibilities when describing short-range structural features.

With our study, we are tracking the structural collapse of LaMO<sub>3</sub> transition metal (i.e. Fe, Co, Ni) perovskites into nanostructured amorphous oxides, by evaluating different acidifying agents (e.g. FeCl<sub>3</sub>, HCl, HNO<sub>3</sub>) and various transition metal compositions of the initial perovskite (e.g. LaNiO<sub>3</sub>, La(NiFe)O<sub>3</sub>, La(NiFeCo)O<sub>3</sub>). Collapse of the perovskites can be observed through time-resolved X-ray total scattering measurements and subsequent PDF analysis (Fig. 1). The loss of long-range features related to the crystalline perovskite, together with observable changes in the first interatomic distances (< 5 Å), allow us to follow the leaching of the La ions and the structural rearrangements taking place in the remaining structure. These reactions will provide valuable insight into alternative ways of formation of amorphous oxides, and to the relationship between the oxide structural stability against their composition and acidic conditions, from an atomic perspective.

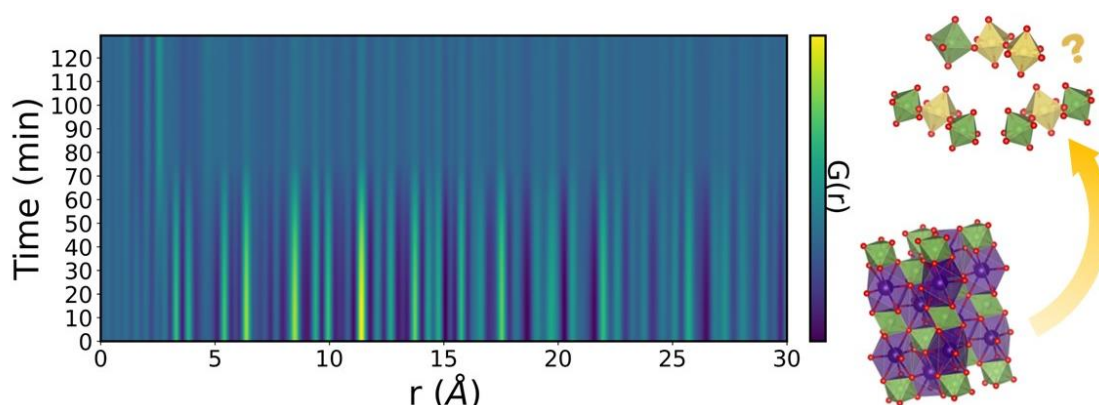


**Figure 1.** Time resolved Pair Distribution Function (PDF) following the breakdown of the initial perovskite. Insets show the evolution from LaMO<sub>3</sub> crystal structure into amorphous transition metal oxides.

- [1] Monama, G. R., Ramohlola, K. E., Iwuoha, E. I., Modibane, K. D. (2022). *Results in Chemistry*, 4, 100321.
- [2] Guo, T., Li, L., Wang, Z. (2022). *Adv. Energy Mater.*, 12, 2200827.
- [3] Chen, G., Zhu, Y., Chen, H.M., *et al.* (2019). *Adv. Mater.*, 31, 1900883.
- [4] Geiger, S., Kasian, O., Ledendecker, M., *et al.* (2018). *Nat. Catal.*, 1, 508.

## **Industrial Impact Through Advanced X-ray and Neutron Analysis**

FORCE Technology supports Danish industry by applying advanced X-ray and neutron techniques to solve real-world materials challenges. Through methods such as synchrotron X-ray and neutron-based analysis, we provide deep insight into material structures and properties—enabling innovation in areas including Power-to-X, advanced manufacturing, medical technology, electronics, and quality assurance.

With strong industrial know-how and access to world-class research infrastructure, we act as a bridge between cutting-edge science and practical application. Our specialists translate complex experimental data into actionable knowledge that improves product performance, ensures quality, and shortens development timelines.

As materials and manufacturing technologies evolve, the demand for precise, science-based understanding grows. FORCE Technology is committed to making advanced characterization methods available and useful to Danish companies—helping translate research excellence into industrial impact.

# Combined imaging and diffraction characterisation of Martian meteorite Black Beauty to identify H-rich phases

*E.B. Naver<sup>1,2</sup>, M. S. Carøe<sup>3</sup>, K. W. Nikolajsen<sup>4</sup>, J. S. Jørgensen<sup>3</sup>, M. Bizzarro<sup>4</sup>, J. Frydenvang<sup>4</sup>, H. Birkedal<sup>5</sup>, T.E. K. Christensen<sup>6</sup>, I. Kantor<sup>6</sup>, H. F. Poulsen<sup>2</sup>, and L. Theil Kuhn<sup>1</sup>*

<sup>1</sup>DTU Energy, Kgs. Lyngby, Denmark, <sup>2</sup>DTU Physics, Kgs. Lyngby, Denmark, <sup>3</sup>DTU Compute, Kgs. Lyngby, Denmark, <sup>4</sup>GLOBE institute, Univ. Copenhagen, Copenhagen, Denmark,

<sup>5</sup>Department of Chemistry, Aarhus University, Denmark, <sup>6</sup>MAX IV Laboratory, Lund University, Lund, Sweden.

Presenting author: E.B. Naver [ebna@dtu.dk](mailto:ebna@dtu.dk)

Meteorites originating from Mars represent the only tangible samples that allow us to investigate the geologic history of this planet, including its potential early habitability. The discovery of the polymict regolith breccia NWA 7034 meteorite and its pairs, informally known as Black Beauty, provides, for the first time, a direct time window into the earliest crustal processes on Mars [1,2]. Analyses of the crustal fragments from this meteorite indicates that water was present on the Martian surface 4450 million years ago [3]. Neutron tomographic imaging is a method for non-destructively characterising samples in 3D and as neutrons are sensitive to H it is possible to directly locate H-rich phases. When combined with X-ray tomographic imaging one can confirm the identification of H and determine which minerals are hosting the H [4].

Two pieces of the Martian meteorite NWA 7034 have been analysed using neutron and X-ray imaging. High-resolution neutron CT was performed at ICON at the Paul Scherrer Institute in Switzerland. X-ray CT was performed at the B05 beamline at European Synchrotron Radiation Facility in France by Phil Cook. The 3D volumes from each measurement were co-registered and high attenuation phases were segmented and identified, see Fig. 1. X-ray powder diffraction tomography was performed at the DanMAX beamline at MAX-IV in Sweden.

Comparison to theoretical attenuation values of minerals in the sample shows that high X-ray attenuation stems from Fe-oxides and high neutron attenuation stems from hydrous phases. There are more high attenuation X-ray spots than high attenuation neutron spots, which shows that not all Fe-oxides contain H. Segmentation also shows that all hydrous phases overlap with the Fe-oxide phases. As such, the analysis performed so far suggests that the water-related H in the meteorite is stored in Fe-oxides. X-ray diffraction allows us to identify these Fe-oxides as ilmenite and magnetite.

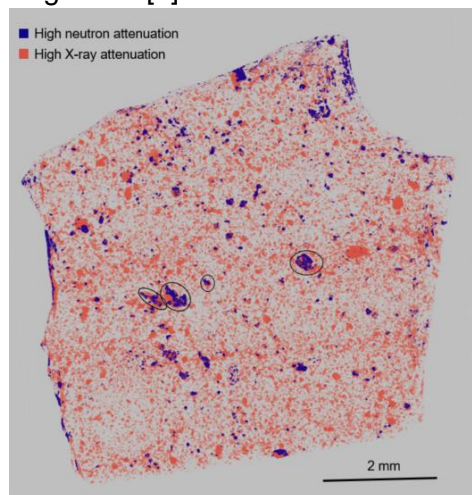


**Fig. 1:** Segmented high neutron att. (blue) and high X-ray att. phases (red).

- [1] M. Humayun et al., Nature 503 (2013), 513–516
- [2] A. Goodwin et al., Astrobiology 22 (2022), 755-767
- [3] Z. Deng et al., Science Advances 6 (2020), eabc4941
- [4] J. Martell et al., Science Advances 8 (2022), eabn3044

## **Looking inside porous activated supercapacitor electrodes**

*Fernando Gabriel Benitez Jara<sup>1,3,4</sup>, Jorge David Barrios Lémus<sup>2</sup>, Jan Peter Embs<sup>5</sup>, Heloisa Nunes Bordallo<sup>3</sup>, Rubens Nunes Faria Jr<sup>1</sup>.*

*1- Nuclear and Energy Research Institute - São Paulo (IPEN-SP),*

*2- Universidad Católica Nuestra Señora de la Asunción - Alto Paraná - Paraguay*

*3 Niels Bohr Institute – University of Copenhagen*

*4- Facultad de Ciencias Exactas y Naturales/Facultad Politécnica – Universidad Nacional de Asunción - Paraguay*

*5- Paul Scherrer Institute (PSI) - Villigen – Switzerland*

### **Abstract**

*Quasi-elastic neutron scattering represents an optimal methodology for the measurement of molecular displacements in both time and space, from peaks of hundreds of femtoseconds to tens of nanoseconds, and from Angstroms to nanometers, respectively. Through this technique, it is possible to investigate the dynamic behavior of molecules, encompassing fast vibrational modes and slow diffusive motions. Thus, showing exactly where the atoms are located and how they move. The aim of this study was to combine TGA-FTIR-MS with neutron spectroscopy supported by QENS analysis, an attempt to understand the behavior of nanoscale mobility of aqueous potassium hydroxide (KOH) solution and eutectic choline chloride-ethylene glycol (ChCl-EG) solution used in porous activated carbon (AC) and reduced graphene oxide (rGO) supercapacitor electrodes under confinement. QENS analysis revealed a self-diffusion translational motion in the liquid confined within the porous AC-KOH electrodes. However, the results at the rGO electrodes and their fit differed in ChCl-EG solution. Moreover, the electrochemical behavior was studied by cyclic voltammetry in order to obtain the specific capacitance and galvanostatic charge-discharge cycles, and then, the equivalent series resistance. Very low specific capacitance, high resistance and electrolyte with localized dynamics in samples with ChCl-EG eutectic electrolyte. Capacitance close to the values of commercial supercapacitors, high resistance and electrolyte with diffusive motion were found in the ACMag-KOH category samples. Capacitance and resistance comparable to those of commercial capacitors (around 30 F/g and resistance around tens of  $\Omega \cdot \text{cm}^2$ ) in ACNUag-KOH sample. No quasielastic signal were observed in the rGOag-Dry, ACNUag-Dry and ACNUag-KOH category samples. These results are due to presence of unwanted solvents, as confirmed by TGA. High specific capacitance, relatively low resistance and no quasi-elastic signal were observed in the rGOag-KOH sample.*

*Work supported by National Scholarship Program “Don Carlos Antonio Lopez - BECAL” of the Ministry of Finance of the Government of the Republic of Paraguay. Contract number: 171/2024, Carlsberg Foundation [CF21-0308, 2013\_01\_0589, CF14-0230, CF19-0521] and DANSCATT.*



# Tackling Real-World Crystal Structure Prediction from Powder Diffraction Data with Generative Language Models

Frederik Lizak Johansen<sup>\*†‡</sup>, Ulrik Friis-Jensen<sup>†‡</sup>, Erik Bjørnager Dam<sup>‡</sup>,  
Kirsten Marie Ørnsbjerg Jensen<sup>†</sup>, Rocío Mercado<sup>‡</sup>, and Raghavendra Selvan<sup>‡</sup>

<sup>‡</sup>Department of Computer Science, University of Copenhagen, Denmark

<sup>†</sup>Department of Chemistry & Nano-Science Center, University of Copenhagen, Denmark

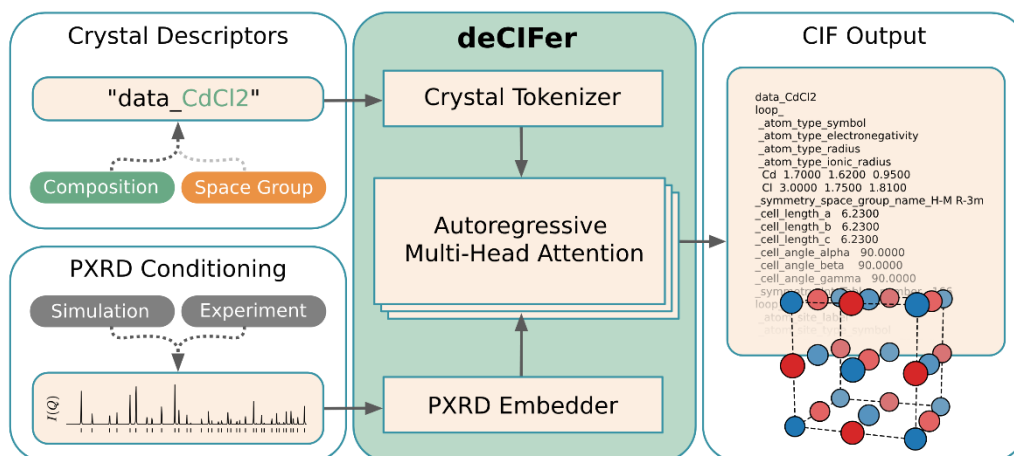
<sup>‡</sup>Department of Computer Science & Engineering, Chalmers University of Technology, Sweden

[\\*frjo@di.ku.dk](mailto:*frjo@di.ku.dk)

Crystal structure prediction (CSP) from powder X-ray diffraction (PXRD) remains a central challenge in materials chemistry. Recent large-scale models such as MatterGen [1] and GNoME [2] have made headlines by generating thermodynamically stable structures conditioned on composition or target properties. However, these models are not designed to address the inverse problem faced by experimentalists. We introduce *deCIFer*, a transformer-based autoregressive language model that generates complete crystal structures directly from PXRD input. Crucially, *deCIFer* treats PXRD as a soft constraint: the diffraction pattern influences generation through a learned embedding, but does not rigidly fix the output. Instead, PXRD must compete with other cues, such as composition and space group, allowing *deCIFer* to navigate uncertainty and propose plausible structural hypotheses when information is limited. This flexibility enables a new form of guided exploration in structural modeling. Trained on over 2.3 million CIF-PXRD pairs, *deCIFer* generates structures that align well with input PXRD while retaining chemical validity. Beyond synthetic benchmarks, the model performs well on the experimentally curated CHILI-100K dataset [3]. By enabling generation of multiple candidate structures per PXRD profile, *deCIFer* aligns with traditional crystallographic workflows and has the potential to offer a practical, flexible tool for CSP in experimental settings.

## References

- [1] Zeni, C., Pinsler, R., Zügner, D. et al. A generative model for inorganic materials design. *Nature* (2025).
- [2] Merchant, A., Batzner, S., Schoenholz, S.S. et al. Scaling deep learning for materials discovery. *Nature* (2023).
- [3] Friis-Jensen et al., CHILI: Chemically-Informed Large-scale Inorganic Nanomaterials Dataset for Advancing Graph Machine Learning. *ACM SIGKDD* (2024).



## ***In-situ synchrotron X-ray diffraction and imaging of solid-state lithium batteries***

*Giulia Dalmonte<sup>1</sup>, Salvatore De Angelis<sup>1</sup>, Poul Ægidius Norby<sup>1</sup>,  
Mads Ry Jørgensen<sup>2</sup>, Innokenty Kantor<sup>2</sup>*

1. Technical University of Denmark, Kgs. Lyngby 2800, Denmark

2. MAX IV Laboratory, Lund University, Lund 22594, Sweden

Solid-state batteries are promising new battery technologies, which will offer a safer alternative to conventional lithium-ion batteries: the flammable organic solvent and fluoride-based salt will be replaced by a non-flammable solid electrolyte. In traditional lithium-ion batteries, the liquid electrolyte conformally coats a porous electrode, maximizing the electrode/electrolyte contact area and creating an ionic transport path. In solid-state batteries instead, charge transport is a key challenge: electrodes should be dense to maximize the contact between particles, and the morphology should include percolating electronic and ionic pathways. By applying significant pressure on the cell during operation, transport properties may be improved, however this solution is not commercially viable for solid-state batteries, which should operate at ambient pressure.

Our experiments probe ionic transport properties as well as interface reactions to obtain better understanding of transport limitations. From spatially and time-resolved operando X-ray diffraction experiments we follow the structural changes in the active materials (using Rietveld refinement) as a function of time and distance in the cathode layer, an example of raw data from a Li/In/LYC/LNO-LYC cell is shown in Fig. 1. We combine this with X-ray computed tomography, to visualize morphology changes during charge-discharge, and at different applied pressures. To do so, at the DanMAX beamline (MaxIV) we used a home-built setup which hosts a 3 or 5 mm diameter in-situ battery cell, and monitors the pressure applied with an adjustable screw. Despite the high absorption from heavy elements (in  $\text{Li}_3\text{YCl}_6$  electrolyte and Li-In anode), we were able to get good resolution data using 35 keV synchrotron radiation.

By gaining information on the kinetics and spatial progression of the lithiation / delithiation process, we can understand interface reactions and ionic transport properties in composite electrodes.

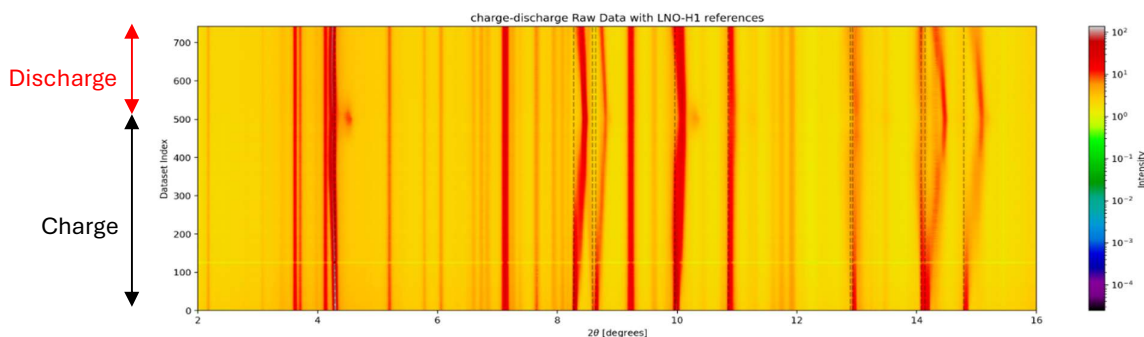


*Figure 1: Integrated intensity of the diffraction pattern during the first cycle of charge and discharge of a Li/In/LYC/LNO-LYC cell. LNO phase changes are visible.*

# Electrolytes in Action: Unraveling Cation Size Effects and Structural Dynamics in NiFe-Layered Double Hydroxides for OER Performance

Ida Kær Mønge<sup>\*a</sup>, Jordy Eggebeen<sup>b</sup>, Marc Koper<sup>b</sup> and Rebecca Pittkowski<sup>a</sup>

<sup>a</sup>Department of Chemistry, University of Copenhagen, Universitetsparken 5, 2100 Denmark

<sup>b</sup>Leiden Institute of Chemistry, Leiden University, Einsteinweg 55, 2333 CC, The Netherlands

\*ikm@chem.ku.dk

NiFe-layered double hydroxides (LDH) are state-of-the-art electrocatalysts for the oxygen evolution reaction (OER) under alkaline conditions. While intrinsic catalyst properties are crucial for their activity, the interaction between the LDH catalyst and the electrolyte can significantly influence the electrocatalytic performance. It has been shown previously that increasing electrolyte cation size ( $\text{CsOH} > \text{KOH} > \text{NaOH} > \text{LiOH}$ ) enhances the NiFe-LDH OER performance. This is hypothesized to be related to the cation intercalation and following changes in LDH layer spacing[1]. *Operando* X-ray diffraction (XRD) and X-ray total scattering with Pair Distribution Function (PDF) analysis are powerful structural characterization techniques, which allow us to follow changes in catalyst structure during operation[2]. With *operando* XRD and PDF, we can probe the relationship between structural dynamics and electrochemical behavior which is mediated by the electrolyte environment. We show that the layer distance of NiFe-LDH changes reversibly with potential, contracting during Ni oxidation and expanding back to larger d-spacing during Ni reduction. Moreover, the LDH interlayer spacing appears to vary when different electrolyte cations are applied. In the OER region, the different alkali cations appear to have distinct influences on the catalyst's structural dynamics, highlighting the importance of studying the electrode-electrolyte interactions in *operando*.

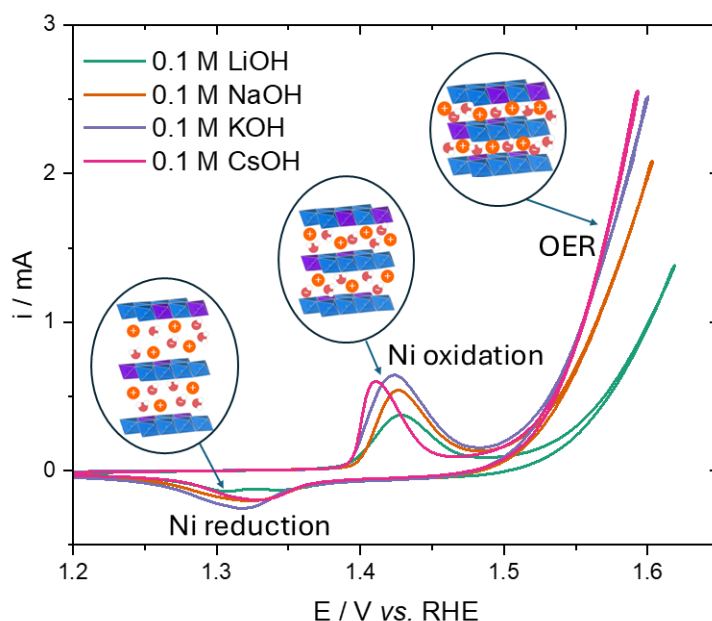


**Figure 1** Cyclic Voltammograms of different electrolytes with inserts showing the structural effect on NiFe-LDH at different potential steps.

- [1] van der Heijden, O., Eggebeen, J. J., Trzesniowski, H., Deka, N., Golnak, R., Xiao, J., ... & Koper, M. T. (2024).  $\text{Li}^+$  cations activate NiFeOOH for oxygen evolution in sodium and potassium hydroxide. *Angewandte Chemie International Edition*, 63(18), e202318692.
- [2] Aalling-Frederiksen, O., Schlegel, N., Punke, S., Anker, A. S., Wiberg, G. K., Wang, B., ... & Jensen, K. M. (2025). Structural Changes of NiFe Layered Double Hydroxides During the Oxygen Evolution Reaction: A Diffraction and Total Scattering *Operando* Study. *Small*, 2411211.

# Imaging instrument at DanMAX: current status and recent developments.

Innokenty Kantor<sup>a,c</sup>, Mads Ry Jørgensen<sup>b,c</sup>, Thorbjørn Erik Køppen Christensen<sup>a,c</sup>, Frederik Holm Gjørup<sup>b,c</sup>

a – DTU, b – Aarhus University, c – MAX VI,

The full-field imaging instrument at DanMAX has been in user operation for approximately one year, during which a series of successful experiments have been conducted. Full-field tomography, offering a field of view of about  $1.3 \times 1.3 \text{ mm}^2$  and voxel sizes of 550 or 275 nm, provides excellent contrast – including phase contrast – and sub-micron resolution across a broad range of sample types, from soft organic tissues to metallic foams and operando batteries. Typical scan times range from several seconds to a few minutes, enabling time-resolved studies such as mechanical deformation, electrochemical cycling, and temperature-induced phase transitions.

An advanced data reconstruction pipeline, leveraging the MAX IV high-performance computing cluster, delivers fully reconstructed volumes to users by the end of their beamtime.

Recent developments include beam expansion and automated stitching techniques to extend the effective field of view, achieving high spatial resolution ( $\sim 100 \text{ nm}$ ) using a multilayer Laue lens, and the integration of an ultra-high-resolution 150 Mpx sensor detector.

## Imaging facilities at MAX IV

Synchrotron-based imaging has emerged as a transformative tool for life sciences, offering unparalleled spatial resolution, elemental sensitivity, and phase contrast for probing biological systems under near-native conditions. At MAX IV, four complementary beamlines—**NanoMAX**, **SoftiMAX**, **ForMAX**, and **DanMAX**—offer a versatile toolkit for comprehensive multiscale, multimodal characterization of cells, tissues, and macromolecular assemblies.

**NanoMAX** delivers a highly focused, coherent hard X-ray beam (5–28 keV) down to 50–100 nm: **STXM** (Scanning Transmission X-ray Microscopy) with single photon counting detectors provide quantitative absorption images of cells, organelles, and protein assemblies. **XRF** (X-ray Fluorescence Mapping) pinpoints trace elements (e.g., metal cofactors) within tissues. **Ptychography** using a fast in-vacuum pixel detector (EIGER2 X 4M) reconstructs both shape and internal density of subcellular structures beyond the beam's spot size.

**SoftiMAX** operates in the soft X-ray range (275 eV–2.5 keV), ideal for carbon, nitrogen, and oxygen contrast: One branch offers sub-100 nm STXM with PMT detectors and ptychography using Andor-Zyla pixel detector for membrane and macromolecule imaging. A second branch provides full-field and coherent imaging with beam sizes up to 20  $\mu\text{m}$  for rapid surveys of cell populations or biofilms.

**ForMAX** bridges scales from 1 nm to 1 mm (8–25 keV) by combining full-field synchrotron x-ray microtomography with scanning SWAXS (small- and wide-angle X-ray scattering) imaging in one instrument. Ultrafast X-ray imaging techniques in 2D (radiography) and 3D (XMPI, X-ray multi projection imaging) are also available. All techniques are applicable to a wide range of materials and suitable for temporally resolved experiments.

**DanMAX** is a materials science beamline, dedicated to in situ and operando experiments on real materials. The beamline operates in the 15–35 keV range and has three endstation instruments: one for full field imaging instrument, one versatile powder diffraction setup using an area detector and a high resolution powder X-ray diffraction instrument using a microstrip detector.

Together, these beamlines can enable life scientists to visualize everything from protein complexes to whole tissues—with elemental, phase, and 3D contrast—under near-physiological conditions.

# Structural characterization of a semiconducting 'paddlewheel' MOF, $[M_2(TCS)(BPY)]$

Jacob Rixen Østerbro, B. B. Iversen

Department of Chemistry, Aarhus University, Denmark

Metal-organic frameworks (MOFs) have gained a lot of popularity in recent years due to their wide range of physical properties, originating from their inherent structural tunability. I am currently investigating a semiconducting MOF with the abbreviated formula  $[M_2(TCS)(BPY)]$  ( $M = Co$  or  $Cu$  in this study;  $H_4TCS = 4,4',4'',4'''$ -silanetetrayltetrabenzoic acid;  $BPY = 4,4'$ -bipyridine). The compound has been shown to be able to photocatalyze the conversion of  $CO_2$  into  $CH_4$  under visible light<sup>[1]</sup>. We are currently conducting charge density analysis of this compound to gain a better understanding of the bonding characteristics of the structure. We have recently observed a phase transition for the Co-MOF variant somewhere between 40 and 100 K, but we have so far not been able to determine the space group. Interestingly, this phase transition is only present for the Co-MOF variant. We also plan to measure the magnetic properties of both variants and relate this to observed d-orbital populations gained from our charge density analysis. Note that this study is currently unfinished.

[1] Yang & Zhang et al., (2017) *Dalton Transactions*, 46(25), 8204-8218

# Curiosities of Terbium Iron Garnet, Diffraction from a Canted Compensated Ferromagnet

J. Thomas-Hunt<sup>1\*</sup>, Navid Qureshi<sup>2</sup>, Claire Colin<sup>3</sup>, B. Tomasello<sup>4</sup>, T. Ziman<sup>2</sup>, S. Geprägs<sup>5</sup>, M. Christensen<sup>1</sup>, D. Mannix<sup>6</sup>.

<sup>1</sup>Aarhus University, Denmark. <sup>2</sup>Institute Laue-Langevin, Grenoble, France., <sup>3</sup>Institute Néel, CNRS, Université Grenoble Alpes Grenoble, France., <sup>4</sup>University of Catania, Catania Italy., <sup>5</sup>Walther Meissner Institute, Munich, Germany., <sup>6</sup>European Spallation Source, Lund, Sweden  
\*jth@chem.au.dk

Terbium iron garnet, (Tb<sub>3</sub>Fe<sub>5</sub>O<sub>12</sub>, TbIG, (Ia-3d, 12.43 Å)), has a complex canted magnetic structure with a wave vector of  $k = 0$  characterized by magnetic reflections of  $hkl = \text{odd, odd, even}$  [1]. The structure is a classic example of Néel's ferrimagnetism with a high ordering temperature of 560 K, it has a point of vanishing net magnetization (compensation point) at 250 K. With the generous unit cell allowing for tuning of this compensation point. The dynamic magnetic structure is seeing a 21st Century renaissance for spin-caloritronics [2,3], the interconversion of spin, heat, and electric currents, by utilizing a bilayer device structure of a ferrimagnetic insulator (e.g. TbIG) and a heavy metal top layer (e.g. Pt). The renewed theoretical understanding of TbIG dynamics[4] prompted a renewed structural investigation supporting a room temperature structure.

Single crystal neutron diffraction was utilised to perform structural analysis at room temperature and base temperatures of 15 and 4 K. Complementary resonant x-ray diffraction (REXS) was performed on TbIG thin films for prototypal spin-caloritronic devices. The single-crystal diffraction data revealed canted magnetic reflections at room temperature, providing the direct evidence of this structure above the compensation point. This observation confirms the theoretical prediction of a cubic canted magnetic structure without requiring symmetry reduction to a rhombohedral nuclear cell. Similar temperature dependencies were observed with REXS on thin films. The improved understanding of the complex canted magnetic structure at room temperature allows further conceptualisation of TbIG for prototypal spin-caloritronic devices at technically feasible conditions.

## References

- [1] Lahoubi, M.; et al., IEEE Transactions on Magnetics 1984, 20 (5), 1518-1520.
- [2] Uchida, K.; et al., Nature 2008, 455 (7214), 778-781.
- [3] Geprägs, S.; et al., Nature Communications 2016, 7 (1), 10452
- [4] Tomasello, B.; et al., Annals of Physics 2022, 447, 169117.

# SiENAH: *In situ* furnace for fast and high-temperature sintering in air

J. Simonsen<sup>1</sup> (js@chem.au.dk), T.O. Kessler<sup>1</sup>, M. Christensen<sup>1,2</sup>

<sup>1</sup>Department of Chemistry, Aarhus University, Aarhus, Denmark, <sup>2</sup>Interdisciplinary Nanoscience Center, Aarhus, Denmark

Magnets are the key to the green transition as they can interconvert between motion and electricity. To tune the properties of permanent magnetic materials a detailed description and control over six orders of magnitude in length scales are required - from the atomic to the macroscale.[1] The atomic structure and crystallinity determine the intrinsic magnetic properties, whilst the crystallite size and morphology determine extrinsic properties.[2] The atomic structure and crystallite size are formed by the synthesis whilst the compaction of the magnet directs the crystallographic preferred orientation or texture. These length scales can be investigated using 2D X-ray diffraction and measuring the sintering *in situ* allows us to follow the development as a function of time, temperature, and heating rate.

To study the formation of hexaferrites in real production conditions *in situ* a furnace that allows for fast heating and high temperatures in air has been developed. For heating the furnace uses silicon nitride heating elements and the design allows for temperatures over 1400 °C and heating rates >80 °C/second. Preliminary *ex situ* experiments have been very successful being able to synthesise phase pure strontium M-type hexaferrite ( $\text{SrFe}_{12}\text{O}_{19}$  or SrM) in under five minutes with promising magnetic properties and nanosized crystallites. Here preliminary benchmarks and results from the *in situ* sintering of SrM in air from P21.2 @ PETRA III will be shown. Fig. 1 a) shows a computer aided design drawing of SiENAH and Fig. 1 b) shows a time-resolved diffraction pattern for the heating of alumina and sodium chloride to 1100 °C with a heating rate of 10 °C/second.

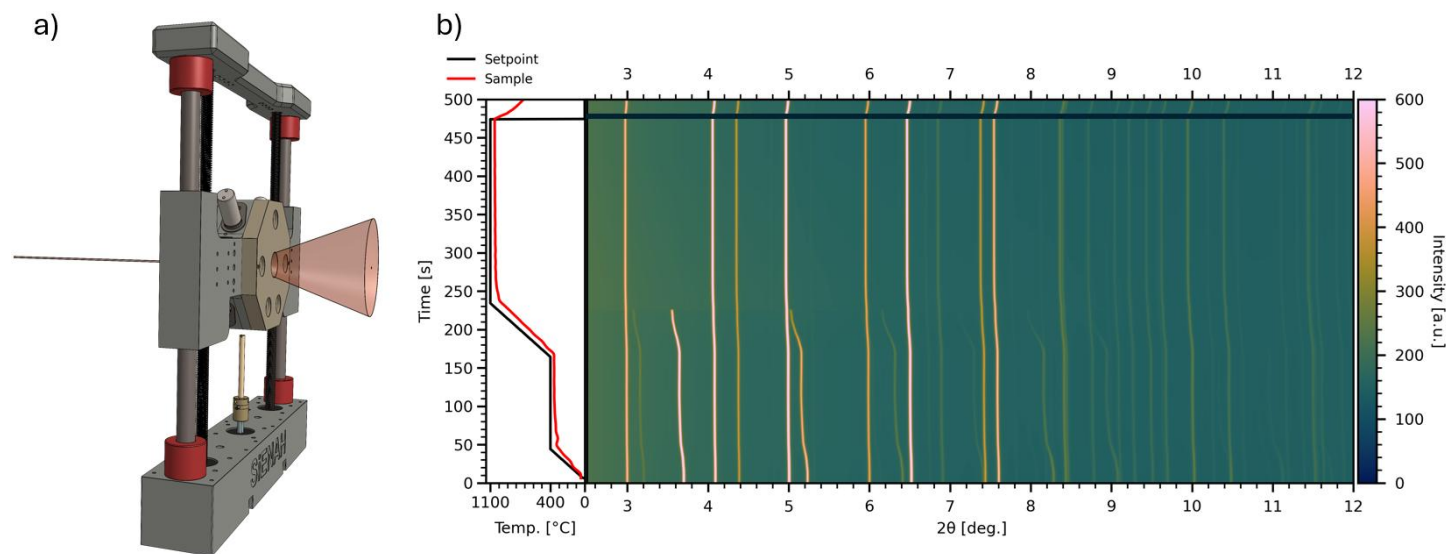


**Figure 1.** a) Computer aided design drawing of SiENAH. b) Time-resolved diffraction pattern for the heating of alumina and sodium chloride to 1100 °C with a heating rate of 10 °C/second.

[1] Leslie-Pelecky, D. L. & Rieke, R. D. (1996). Chemistry of Materials, 8, 1770.

[2] Sander, D., Valenzuela, S. O., Makarov, D., Marrows, C. H., Fullerton, E. E., Fischer, P., McCord, J., Vavassori, P., Mangin, S., Pirro, P., Hillebrands, B., Kent, A. D., Jungwirth, T., Gutfleisch, O., Kim, C. G. & Berger, A. (2017). J. Physics D, 50, 363001.



## Kick starting the Scandinavian Crystallography Service

Kirsten E. Christensen<sup>a,b</sup> and Lennard Krause<sup>a,b</sup>

a) Department of Chemistry, Aarhus University, Aarhus, Denmark

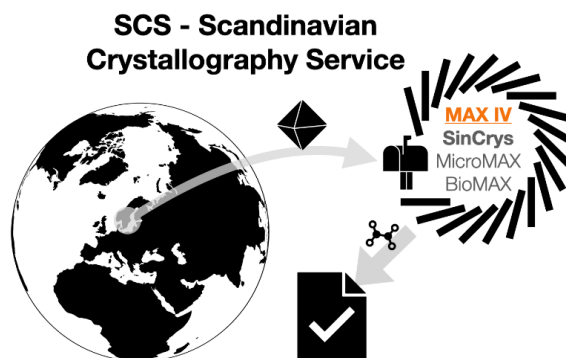
b) MAX IV Laboratory, Lund University, Lund, Sweden

Single crystal X-ray diffraction is the preferred technique to solve the atomic structure of a crystalline material. Today, it is a routine technique in many research laboratories, however, the limited flux, spectral purity and focusing ability of a lab-source severely limits the size and quality of the crystals that can be measured. Moreover, many materials do not grow crystals that are large enough to be studied by this technique. Synchrotrons can close this gap; however, they are not commonly used for routine small molecule crystallography due to the required additional technical expertise and long lead times in the proposal-based access policy.

The Scandinavian Crystallography Service (SCS) seeks to remove this barrier and establish a point-of-entry for service crystallography inspired by the successful UK National Crystallography Service. It covers fundamental materials research as well as deep strategic studies of commercial interest and provides new synergies, scientific projects and structural insights using single crystal X-ray diffraction. The target demographic is any commercial or academic user, independent of the level of crystallographic experience.

SCS has access to SINCRYS, BioMAX and MicroMAX beamlines. This allows for data collections on a wide range of compounds with smaller unit cells that can benefit to be measured with higher intensity. Depending on user experience with X-ray single crystal diffraction there are different access levels such as 'Data Only', and 'Full Structure analysis'. Samples are submitted by users throughout Scandinavia and further abroad.

SCS aims to offer easy, paid-for access to collect data on single crystals. For more details, please contact us on [scs@maxiv.lu.se](mailto:scs@maxiv.lu.se)



# Ultra small iridium oxide nanoparticles – from synthesis to oxygen evolution reaction catalyst

Laura Graversen\*, Freja B. Holde, Stefanie Punke, Rebecca Pittkowski & Kirsten M. Ø. Jensen

Department of Chemistry & Nano-science center, University of Copenhagen, 2100 Copenhagen Ø, Denmark

\*Lgg@chem.ku.dk

Electrochemical water splitting plays a key role in efficient storage of green energy. However, the oxygen evolution reaction (OER) occurring at the anode represents a significant bottleneck owing to its sluggish reaction kinetics [1]. The harsh conditions present in the acidic OER reaction necessitate the need for precious metal-based catalysts such as  $\text{IrO}_2$  and  $\text{RuO}_2$ . To optimize the catalytic properties of these scarce materials, we need an understanding of the catalysts at an atomistic level, since crystal structure and oxidation state impact the catalyst performance. Small iridium nanoparticles with high dispersion can reduce the amount of precious metal, but they show increased degradation and eventually reduced catalytic activity [2]. Thus, knowledge of the structure-performance relationship in high-surface-area particles is crucial in the quest towards designing new materials with smaller loadings of scarce metals.

Using an easy hydrothermal synthesis method, sub 1 nm  $\text{IrO}_x$  particles have been prepared. Subsequent calcination at different temperatures allows tuning of the particle sizes (see Figure 1a). The  $\text{IrO}_x$  sizes have been determined through multimodal analysis using small angle X-ray scattering (SAXS) and total scattering with pair distribution function (PDF) analysis. These two complementary techniques reveal the growth of spherical 1 nm NPs at 400 °C into 3 nm spherical NPs at 450 °C. Growth through oriented attachment leads to the formation of 3 nm wide and 9 nm long rods at a temperature of 500 °C. PDF analysis reveals a size-dependent atomic structure of the  $\text{IrO}_x$  catalysts (see Figure 1b, c), where a smaller crystallite size is correlated with an increased amount of edge-sharing (ES)  $[\text{IrO}_6]$ -octahedra compared to the rutile  $\text{IrO}_2$  structure. Using operando PDF and X-ray absorption fine structure (XAFS) analysis, we study how  $\text{IrO}_x$  size, structure, and morphology impact the structural changes in the catalyst structure upon activation. The operando studies reveal a high structural stability of the nanosized OER catalyst, which may originate from an increased amount of ES  $[\text{IrO}_6]$ -octahedra present in the  $\text{IrO}_x$  structure.

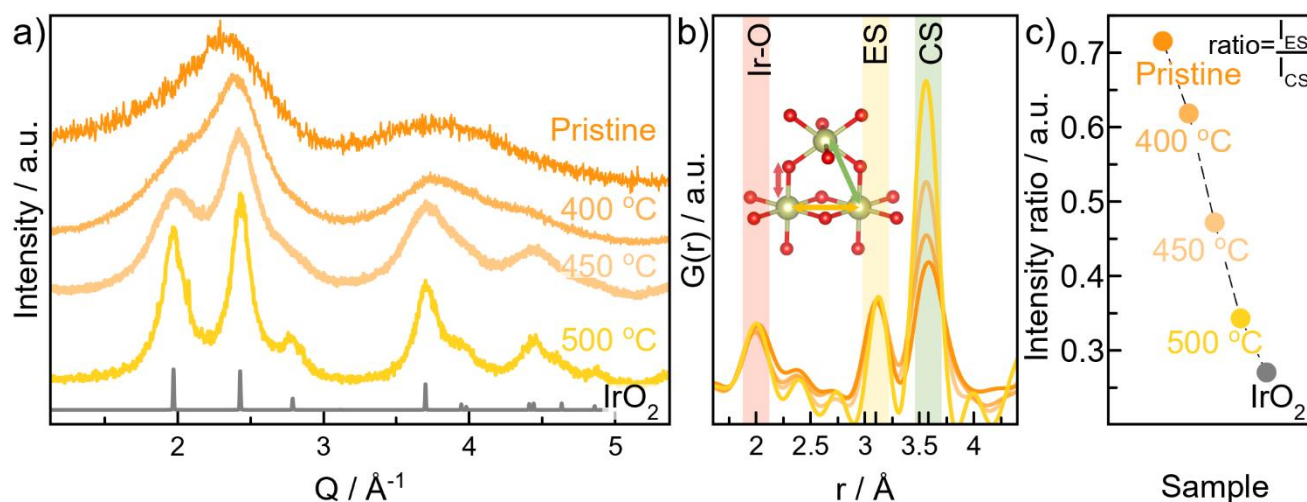


**Figure 1.** Diffraction patterns of hydrothermally synthesized  $\text{IrO}_x$  “Pristine”, and subsequently calcined at 400 °C, 450 °C, or 500 °C. a) PXRD showing sharper Bragg peaks at higher calcination temperatures. b) Local PDF range showing ES/CS intensity differences. c) Ratio of ES/CS PDF peak intensity illustrating less structural disorder with higher calcination temperature.

[1] Carmo, M., Fritz, D.L., Mergel, J. & Stolten, D. (2013). *Int. J. Hydrog. Energy.*, **38**, 4901-4934.

[2] Bornet, A., Pittkowski, R., Nielsen, T. M., Berner, E., Maletzko, A., Schröder, J., Quinson, J., Melke, J., Jensen, K. M. Ø. & Arenz, M. (2023). *ACS Catal.*, **13**, 7568-7577.

# Serial Synchrotron X-ray Crystallography studies of Lytic polysaccharide monooxygenase

Zhiyu Huang<sup>1</sup>, Monika Bjelcic<sup>2</sup>, Jie Nan<sup>2</sup>, Yusuf Theibich<sup>1</sup>, Mohannad Khaled Aloula<sup>1</sup>, Leila Lo Leggio<sup>1§</sup>

<sup>1</sup> Department of Chemistry, University of Copenhagen, Universitetsparken 5, DK-2100, Denmark.

<sup>2</sup> MAX IV Laboratory, Fotongatan 2, 224 84 Lund, Sweden.

§leila@chem.ku.dk

Lytic polysaccharide monooxygenases (LPMOs) are enzymes copper-dependent enzymes that degrade polysaccharides oxidatively and used in second-generation bioethanol production and virulence factors in some pathogens. LPMOs are classified within the Auxiliary Activities (AA) family of CAZymes [1] and histidine brace is highly conserved. The mechanism of LPMOs reaction is highly complex, and it is now widely recognized that hydrogen peroxide serves as a co-substrate in facilitating the catalytic process [2]. However, further in-depth mechanistic investigations are required to elucidate the underlying details. Serial synchrotron X-ray crystallography (SSX) can potentially capture the dynamic action of LPMOs at room temperature in a time-resolved (TR) manner, offering insights into their catalytic mechanism at the molecular level. In this study, *LsAA9A*, derived from *Lentinus similis* and classified within the AA9 family, has served as an important model system due to its activity on soluble oligosaccharide substrates. SSX structural analysis of *LsAA9A* has been initiated using both T-REXX (DESY, Hamburg) and Biomax/Micromax (MAXIV). Microcrystals of *LsAA9A* were successfully produced and diffracted and preliminary structures obtained. This study provide a solid foundation for future time-resolved serial crystallography experiments on LPMOs.

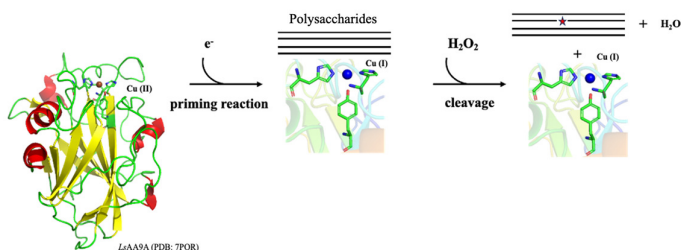


**Figure:** Left: the “priming reduction” initiates the catalytic cycle of LPMOs reaction.

## References

1. Cantarel, B. L. et al. Nucleic Acids Res, 37, D233–D238 (2009).
2. Bissaro B. et al. Nat Chem Biol, 13(10), 1123-1128 (2017).

# The lack of long range magnetic order in deuteronium jarosite, elucidated by neutron scattering

## Abstract

Jarosites,  $\text{AFe}_3(\text{SO}_4)_2(\text{OD})_6$ , contain layers of  $\text{Fe}^{3+}$  in a frustrated kagomé lattice structure. The common potassium jarosite,  $\text{A} = \text{K}$ , exhibits magnetic order at around 65 K. The aim is to investigate how changing the  $\text{K}^+$  ion on the A-site to  $\text{H}_3\text{O}^+$ ,  $\text{D}_3\text{O}^+$ , or  $\text{ND}_4^+$  affects the magnetic properties of the material. Based on existing literature, it is known that the  $\text{ND}_4$ -jarosite has a reduced ordering temperature,  $T_N = 52$  K, while the hydronium and deuteronium jarosites have a phase transition to spin glass between 12 and 18 K.

The magnetic properties of all 4 jarosites were investigated using inelastic neutron scattering at FOCUS, the Time-of-Flight spectrometer at PSI, and the magnetic and crystal structure was studied with the powder diffractometer HRPT, PSI. Based on the FOCUS data recorded for different temperatures, it is concluded that the centre of neutron scattering occurs around  $Q = 1 \text{ \AA}^{-1}$  to  $Q = 1.1 \text{ \AA}^{-1}$ . This is the Q-value of the first 3D antiferromagnetic peak in jarosites. For the deuteronium jarosite, quasi-elastic magnetic scattering is observed with a peak in intensity at 35 K. In contrast, for  $\text{ND}_4$ -jarosite and potassium jarosite, there is an inelastic signal resembling spin waves below the ordering temperature. We aim to help elucidate the nature of magnetic transitions of different jarosites.

Title: Flexible 3D ptychographic tomography at grazing incidence with hard X-rays for arbitrary surface structures

Abstract:

Coherent diffraction imaging techniques in reflection geometry offer exceptional surface sensitivity, making them a powerful tool for resolving buried surface structures. In this work, we introduce a new framework for reconstruction of 3D objects from experimental grazing incidence ptychographic data using multislice as a forward model with automatic differentiation. We further demonstrate the framework's flexibility by incorporating multiple incidence angles and rotational angles into a single reconstruction. Example applications include the reconstruction of randomly dispersed Si nanoparticles on an Au substrate and a multilayer thin film with nanoscale thickness variations. The framework is available as an open-source package, providing an accessible and versatile tool for reconstructing arbitrary 3D surface structures in grazing incidence.

# **Operando mapping of morphology, phase transformations, and current patterns in energy devices by time-of-flight neutron diffraction and polarised neutron imaging**

Luise Theil Kuhn

DTU Energy, Technical University of Denmark, Kgs. Lyngby, Denmark

A core activity in the ESS Lighthouse Hard Materials in 3D, SOLID (<https://solid.dtu.dk/>), has been to develop advanced neutron imaging methods for operando analysis of microstructure, phase transformations, and current patterns in energy devices. Here, I will present two cases where we have investigated the battery cell degradation of Na-ion batteries while being charged and discharged, and the current pattern formation in a proton exchange membrane water electrolysis (PEMWE) cell under operation.

Na-ion batteries are one of the promising next-generation battery technologies since they can deliver a capacity comparable to Li-ion batteries while constituting cheap, non-flammable, and sustainable materials. However, the chemical and mechanical stability during cycling is a challenge. The Na-ion battery is inherently difficult to directly image as Na has a very low X-ray and neutron scattering cross-section and can't sustain post-mortem disassembly and analysis. At the SENJU beamline at J-PARC, we have successfully performed the first multimodal operando neutron studies combining time-of-flight diffraction and Bragg edge imaging to investigate the microstructural changes and phase transformations of the battery electrodes and link them to the electrochemically active regions.

PEMWE cells are considered one of the key technologies for sustainable hydrogen production. PEMWE can be operated under relatively flexible conditions, making them ideal for varying electricity production by e.g. wind turbines or solar cells. A central component is the porous transport layer (PTL), which is used for managing the distribution of water and release of produced gasses. The PTL is subject to a very harsh environment and is often based on Ti coated with Pt or Ir. The morphology of the PTL is crucial for the performance of the PEMWE since this is directly linked to the oxygen bubble formation and the current pattern formation in the cell. At the RADEN beamline at J-PARC and NeXT at ILL, we have performed the first polarised neutron imaging studies of the current pattern formation in the PEMWE cell under operation while linking it to the electrochemical performance with different types of PTLs.

# ESS DMSC Summer School

*Aaron Finke, Ales Kutsepau, Alexandre Stefanov, André Costa, Andrew Sazonov, Carina Lobley, Celine Durniak, Christian Vedel, Cosmina Somani, George Oneil, Henrik Jacobsen, Jan-Lukas Wynen, Joanna Lewis, Johannes Kasimir, Mads Bertelsen, Martin Trajanovski, Massimiliano Novelli, Mridul Seth, Neil Vaytet, Oliver Hammond, Peter Willendrup, Raquel Costa, Sunyoung Yoo, Torben Roland Nielsen*

The European Spallation Source (ESS) aims to be the world's brightest neutron source and is currently under construction in Lund, Sweden. The project is nearing the end of its construction phase and will soon start commissioning of neutron scattering instruments and thus start production of data. The Data Management and Software Centre (DMSC) located in Lyngby, Denmark, have been preparing handling this data by developing a suite of scientific software. Among the capabilities of the software is simulation / control of neutron scattering instrumentation, data reduction, data analysis and data storage. We refer to this as the DMSC data pipeline, as the data moves through these stages. In addition, DMSC provides remote access to the data as well as the necessary software.

The ESS DMSC Summer School is a 5-day school held at the DMSC in Lyngby that prepares potential future users of ESS for using the software effectively. The school was held in 2023 and 2024, with registration now open for 2025. Participants will be taught about the ESS facility and how to apply for beamtime. As all the software uses Python, an introduction is included in the school programme. Participants will learn about instrument simulation using McStas and choose between 3 different exercise tracks, QENS, SANS or powder diffraction. The created data will be reduced with the Scipp library, and the analysis will be performed with EasyScience, both developed at the DMSC. Finally, the data created by each participant will be uploaded to our data catalogue using SciCat.

The school had participants from High School to senior scientists, and we are proud to say the entire spectrum had a useful experience. This is partly because this software stack is new to the entire community. Anyone interested in performing an experiment at ESS or using the resulting data are welcome to apply to join our school, the only requirement is an abstract for a poster used to choose among the applications. Costs are reduced to a minimum by applying for external sponsorships, in the past we have been sponsored by DanScatt, the Carlsberg Foundation and 2FDN, and have so far avoided a registration fee.

# Valence transitions in lanthanide-organic polymers

M. A. Dunstan<sup>1</sup>, A. Viborg<sup>1</sup>, N. J. Yutronkie<sup>2</sup>, G. Garbarino<sup>2</sup>, F. Wilhelm<sup>2</sup>, A. Rogalev<sup>2</sup>, K. S. Pedersen<sup>1</sup>

<sup>1</sup>Department of Chemistry, Technical University of Denmark, <sup>2</sup>European Synchrotron Radiation Facility  
majdu@kemi.dtu.dk

Molecular materials based off redox-active building blocks hold great promise for the realisation of materials with unique magnetic, conductive, and photophysical properties which can be switched on or off by application of an external stimulus (e.g. pressure, light, or temperature).<sup>[1,2]</sup> We have synthesised a family of molecular lanthanide (Ln) materials of general formula  $\text{LnI}_2(\text{pyz})_3$  (pyz = pyrazine; Fig 1a).<sup>[2-4]</sup> Incorporating the strongly reducing Sm(II) allows for observation of a valence tautomeric transition in  $\text{SmI}_2(\text{pyz})_3$  (Fig. 1b).<sup>[3]</sup> Here,  $\text{Sm(III)-pyz}(\bullet-)$  and  $\text{Sm(II)-pyz}(0)$  redox tautomers exist in close energetic proximity, engendering a tunable thermal switching between two distinct electronic states. Samarium  $L_{2,3}$  XANES provides unambiguous elucidation of the Ln valency, and has been used to track the temperature- and pressure-dependence of the valence transition (Fig 1b), leading to the the first observation of a pressure-induce valence tautomeric transition in a molecular lanthanide material.

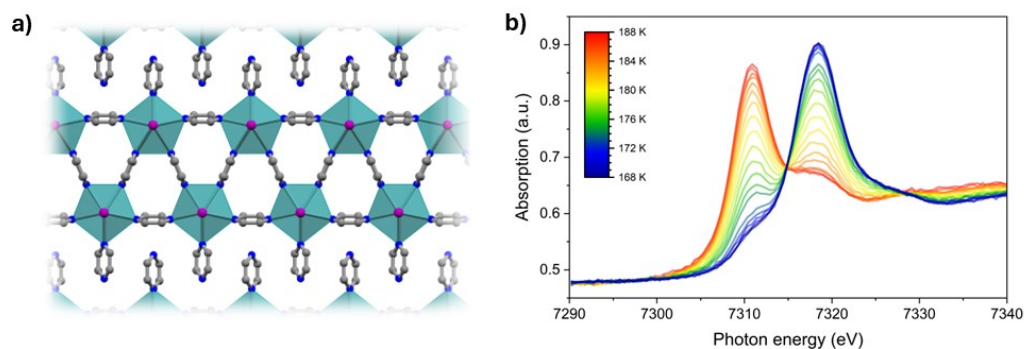


**Figure 1. a)**  $\text{LnI}_2(\text{pyz})_3$ . **b)** Variable temperature Sm  $L_2$ -edge XANES of  $\text{SmI}_2(\text{pyz})_3$ .

## References

- [1] O. Sato, *Nat. Chem.*, **2016**, 8, 644.
- [2] M. A. Dunstan, K. S. Pedersen, *Chem. Commun.*, **2025**, 61, 627.
- [3] M. A. Dunstan, K. S. Pedersen *et al.*, *Nat. Chem.*, **2024**, 16, 735.
- [4] A. Viborg, M. A. Dunstan, K. S. Pedersen *et al.*, *Chem. Sci.*, **2025**, accepted article.  
DOI: 10.1039/d5sc01246e.



## To the nanoscale and beyond: imaging the cellular voids and connections in bone tissue with nano-CT

M. Østergaard,<sup>1</sup> L. Burc,<sup>1</sup> A. Pacureanu,<sup>2</sup> T.T. Sikjær,<sup>3,4</sup> L. Rejnmark,<sup>3</sup> H. Birkedal<sup>1</sup>

1: Dept. of Chemistry and iNANO, Aarhus University, Aarhus, Denmark

2: ESRF, The European Synchrotron, Grenoble, France

3: Dept. of Endocrinology and Internal Medicine, Aarhus University Hospital, Aarhus, Denmark

4: Dept. of Clinical Medicine, Aarhus University, Aarhus, Denmark

Bone is a complex hierarchical composite material made up mostly of collagen and nanocrystalline apatite, but it also contains crucial minor components e.g. controlling mineralization mechanisms. Bone also contains a network of cells called osteocytes which are contained in lacunae and interconnected by canaliculi (channels in bone some 100s of nm wide). These cells are thought to be the orchestrators of the ever-ongoing bone remodeling process and are thus critical for bone health. Hence, accurate characterization of the 3D morphology of the osteocyte lacunae and their signaling interconnections is vital when investigating the osteocyte function under various physiological and pathological conditions but remains challenging as the lacuno-canalicular network (LCN) is situated deeply within the mineralized bone matrix. Nano-CT allows for 3D investigations at resolutions sufficient to visualize even canalicular structure and with the emergence of fourth-generation synchrotrons the technique will be more readily available.

We aim to investigate the LCN in small samples from hypoparathyroidism patients treated with PTH(1-84) for 6 months. As the PTH treatment leads to renewed bone formation, these samples offer the chance to detect lacunae during the remodeling process, when the cells are actively laying down new bone. Samples were from iliac crest biopsies that were embedded in plastic and cut to square rods using a diamond saw. Nano-CT was performed in a holographical manner using a 50 nm isotropic voxel size at the ID16A beamline at the European Synchrotron Radiation Facility.

Using nano-CT we captured these lacunae and their protruding canaliculi in regions of differently mineralized bone, both a strong side and a downside to the study. Due to this difference in mineralization density across a single sample, the tracing of canaliculi between the cells is a challenging task. The data obtained is 3D, so after extracting LCN we can get information about size and shape of both the lacunae and the canaliculi.

Nano-CT as a technique offers 3D morphologic information of the LCN even from plastic embedded samples. With standard  $\mu$ CT the contrast only offers to observe lacunae, the cellular ghosts, and not the cells themselves. But the contrast offered from nano-CT on fourth-generation synchrotrons is going to enable observations of cells within the lacunae. With more datasets like this from fourth-generation synchrotrons we hope, in the future, to be able to link LCN morphology to cell types. With that, this technique could offer both morphological and cell specific information.

# Spectroelectrochemical neutron reflectometry of photosynthetic membranes

Mary Wood, Rebecca J. L. Welbourn, Joshua Lawrence  
Niels Bohr Institute  
Blegdamsvej 17, Copenhagen, Denmark  
mary.wood@nbi.ku.dk

Photosynthesis is one of the most important processes for life on our planet, yet many important questions regarding its fundamental mechanisms remain unanswered. The rapidly developing field of bioelectronic devices that use photosynthetic organisms such as cyanobacteria wired to electrodes has given an urgency to addressing these questions; in particular, development of such technologies requires a detailed understanding of the electron transfer mechanisms at the biofilm/electrode interface, which currently represents the bottleneck in improving efficiency<sup>1</sup>.

A more efficient method has been to extract the photosynthetic thylakoid membranes and deposit these directly onto the electrode<sup>2,3</sup>. However, these systems are still highly complex and deconvoluting their components and the parameters that contribute to their electron-transfer mechanisms from a top-down perspective is non-trivial. To address this, we have developed neutron reflectometry coupled with spectroelectrochemistry *in situ* to compare electrodes with extracted thylakoid membranes to those using a model lipid/protein mixture. We have shown that bilayer formation is not induced for the natural vesicles but can be initiated by an applied potential for the model system. We also observed light-dependent movement of the model thylakoid membranes representing the first time neutron reflectometry has been used to measure such spectroelectrochemical structural changes.

This work has demonstrated the potential of our neutron reflectometry/spectroelectrochemistry system as well as establishing a platform for further fundamental studies both of photosynthesis in model membranes and also for screening potential improvements to bioelectronic technologies.

- (1) McCormick, A. J.; Bombelli, P.; Bradley, R. W.; Thorne, R.; Wenzel, T.; Howe, C. J.. *Energy Environ. Sci.* **2015**, *8*, 1092–1109.
- (2) Liu, Y.; Daye, J.; Jenson, D.; Fong, S. *Bioelectrochem.* **2018**, *124*, 22–27.
- (3) Pankratov, D.; Pankratova, G.; Gorton, L. *Curr. Opin. Electrochem.* **2020**, *19*, 49–54.

# Slot-Die Coater for In-Situ Multimodal Characterization of Functional Thin Films

Matteo Ciambezi  
FOM Technologies, Copenhagen, Denmark  
Email: [mac@fomtechnologies.com](mailto:mac@fomtechnologies.com)

Solution-processable materials for applications in photovoltaics, batteries, sensors, and optoelectronics are increasingly studied due to their performance, scalability, and cost-effectiveness.<sup>1-3</sup> Understanding the mechanisms of film formation during deposition is essential for improving film quality and device performance.

We present a compact roll-to-roll slot-die coating platform designed for high-throughput research and integration into in-situ characterization setups. The system includes a remote-controlled slot-die coater with precise ink delivery, thermal annealing (up to 200 °C), and gas quenching. Its modular design makes it flexible to various experimental requirements, including synchrotron beamlines.

This platform supports simultaneous in-situ measurements using multiple techniques, including X-ray absorption spectroscopy (XAS), X-ray fluorescence (XRF), X-ray diffraction (XRD), grazing-incidence small-angle X-ray scattering (GISAXS), and optical spectroscopy. These techniques can be employed simultaneously at the same sample location, enabling comprehensive analysis of chemical composition, oxidation states, crystalline structure, and nanoscale morphology during film deposition and post-processing.

The system's automation and reproducibility facilitate systematic exploration of processing parameters. Its compact footprint allows installation in standard laboratory environments, including fume hoods, making it accessible for both academic and industrial research.

This platform provides a valuable tool for advancing the understanding and optimization of functional thin-film materials through real-time, in-situ, multimodal analysis.

## References:

<sup>1</sup>Nishide, Hiroyuki, and Kenichi Oyaizu. "Toward flexible batteries." *Science* 319.5864 (2008): 737-738.

<sup>2</sup>Burschka, Julian, et al. "Sequential deposition as a route to high-performance perovskite-sensitized solar cells." *Nature* 499.7458 (2013): 316-319.

<sup>3</sup>Li, Jinzhao, et al. "20.8% slot-die coated MAPbI<sub>3</sub> perovskite solar cells by optimal DMSO-content and age of 2-ME based precursor inks." (2020).

# Competing mechanisms involved in the autofluorescence of cetyltrimethylammonium-modified cellulose nanocrystals

Marcus A. Johns,<sup>a</sup> Dorthe Posselt,<sup>b</sup> Wang Zhang Yuan,<sup>c</sup> Emily D. Cranston,<sup>d</sup> Jacek Fiutowski<sup>a</sup>

- a) Mads Clausen Institute, University of Southern Denmark, Denmark
- b) IMFUFA, FRUSTMI, Department of Science and Environment, Roskilde University, Denmark
- c) School of Chemistry and Chemical Engineering, Shanghai Jiao Tang University, China
- d) UBC Bioproducts Institute, University of British Columbia, Canada

Cluster-triggered emission (CTE) photoluminescence is an emerging phenomenon that allows non-conjugated compounds rich in heteroatoms, such as oxygen or nitrogen, to exhibit luminescence upon aggregation or clustering. Essentially, this mechanism describes fluorescence from nontraditional fluorophores. We have previously used the technique to characterise key physicochemical properties of cellulose nanocrystals (CNCs) - rod-like nanoparticles made of chains of  $\beta$ -(1 $\rightarrow$ 4) linked glucose units arranged into a highly crystalline structure, typically featuring anionic sulfate half-ester surface groups – and to identify microplastic polymer types.<sup>1-3</sup>

Recently, Stephens et al. computationally demonstrated that increasing hydrogen bond length decreases the likelihood of CTE photoluminescent decay, while an ammonium cation increases the likelihood.<sup>4</sup> We tested this by substituting the counterion for the sulfate half-ester groups on the CNCs with cetyltrimethylammonium (CTA) cations. We hypothesised that two competing mechanisms are involved in the resulting photoluminescence properties:

1. **Fluorescence enhancement** due to CTA's quaternary ammonium groups promoting aggregation and charge-assisted emission.
2. **Fluorescence quenching** at higher modification levels, where long alkyl chains disrupt CNC clustering.

Preliminary results suggest that our hypothesis is correct, showing an initial increase in the fluorescence quantum yield, followed by a decrease. Critically, the turning point may occur when the CNCs switch from amphiphilic to hydrophobic, specifically when the surface coverage of the nanoparticles by the CTA cation is sufficient to disrupt the intermolecular interactions between the CNCs. Furthermore, SAXS/WAXS analysis supports this with a distinct difference in the relationship between the apparent crystallinity index and packing density of the CNCs, depending on whether they are amphiphilic or hydrophobic (Fig. 1). Finally, for the hydrophobic CNCs, an increase in the apparent packing density, as determined by SAXS/WAXS, leads to a decrease in the quantum yield. This indicates that within this region, the effective number of fluorescent sources, namely the number of CNCs per unit volume, determines the quantum yield rather than any changes in intermolecular interactions due to the increasing concentration of the ammonium cation.

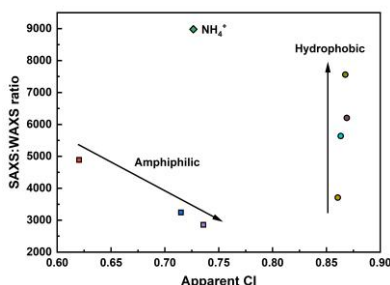


**Figure 1.** Relationships between apparent packing density (SAXS/WAXS ratio) and apparent crystallinity index.

## References

1. Johns et al., *Nanoscale*, **2022**, 14:16883.
2. Johns et al., *Cellulose*, **2023**, 30:8259.
3. Johns et al., *Analyst*, **2024**, 149:4747.
4. Stephens et al. *Proc. Nat. Acad. Sci.*, **2021**, 118:e2020389118.

# Structural Changes in NiFeCoCuMn Layered Double Hydroxides During Oxygen Evolution, Followed *Operando* with Simultaneous Diffraction, Total Scattering and X-ray Absorption

Melissa J. Marks, Ida K. Mønge, Rebecca K. Pittkowski  
Department of Chemistry, University of Copenhagen  
Universitetsparken 5, 2100 Copenhagen Ø, Denmark  
mjm@chem.ku.dk

Transition metal layered double hydroxides (LDHs) (Figure 1) are emerging as promising electrocatalysts for the oxygen evolution reaction (OER) in alkaline conditions, with NiFe and CoFe LDHs among the most active OER catalysts comprised of earth-abundant elements. Under oxidative conditions, these LDHs undergo a reversible structural transition from the synthesized  $\alpha$ -phase to the catalytically-active  $\gamma$ -phase, involving contraction of the interlayer spacing and exchange of intercalated ions between the layers.<sup>1</sup> Irreversible structural changes including increased stacking disorder and a breakdown of the in-plane LDH sheets have also been reported during operation.<sup>2</sup> These fundamental structure-property insights on catalytically-active species and stability are enabled only by *operando* studies, where the structural evolution of the OER-active catalyst is studied under an applied potential. The present *operando* study utilizes a home-built setup<sup>3</sup> to track the structural changes in LDHs comprising up to five transition metals (Ni, Fe, Co, Cu, and Mn) during OER, via simultaneous X-ray diffraction (XRD), total scattering (TS) and subsequent pair distribution function (PDF) analysis, and X-ray absorption spectroscopy (XAS). This combination of techniques facilitates simultaneous examination of the evolution in long-range structure (e.g. interlayer spacing), local atomic arrangement (e.g. atomic-level disorder and sizing of the LDH sheets) and oxidation state of the active OER catalyst, which can aid in uncovering the active metal sites. Our results demonstrate the high OER activity of the novel LDH structure incorporating 5 elements, and highlights the complex structural transitions which occur simultaneously with oxidization of the active metal(s) during operation.

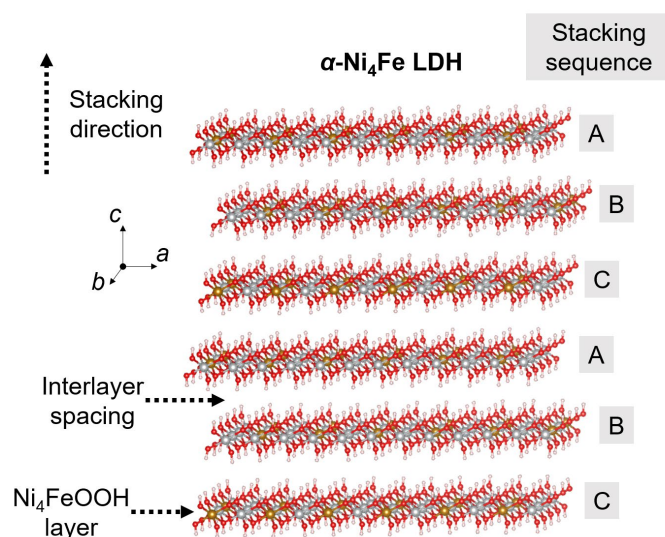


**Figure 1.** Crystal structure of  $\alpha$ -Ni<sub>4</sub>Fe LDH, highlighting the layer stacking sequence and direction. Ni, Fe, O and H atoms are shown in grey, brown, red and white, respectively. The intercalated ions between the Ni<sub>4</sub>FeOOH layers have been omitted for clarity.

- (1) Dionigi, F. et al., *Nature Comms* **2020**, 11 (1).
- (2) Aalling-Frederiksen, et al., *Small* **2025**.
- (3) Wiberg, G. K. H. et al., *Chimia* **2024**, 78 (5), 344-348.

## **MicroMAX – a beamline with time-resolved macromolecular crystallography capabilities at the MAX IV Laboratory**

M. Bjelčić, D. Lang, O. Aurelius, M. Milas, M. Chenchiliyan, C.M. Casadei, J. Nan, I. Gorgisyan, S. Aggarwal, A. E. Jagudin, M. Eguiraun, A. Nardella, A. Gonzalez, M. Malmgren, E. Panepucci, and T. Ursby

MAX IV Laboratory, Lund University, Fotongatan 2, 224 84 Lund, Sweden

The rise of 4<sup>th</sup> generation sources, including the MAX IV Laboratory 3 GeV ring, has enabled new possibilities to study dynamics using crystallography. The MicroMAX beamline is focussed on providing optimal X-ray characteristics for serial and time-resolved crystallography. The beamline offers a flexible sample environment for bespoke experimental setups and also supports high-throughput single crystal data collections.

MicroMAX recently started user operations and has performed experiments with SPINE-based fixed targets, flow injectors (high viscosity extrusion, capillary), and customized microfluidics mounted to an MD3-up diffractometer. Time-resolved SSX measurements have also been performed using a nanosecond pump laser (210-2600 nm). An X-ray chopper (0,8-70% duty cycle) in conjunction with a Jungfrau 9M Si integrating hybrid pixel detector (on-loan from PSI) also enables 2 kHz data collections at 10  $\mu$ s resolution. Standard collections are also enabled by an Eiger2 X 9M CdTe photon counting hybrid pixel detector, with automatic changes between both detectors in under a minute. The end station is also equipped with an automatic sample changer (ISARA2) that can be used in cryogenic conditions housing up to 29 unipucks but can also exchange crystallisation plates and room-temperature spine-based sample holders. Experiments are controlled by MXCuBE with ISPyB and automated analysis in CrystFEL.

The second experimental hutch at MicroMAX can be used for other activities while the first hutch is in X-ray operation. The second hutch is currently used as an off-line laser and spectroscopy laboratory for sample pre-characterization studies, but will also be used to support fully-customized user setups on a breadboard optical table

The beamline has two monochromators, a crystal monochromator giving a narrow bandwidth beam with up to  $10^{13}$  photons/s and a multilayer monochromator giving a wider bandwidth (up to 1%) with more than  $10^{14}$  photons/s. The X-ray beam is initially focused by beryllium X-ray lenses down to around 10  $\mu$ m, with further focussing using a K-B mirror system planned in 2026

MicroMAX has been funded by the Novo Nordisk Foundation grant number NNF17CC0030666.

# The Powder Diffraction and Total Scattering Beamline P02.1 at PETRA III, DESY

M. Etter<sup>1</sup>, V. Baran<sup>1</sup>, M. A. Karlsen<sup>1</sup>, A. Schökel<sup>1</sup>, T. Schoof<sup>1</sup>, M. Wendt<sup>1</sup> and S. Wenz<sup>1</sup>

<sup>1</sup>*Deutsches Elektronen-Synchrotron (DESY), Notkestraße 85, 22607 Hamburg, Germany*

*martin.etter@desy.de*

Powder Diffraction is a well-established method which allows to investigate long-range order structural properties of crystalline materials. On the other hand, Total Scattering measurements in combination with the Pair Distribution Function method is an expanding and powerful technique which allows to investigate the short-range and/or long-range order at the same time, making it possible not only to investigate crystalline materials, but also amorphous solids or liquids. Therefore, the combination of both methods provides a detailed insight into the structure of a wide range of material systems, including organic materials such as pharmaceuticals, co-crystals, covalent-organic frameworks, polymers and fibers, metal-organics such as metal-organic frameworks and inorganic materials such as nanoparticles, ceramics, cements, battery materials, metals and steels, metallic glasses, minerals and mineral glasses, superconductors, strongly (electron-)correlated materials, corrosion products, melts, liquids and so forth. For this huge range of crystalline and non-crystalline materials, structural properties, phase transitions or phase mixtures can be investigated at synchrotron facilities in *ex situ*, *in situ* or *in operando* experiments utilizing either beamline-offered or user-developed sample environments. With this widely covered range of material systems, Powder Diffraction and Total Scattering are extremely suited to investigate the state and consistency of all kinds of cultural heritage objects in a non-destructive way.

The Powder Diffraction and Total Scattering Beamline P02.1 at the PETRA III synchrotron at the DESY facility in Hamburg, Germany, is a specialized station, where researchers from science and industry have the possibility to collect Powder Diffraction and Total Scattering data simultaneously with a fixed energy of 60 keV [1, 2]. In recent years, the station has undergone major upgrades. For example, instead of using a single area detector, a custom-made tandem detector setup was installed, allowing users to measure simultaneously high-resolution Powder Diffraction data and Total Scattering / Pair Distribution Function data on the same sample or the same in situ process. Moreover, the old collimator tube was replaced by a flexible telescopic collimator tube allowing the last pin hole to get close to the sample or experiment. This suppresses the undesirable air scattering in front of the sample and therefore leads to a better data quality especially when Total Scattering data is collected. On the sample environment side, a new cryostat with a wide-opening angle was purchased, which will allow also to measure Total Scattering data down to temperature of 4 K. Currently this device is commissioned still under commission but will be available soon.

Besides regular on-site synchrotron experiments, users can also apply for mail-in / rapid access services for Powder Diffraction and/or Total Scattering / Pair Distribution Function measurements of samples packed in capillaries.

In this presentation, we will inform the scientific community as well as industrial customers about the latest developments at beamline P02.1.

[1] Dippel, A.-C., Bindzus, N., Saha, D., Delitz, J. T., Liermann, H.-P., Wahlberg, N., Becker, J., Bøjesen, E. D. & Iversen, B. B. (2014). *Z. Anorg. Allg. Chem.* **640**, 3094.

[2] Dippel, A.-C., Liermann, H.-P., Delitz, J. T., Walter, P., Schulte-Schrepping, H., Seeck, O. H. & Franz, H. (2015). *J. Synchrotron Radiat.* **22**, 675.

## Investigation of the synthesis and structure of CoNiGa spinels

The reduction of CO<sub>2</sub> to fuels is a promising approach to address the challenges of decoupling sectors such as aviation from fossil fuel, where battery based solutions are unsuitable due to their weight.

Cobalt (Co) and Nickel (Ni) have shown potential as catalyst for CO<sub>2</sub> reduction, however they tend to bind too strongly with CO, which limits their effectiveness. Incorporating gallium (Ga) can help mitigate this issue by weakening the CO binding strength to the entire catalyst.

In this project, we aim to synthesize and characterize CoNiGa oxides, specifically with the spinel structure as this will promote mixing of the transition metals and Ga. These materials can be reduced either electrochemically in situ or via a reducing atmosphere in order to obtain the alloy, which is the most promising for catalysis.

A solvothermal synthesis approach was employed to prepare the CoNiGa spinels due to the simplicity and scalability of this approach. Screening different solvents and metal ratios revealed that phase-pure spinels containing all three metals could be synthesized using dimethylformamide (DMF) as a solvent and a 1:1:4 metal ratio (Co:Ni:Ga). Subsequent annealing led to an increase in particle size.

To explore the broader applicability of this synthesis method, binary CoGa and NiGa spinels were also prepared using the same conditions. These systems also adopted the spinel structure, confirming the versatility of the synthesis route.

Total X-ray scattering, coupled with pair distribution function (PDF) analysis, was used to investigate the local structure of the nanosized spinel particles. Future work will involve in-situ total scattering measurements during annealing to monitor structural evolution and particle growth, enabling a deeper understanding of how these processes influence local atomic arrangements in CoGa, NiGa, and CoNiGa systems.



# Decoupling Dopant Effects on Air Stability and Structural Evolution During Cycling in Layered Na<sup>+</sup>-ion Batteries

Nathalie H. Richter-Mikkelsen<sup>a</sup>, Kirsten M. Ø. Jensen<sup>a</sup>, Søren Dahl<sup>b</sup>, and Lars F. Lundegaard<sup>b</sup>

<sup>a</sup>Department of Chemistry, University of Copenhagen, and <sup>b</sup>Topsoe A/S

E-mail: natharich@gmail.com

With the growing demand for sustainable energy storage, sodium-ion batteries (SIBs) have emerged as a viable alternative to lithium-ion batteries due to the abundance and low cost of sodium. Among SIBs, layered Na<sup>+</sup>-ion transition metal oxides, O3-Na<sub>x</sub>MO<sub>2</sub>, are promising cathode materials because of their tunable composition and high sodium content.<sup>1</sup> However, their application is limited by air sensitivity and structural degradation during cycling. This study systematically introduces dopants into the transition metal (TM) layer to improve air stability, enhance electrochemical performance, and reduce structural changes during cycling.<sup>2</sup> A series of O3-Na<sub>x</sub>MO<sub>2</sub> samples were synthesized via a solid-state approach, where Ni, Mn, and Fe were included in all samples, while Ti, Zn, and Li systematically were added. Air stability was assessed using *ex situ* PXRD and thermogravimetric analysis (TGA) coupled with DSC and MS. The NMF-TLZ sample, containing all six metals in the TM layer, exhibited the highest air stability, with Ti identified as the key stabilizing factor. Structural changes during cycling were examined using *operando* PXRD, where the NMF-TLZ sample displayed highly reversible O3→P3→High-V→P3→O3 phase transitions, while the NMF sample showed significant irreversibility, with the High-V phase diminishing after the first cycle. While the O3→P3 phase transition is well-documented in the literature, the mechanisms governing phase transitions at high voltage remain poorly understood.<sup>3</sup> To investigate the high-voltage phase, two structural models were applied: the Stacking-Faulted Model and the Monoclinic Model. While the Stacking-Faulted Model captured some features, the Monoclinic Model successfully tracked structural changes across all cycles by allowing a gradual glide in the ab-plane. These findings highlight the importance of TM-layer composition and structural modeling in improving the stability and performance of O3-Na<sub>x</sub>MO<sub>2</sub> cathodes.

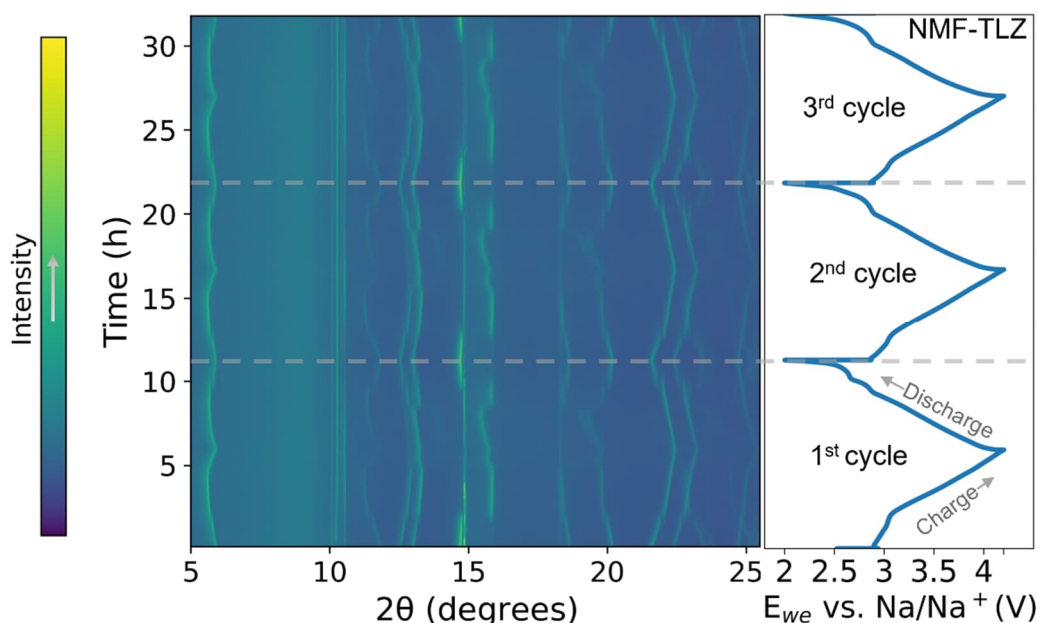


Figure 1: *Operando* PXRD data of the NMF-TLZ sample. Left: Contour plot of  $2\theta$  as a function of time with intensity scale seen in the color bar to the left. Right: Voltage ( $E_{we}$  vs. Na/Na<sup>+</sup>) as a function of time in the range [2.0–4.2]V.

- (1) Zhang, H.; Wang, L.; Zuo, P. J. *Mater. Chem. A* **2024**, 12, 30971–31003
- (2) Yang, Y.; Wang, Z.; Du, C.; Wang, B.; Li, X.; Wu, S.; et al. *Science* **2024**, 385 (6710), 744–752.
- (3) Li, X.; Fan, Y.; Johannessen, B.; Xu, X.; See, K. W.; Pang, W. K. *Batteries Supercaps* **2024**, 75

# Using MC simulations to compute neutron time-of-flight at ESS

## Abstract:

The long ESS pulse presents challenges when it comes to computing the time-of-flight (and hence wavelength) of neutron events recorded by the instruments.

Two neutrons with significantly different wavelengths, originating from different parts of the pulse, can end up hitting the detector at the exact same time.

The problem cannot be resolved at the detector, as according to the difference between time recorded at the detector and the measured start of the source pulse, both neutrons have the same wavelength.

This is the main reason why pulse-shaping and wavelength-frame multiplication choppers will be widely used at ESS.

This poster will take the reader through the different strategies that were developed over the past years by ESS's Data Management and Software Centre to compute accurate neutron time-of-flight from pulse-shaped neutron events.

We will show how and why we have finally settled on making use of Monte-Carlo simulations, such as McStas, to obtain the best possible results.

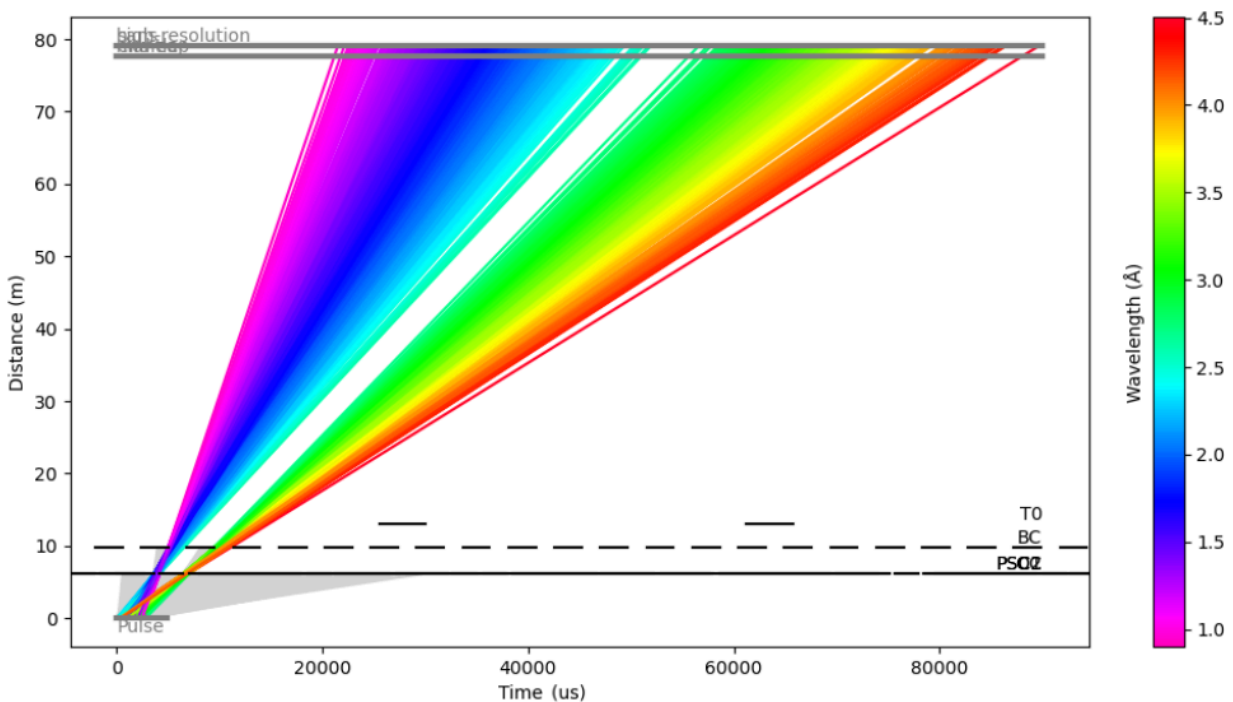


Figure: Time-distance diagram for the DREAM instrument (ESS) chopper cascade with a pulse of neutrons traveling through it.

# One-step synthesis of anatase TiO<sub>2</sub> nanoparticles using a non-mixing continuous flow solvothermal reactor

*Nikolaos Antonios Iakynthos Nemet,<sup>a</sup> Andreas Dueholm Bertelsen,<sup>a</sup> Magnus Kløve,<sup>a</sup> Aref Hasen Mamakhel,<sup>a</sup> and Bo Brummerstedt Iversen<sup>a</sup>*

<sup>a</sup> Center for Integrated Materials Research, Department of Chemistry, Interdisciplinary Nanoscience Center (iNANO), Aarhus University, Langelandsgade 140, 8000 Aarhus C, Denmark.

## Abstract

A non-mixing solvothermal flow reactor has been designed and commissioned to allow for precise control of residence time during synthesis of crystalline nanoparticles. Benchmarking of the reactor was performed against a conventional T-mixing flow reactor at 200 °C, 250 °C, 300 °C, and 350 °C (P = 250 bar) by synthesizing phase-pure anatase TiO<sub>2</sub> nanoparticles from an industrial-grade TiOSO<sub>4</sub> precursor. Characterization was carried out using PXRD, TEM, UV-VIS, and Raman spectroscopy revealing highly anisotropic particles with constant crystallite sizes of ~10 nm in the (100) basal plane and decreasing sizes along the [001] direction with increasing temperatures (from ~19 nm to ~14 nm). A residence time study, using the non-mixing reactor, confirmed that the crystallite size in the (100) plane is invariant to temperature (250-350 °C), residence time, and reactor design. At 350 °C, the crystallite size along [001] was stable at 14 nm, while at 250 °C, larger nanoparticles (16-19 nm) formed with increasing residence time. This study highlights the new reactor's capability for controlled synthesis of anisotropic anatase nanoparticles, and its easy optimization of synthesis parameters.

## Cation Transport Mechanisms across Nafion and Sustainion in MEA Electrolyzers: An In-situ X-Ray Fluorescence Spectroscopy Investigation

The role of large alkali metal cations in improving  $C_2^+$  product selectivity during  $CO_2$  electrolysis on Cu catalyst is well documented.<sup>1–4</sup> In membrane electrode assembly (MEA) electrolyzers, these cations are transported from the anolyte to the cathode surface via ion exchange membranes. The efficiency and durability of MEA electrolyzers are intricately linked to the type of membrane used, as cation transport directly influences water management, which in turn, affects long-term system stability. Essential membrane attributes, such as cationic head group composition, ion exchange capacity, and water uptake, and other dynamic parameters such as membrane resting potential, and Donnan potential determine the transport mechanisms of these cations during electrolysis. Optimizing these characteristics is vital for preventing gas diffusion electrode (GDE) flooding and facilitating efficient cation transport. This investigation evaluates the transport behavior of  $Cs^+$  (used as a model cation) across two commercial ion exchange membranes namely Sustainion (anion exchange membrane) and Nafion (cation exchange membrane), applying advanced in-situ methodologies to observe dynamic changes throughout the electrolysis process. Through the combined use of Wide-Angle X-ray Scattering (WAXS) for monitoring structural changes in electrolyzer components and water distribution, alongside X-ray Fluorescence (XRF) spectroscopy for dynamic tracking of cations, this study offers a comprehensive analysis of the interplay between cations and water during operation. The results demonstrate substantial differences in cation transport and water dynamics contingent on the membrane type, where the interaction between Donnan potential and solvation shell dynamics emerges as a critical determinant of electrochemical stability. Structural and compositional disparities between membranes strongly influence these mechanisms, providing deeper insights into achieving enhanced performance. The mechanistic insights derived from this study offer a deeper understanding of cation transport dynamics within MEA electrolyzers during electrolysis, emphasizing the critical role of ion-selective and structurally robust membranes in achieving enhanced efficiency and durability.

### References

- (1) Montoya, J. H.; Peterson, A. A.; Nørskov, J. K. Insights into C-C Coupling in  $CO_2$  Electroreduction on Copper Electrodes. *ChemCatChem* 2013, 5 (3), 737–742. <https://doi.org/10.1002/cctc.201200564>.
- (2) Garg, S.; Xu, Q.; Moss, A. B.; Mirolo, M.; Deng, W.; Chorkendorff, I.; Drnec, J.; Seger, B. How Alkali Cations Affect Salt Precipitation and  $CO_2$  Electrolysis Performance in Membrane Electrode Assembly Electrolyzers. *Energy Environ Sci* 2023, 16 (4), 1631–1643. <https://doi.org/10.1039/d2ee03725d>.
- (3) Montoya, J. H.; Shi, C.; Chan, K.; Nørskov, J. K. Theoretical Insights into a CO Dimerization Mechanism in  $CO_2$  Electroreduction. *Journal of Physical Chemistry Letters* 2015, 6 (11), 2032–2037. <https://doi.org/10.1021/acs.jpcllett.5b00722>.

- (4) Resasco, J.; Chen, L. D.; Clark, E.; Tsai, C.; Hahn, C.; Jaramillo, T. F.; Chan, K.; Bell, A. T. Promoter Effects of Alkali Metal Cations on the Electrochemical Reduction of Carbon Dioxide. *J Am Chem Soc* 2017, 139 (32), 11277–11287. <https://doi.org/10.1021/jacs.7b06765>.

# Phase evolution and magnetic performance of SrFe<sub>12</sub>O<sub>19</sub> from anisotropic precursors

P N Subrahmanian<sup>1</sup>, J Simonsen<sup>1</sup>, M I Mørch<sup>2</sup>, M Christensen<sup>1\*</sup>

<sup>1</sup>Aarhus University, Aarhus University Institute of Chemistry, Langelandsgade 140, 8000 Aarhus C, Denmark

<sup>2</sup>Patent og Varemærkestyrelsen, Helgeshøj Alle 81, 2630 Taastrup, Denmark

\*mch@chem.au.dk

Permanent magnets (PMs) play a pivotal role in the green transition and it revolutionized various industries and many aspects of our daily lives. The strength of a permanent magnet is significantly influenced by remanent magnetization, which in turn is tuned by crystallite orientation. Previous studies have demonstrated that SrFe<sub>12</sub>O<sub>19</sub> crystallites can be oriented without external magnetic field by leveraging precursor anisotropy [1,2]. To probe the effect of precursor morphology and size on magnetic performance of SrFe<sub>12</sub>O<sub>19</sub> pellets, hexaferrite was synthesised by a solid-state method, using  $\alpha$ -FeOOH (goethite) precursors of differing size. A series of sintering experiments were carried out by varying the sintering temperature of cold-compacted pellets of precursor mixtures. The phase evolution of hexaferrite was determined by quantitative analysis of temperature-dependent in-situ synchrotron powder X-ray diffraction (PXRD) studies on cold-compacted pellets, which was consistent with previous reports [3]. The structural investigation of ex-situ PXRD of sintered pellets indicate that  $\alpha$ -FeOOH precursor size and morphology significantly improve the final hexaferrite crystallite alignment.

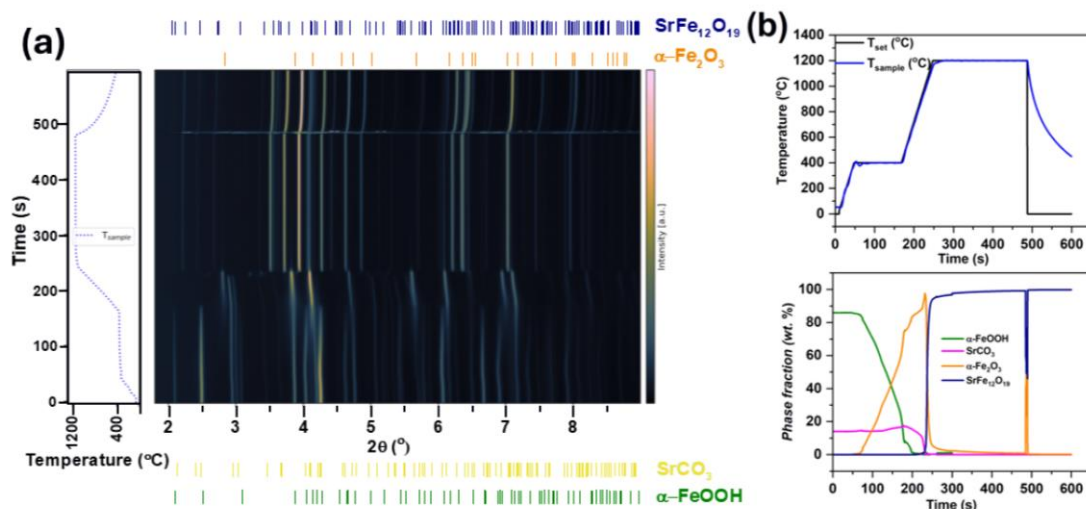


**Figure 1.** (a) The observed TRDP for G 420 - SrCO<sub>3</sub> precursor mix cold-compacted and sintered at 1150°C with increasing experiment time along the y-axis. The Bragg diffraction positions of identified phases are given above and below. (b) Weight percentages of goethite (green),  $\alpha$ -Fe<sub>2</sub>O<sub>3</sub> (Orange), SrFe<sub>12</sub>O<sub>19</sub> (blue) and SrCO<sub>3</sub> (magenta) along with temperature ramp of the experiment in the lower panel.

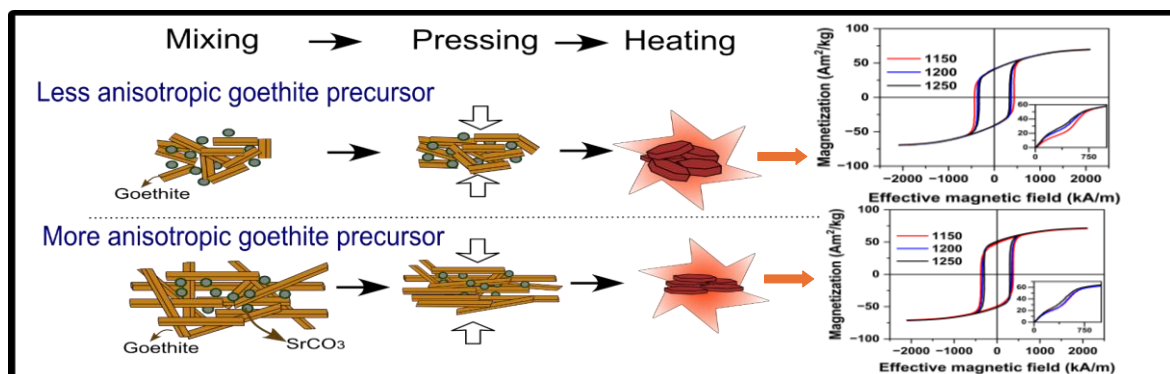


**Figure 2.** Overview of the preparation of SrFe<sub>12</sub>O<sub>19</sub> using two differently sized goethite precursors and corresponding magnetic properties of hexaferrite pellets sintered at various temperatures

The hexaferrites from more anisotropic  $\alpha$ -FeOOH displayed superior magnetic properties compared to less anisotropic precursors, which is corroborating the results on crystallite orientation from PXRD data. This work indicates the optimization of precursor morphology and dimensions could play a crucial role in achieving better alignment and magnetic properties in the final hexaferrite pellets.

#### **Acknowledgment**

We acknowledge European Commission for the project funding (Project BEETHOVEN). BEETHOVEN project funded by the European Commission under grant agreement 101129912. Views and opinions expressed herein are however those of the author(s) only and do not necessarily reflect those of the European Union or the European Education and Culture Executive Agency (EACEA). Neither the European Union nor EACEA can be held responsible for them. We also acknowledge DESY, a member of the Helmholtz Association HGF, for time on Beamline PETRA III and DanScatt for providing funding for beamline expenses. Authors would also like to acknowledge funding for the scanning electron microscope from the Carlsberg Foundation and iMAT.

#### **References**

- [1] Thomas-Hunt, J.; Povlsen, A.; Vijayan, H.; Knudsen, C. G.; Gjørup, F. H.; Christensen, M. *Dalt. Trans.* **2022**, *51*, 3884–3893.
- [2] Mørch, M. I.; Thomas-Hunt, J.; Laursen, A. P.; Simonsen, J.; Frandsen, J. P.; Vijayan, H.; Christensen, M. *Chem. Mater.* **2024**, *36*, 1919–1927.
- [3] Laursen, A. P.; Frandsen, J. P.; Shyam, P.; Mørch, M. I.; Gjørup, F. H.; Vijayan, H.; Jørgensen, M. R. V.; Christensen, M. *Adv. Electron. Mater.* **2024**, *2400077*, 1–9.

## Abstract for DanScatt Annual Meeting 2025 (Poster)

**Peter Skjøtt Thorup, Postdoc, Aarhus University**

**Title: Structural origins of ultra-low glass-like thermal conductivity in  $\text{AgGaGe}_3\text{Se}_8$**

Peter Skjøtt Thorup<sup>1</sup>, Rasmus Baden Stubkjær<sup>1</sup>, Kim-Khuong Huynh<sup>1</sup>, Pavankumar Ventrapati<sup>1,2</sup>, Emilie Skytte Vosegaard<sup>1</sup>, Anders Bæk Borup<sup>1</sup>, and Bo Brummerstedt Iversen<sup>1,\*</sup>

<sup>1</sup> Center for Integrated Materials Research, Department of Chemistry and iNANO, Aarhus University, DK-8000 Aarhus, Denmark

<sup>2</sup> Department of Chemistry, SRM University Amaravati-AP, Mangalagiri 522240 Andhra Pradesh, India

Conduction of heat through a material is a fundamental physical property, and understanding the underlying mechanisms that govern heat transport, and relate them to structural features, remain a central goal within material science. Materials that exhibit low thermal conductivity are important for a variety of applications such as thermoelectrics and thermal barrier coatings. Here, we present the remarkable low thermal conductivity observed in the quaternary silver chalcogenide  $\text{AgGaGe}_3\text{Se}_8$ , which exhibit unusual glass-like thermal behavior from 2 K to 700 K with a thermal conductivity value of only  $0.2 \text{ Wm}^{-1}\text{K}^{-1}$  at room temperature. We relate this to a disordered nature of Ag in the structure, where the Ag atoms display extremely large atomic displacement parameters from multi-temperature synchrotron powder X-ray scattering experiments, and Ag ionic conductivity at elevated temperatures. Signs of structural anharmonicity and soft bonding are evident from a low temperature Boson peak in the heat capacity and a low Debye temperature of 158 K. From these findings, we link the low thermal conductivity in  $\text{AgGaGe}_3\text{Se}_8$  to highly disordered Ag sites within the otherwise static  $\text{GaGe}_3\text{Se}_8$  framework that inhibits the propagation of heat conductive phonons. [1]

[1] Peter S. Thorup et al., *Science Advances*, **2025**, Accepted



## Ellipsoidal mineral aggregations, and the mineralization of narwhal tusk

P. A. S. Vibe<sup>1</sup>, A. R. Palomo<sup>1</sup>, A. M. M. Faaborg<sup>1</sup>, M. Østergaard<sup>1</sup>, A. Sadetskaia<sup>1</sup>, T. E. K. Christensen<sup>2</sup>, H. Birkedal<sup>1</sup>

<sup>1</sup>*Dept. of Chemistry and iNANO, Aarhus University, Aarhus, Denmark, <sup>2</sup>MAX IV, Lund, Sweden*

The immense spiralling tusk of the narwhal is an impressive feat of biomineralization due to its chirality, mechanically resilience and size. The tusk consists of the same nanoscale building blocks as bone and tooth, namely hydroxyapatite nanocrystals as the hard mineral part and collagen fibres as the soft part, the combination of which makes for a strong and crack resistant composite material. These building blocks are structured into dentine at the centre of the tusk that encloses a pulp chamber. Surrounding the dentine is a layer of cementum, composed of the same nanoscale building blocks but with a remarkably different structure. Thin and long dentinal tubules stretch throughout the dentin part of tusk, from the pulp chamber to the junction between cementum and dentin, whereas cementum instead contains cementocytes. In the dentin, growth layer groups can be observed as a result of annual growth the tusk.

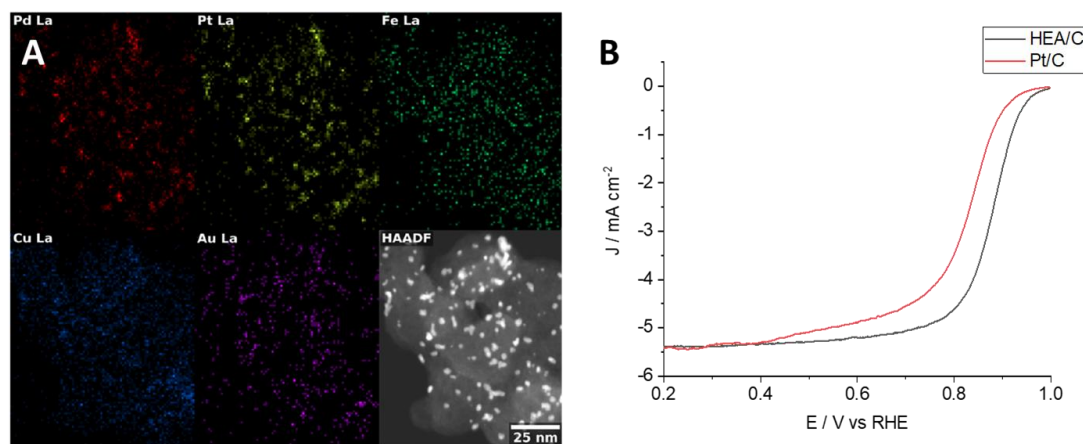
To study the growth and structure of the dentine layer of narwhal tusk. 35 radial square rods of tusk, cut with sides of 1 mm by 1 mm, spanning from the pulp chamber to outer cementum, were imaged with the computed tomography (CT) setup at DanMAX, MAX IV, at 30 keV. This resulted in high-quality CT volumes with voxel sizes of 275 nm. The tusk rods were cut from two different sections of the tusk, one close to the skull and the other close to the tip, corresponding to two vastly different tusk diameters and therefore relative curvature. Where the sample close to the tip is subjected to a much stronger curvature than close to the skull. These CT-volumes revealed a structured aggregation of the mineralization in dentin, into ellipsoidal aggregates. The size of the ellipsoidal aggregates increases as a function of distance from the cementum-dentin junction. To quantify this increase and to examine the relevance of local curvature, the dentin part of the CT volumes was segmented using watershed algorithms. The full data treatment is still underway, but preliminary results are promising. Revealing a steady increase, from the cementum-dentin junction to the pulp chamber, in aggregate volume from about 415  $\mu\text{m}^3$  to 1040  $\mu\text{m}^3$ . Fully completing the data treatment will be an important step towards a mechanistic understanding of the curious biomineralization of the narwhal tusk and will possibly prove the method to be valuable for similar tissues.

# Durable and Active High-Entropy Alloy Nanoparticles for Alkaline Oxygen Reduction Reaction

Péter Gyenes, Ida Kær Mønge, Jan Rossmeisl, Rebecca Katharina Pittkowski  
University of Copenhagen  
Universitetsparken 5, 2100 København, Denmark  
pg@chem.ku.dk

The oxygen reduction reaction (ORR) is a crucial electrode reaction for energy storage and conversion devices based on oxygen electrocatalysis. However, the electrochemical oxygen reduction reaction (ORR) remains the major bottleneck in fuel cells. Considering the importance of this reaction and the research effort devoted to developing more active ORR catalysts, platinum and platinum cobalt remain the state-of-art ORR catalyst.

This materials discovery challenge might be overcome when exploring the phase space available for high-entropy alloys (HEA). These alloys are made up of five or more elements in roughly equimolar ratios.[1] HEAs have unique properties as they allow e.g. fine-tuning of the binding energies of adsorbates by changing the composition.[2] This is useful for achieving higher catalyst activities according to the Sabatier principle. [3] Tuning the composition can also enhance the durability of the catalyst. The number of possible alloys in the HEA composition space of five elements is huge, even when using large increments in composition. Instead of trial-and-error catalyst testing, targeted catalyst design by computational methods is preferred, to gain a deep understanding of the relation of the composition and the properties of the catalyst. Operando XANES measurements can determine the oxidation state and the local coordination environment and thus contribute to understanding the catalytic sites and degradation mechanisms. With this fundamental understanding, we might find catalysts that are more active, more durable or more cost-effective than the current state-of-art. Au-Cu-Fe-Pd-Pt were chosen as the five elements for the HEA (Fig. 1 A). Small nanoparticles of the alloys dispersed on carbon support (HEA/C) were produced in a green synthesis using ascorbic acid as a reducing agent. The synthesis allows to vary the Au content of the HEAs. Some of the prepared alloys showed both superior activity (Fig. 1 B) and durability in alkaline ORR



compared to commercial carbon supported platinum (Pt/C).

Figure 1: (A) STEM-EDX of HEA/C. (B) Voltammogram of commercial Pt/C and HEA/C catalysts in rotating disk electrode setup at 1600 RPM after accelerated degradation protocol. [4] The electrolyte is 0.1 M KOH solution saturated with O<sub>2</sub>.

## References:

- [1] J.-W. Yeh et al., *Adv. Eng. Mater.* **6** (2004), 299.
- [2] T. Löffler et al., *Angew. Chem. Int. Ed.* **60** (2021), 26894.
- [3] T. A. A. Batchelor et al. *Joule* **3** (2019), 834-845.
- [4] E. Pizzutilo et al. *J. Electrochem. Soc.* **163** (2016): F1510.

## **DanScatt Abstract**

Hydrogen is projected to play a pivotal role in the transition toward a more sustainable future, particularly by decarbonizing sectors such as heavy industry and transportation. However, current hydrogen production is predominantly led by fossil fuel and coal-based methods resulting in significant carbon emissions. Alkaline Water Electrolysis (AWE) offers a promising low-emission alternative capable of producing high-purity hydrogen. Despite its potential, AWE faces challenges in terms of energy efficiency, durability and cost-effectiveness which can be mitigated by the development of high-performance, low-cost electrode materials. To optimize AWE performance, it is necessary to understand electrocatalyst behavior during operational conditions. In situ and operando X-ray techniques on Synchrotron facilities offer such opportunities to monitor catalyst surface structural phases during operation. Due to the limitations of X-ray analysis techniques, AWE cells must be specifically designed to facilitate the experiments conducted. Knowledge regarding electrochemistry, materials, heat transfer, flow regimes and pumps are vital for the creation of a representative AWE operando cell for surface analysis.

# Multi-Contrast Imaging of Industrial Catalyst Pellets

Rohde, Rasmus<sup>1</sup>, Gjørup, Frederik H.<sup>2,3</sup>, Lauritsen, Jeppe V.<sup>1</sup>, Bøjesen, Espen D.<sup>1</sup>

1) Interdisciplinary Nanoscience Center & Aarhus University Centre for Integrated Materials Research, Aarhus University, Denmark

2) Department of Chemistry and Interdisciplinary Nanoscience Center (iNANO), Aarhus University, Langelandsgade 140, 8000 Aarhus C, Denmark,

3) MAX IV Laboratory, Lund University, Fotongatan 2, 224 84 Lund, Sweden

Catalysts are essential in facilitating many chemical reactions important to our society such as the Haber-Bosch process, reducing NO<sub>x</sub> gases, or hydroprocessing of fuels. Many heterogenous catalysts consist of catalytically activate particles dispersed on a pellet of porous support material. However, often catalysts are studied either at the reactor level or as crushed powders. With the combination of DanMAX's scattering and imaging facilities, single pellets can be characterized spatially to map out the pellet structure, porosity, crystallographic phases and distribution of certain elements.

Ni-promoted MoS<sub>2</sub> nanoparticles on  $\gamma$ -Al<sub>2</sub>O<sub>3</sub> is an industrially available catalyst being studied for its hydroprocessing capabilities. It has shown promising results in the removal of oxygen from pyrolysis oils derived from biomass waste through hydrodeoxygenation. Unfortunately, it also suffers from low stability, in part due to oxygen being released as water as a byproduct of the reaction. The degradation of the catalyst pellet happens both through a decrease in porosity and a change in the crystallographic phases. With X-ray absorption and diffraction computed tomography ( $\mu$ -CT and XRD-CT), these changes can be imaged at DanMAX by studying pellets exposed to water at 200°C for varying times.

$\mu$ -CT provided 3D images of the pellets from which the pore sizes can be quantified. Furthermore, imaging done with a beam energy above and below the Mo absorption edge showed that Mo was more present towards the surface of the pellet.  $\gamma$ -Al<sub>2</sub>O<sub>3</sub> pellets without catalyst were shown with XRD-CT to degrade uniformly into the hydrated parent structure, boehmite, because of water exposure. Interestingly, this transformation is not seen for pellets with MoS<sub>2</sub>. However, the underlying  $\gamma$ -Al<sub>2</sub>O<sub>3</sub> is found to turn into a sulfate-containing alunogen phase with a nickelalumite structure emerging in the center of the pellet. These insights can not only guide further catalyst pellet development, but also showcase the high potential of combining  $\mu$ -CT and XRD-CT for catalyst pellet characterization.

# Studying Extended-Range Order using Pair-Angle Distribution Functions

Rebekka Klemmt,<sup>a</sup> Alan Salek,<sup>b</sup> Martin A. Karlsen,<sup>c</sup> Dorthe B. Ravnsbæk,<sup>d</sup> Andrew V. Martin,<sup>b</sup> Espen D. Bøjesen<sup>a</sup>

<sup>a</sup>Interdisciplinary Nanoscience Centre and Aarhus University Centre for Integrated Materials Research, Aarhus University, Denmark, <sup>b</sup>School of Science, RMIT University, Melbourne, Victoria, Australia, <sup>c</sup>P02.1 Beamline, PETRA III, Deutsches Elektronen-Synchrotron DESY, Hamburg, Germany, <sup>d</sup>Center for integrated Materials Research, Department of Chemistry, Aarhus University, Denmark.

The lack of long-range order challenges the important characterization of the extended-range order of disordered materials with conventional crystallographic methods based on diffraction. Alternative methods have to be used for investigating disordered materials. A well-established example is the use of pair distribution function (PDF) analysis which provides crucial information on average interatomic distances. Although PDF is a valuable tool to study the structure of disordered materials, it has the limitation that meaningfully different structural models might result in identical PDFs, as angular arrangements between atom pairs are only described indirectly [1]. Hence, advanced methods are needed which are able to describe the angular arrangements in the extended-range order of disordered materials.

A method which has this ability is the pair-angle distribution function (PADF) analysis [2]. It characterizes the atomic structure in terms of two atomic pair distances ( $r$ ,  $r'$ ) and the angle ( $\theta$ ) of three-atom and four-atom pairs. PADF is a method still in its infancy and has mainly been used to characterize the short-range order of materials. With our work, we explore the possibilities of using PADF for elucidating the extended-range order of disordered materials at the example of highly sp<sup>2</sup>-hybridized disordered carbons. In the case of disordered carbon, the information-rich PADF can be used to separately study the disorder within and in between graphite-like layers, which is not possible in comparable ways using PDF analysis. The PADF analysis approach will contribute to an enhanced understanding of the structure of disordered carbons and other layered disordered materials.

[1] Maffettone, P. M., Fletcher, W. J. K., Nicholas, T. C., Deringer, V. L., Allison, J. R., Smith, L. J., & Goodwin, A. L. (2025). When can we trust structural models derived from pair distribution function measurements? *Faraday Discuss.*, 255(0), 311-324.

[2] Martin, A. V. (2017). Orientational order of liquids and glasses via fluctuation diffraction. *IUCrJ*, 4(Pt 1), 24-36.

# Multiscale tomography of an entire sea star ossicle with extreme resolution (Xtreme-CT)

**Richard T. Deyhle Jr.**<sup>1</sup>, Adrian Rodriguez-Palomo<sup>1</sup>, Nis C. Gellert<sup>7</sup>, August L. Høeg<sup>3</sup>, Emma L. Thomson<sup>2</sup>, Thorbjørn E.K. Christensen<sup>3,4</sup>, Innokentiy Kantor<sup>4</sup>, Anders B. Dahl<sup>3</sup>, Tim Dyrby<sup>2,3</sup>, Martin Bech<sup>5,6</sup>, Rajmund Mokso<sup>7</sup>, Henning F. Poulsen<sup>7</sup>, Henrik Birkedal<sup>1</sup>

<sup>1</sup> Department of Chemistry and Interdisciplinary Nanoscience Center (iNANO), Aarhus University, Aarhus, Denmark

<sup>2</sup> Danish Researcher Centre for Magnetic Resonance (DRCMR), Amager and Hvidovre Hospital, Hvidovre, Denmark

<sup>3</sup> Department of Applied Mathematics and Computer Science (DTU Compute), Technical University of Denmark, Kongens Lyngby, Denmark

<sup>4</sup> DanMAX, MAX IV Laboratory, Lund, Sweden

<sup>5</sup> Department of Medical Radiation Physics, Lund University, Clinical Sciences Lund, Lund, Sweden

<sup>6</sup> LINXS Institute for Advanced X-ray and Neutron Science, Lund, Sweden

<sup>7</sup> Department of Physics, Technical University of Denmark, Kongens Lyngby, Denmark

Imaging the hierarchical structure of biomineralized tissue is challenging because it requires images over large volumes with high resolution. This often comes at the cost of losing the relationship between macrostructure and microstructure. Although these constraints have historically limited data collection, recent advances in photon flux and detector performance at 4th-generation synchrotrons — such as MAX IV — now make it possible to image larger 3D volumes (i.e. an expanded volumetric field of view (FOV)) at higher resolution in shorter times.

The Xtreme-CT project at the DanMAX beamline at MAX IV aims to enable multiscale 3D X-ray tomographic imaging. Its ambition is to achieve a voxel-to-image volume ratio of  $10^4$ – $10^5$ , offering significantly greater information density than traditional micro-CT approaches. Our custom-made detector supports a full array of  $14176 \times 10640$  pixels (~151 megapixels (Mpx)), enabling an FOV area exceeding  $0.70 \text{ cm}^2$ . Preliminary scans of dried starfish ossicles were acquired using a windowed region of  $13920 \times 10640$  pixels (~148 Mpx), for a FOV area of  $0.68 \text{ cm}^2$ . The ossicles have been reported to form a lattice with micron-scale ordered walls containing calcite crystals<sup>1</sup>.

The Xtreme-CT setup represents a substantial increase in both the volumetric field of view and the image matrix while maintaining sub-micron spatial resolution — allowing, for the first time, the unique microlattice patterns of an entire ossicle to be visualized in a single scan. The goal of this study is to assess the heterogeneity of microlattice alignment within a full ossicle, showcasing the capabilities of the new detector system at DanMAX.

1. Yang, Ting, et al. "A damage-tolerant, dual-scale, single-crystalline microlattice in the knobby starfish, *Protoreaster nodosus*." *Science* 375.6581 (2022): 647-652.

## Abstract Danscatt 2025 – Poster

**Title: The AUREX cell: a versatile *operando* electrochemical cell for studying catalytic materials using X-ray diffraction, total scattering and X-ray absorption spectroscopy under working conditions**

Authors: Sara Frank<sup>a</sup>, Marcel Ceccato<sup>a</sup> Henrik S. Jeppesen<sup>b</sup>, Melissa J. Marks<sup>a,c</sup>, Mads L. N. Nielsen<sup>c,d</sup>, Ronghui Lu<sup>c,d</sup>, Jens Jakob Gammelgaard<sup>c</sup>, Jonathan Quinson<sup>a</sup>, Ruchi Sharma<sup>a</sup>, Julie S. Jensen<sup>a</sup>, Sara Hjelme<sup>a</sup>, Cecilie Friberg Klysner<sup>c</sup>, Simon J. L. Billinge<sup>e</sup>, Justus Just<sup>f</sup>, Frederik H. Gjørup<sup>c,f,g</sup>, Jacopo Catalano<sup>a</sup>, and Nina Lock<sup>c,d</sup>

Affiliations: <sup>a</sup>Department of Biological and Chemical Engineering, Aarhus University, Åbogade 40, 8200 Aarhus N, Denmark, <sup>b</sup>Deutsches Elektronen-Synchrotron (DESY), Notkestrasse 85, 22607 Hamburg, Germany, <sup>c</sup>Interdisciplinary Nanoscience Center (iNANO), Aarhus University, Gustav Wieds Vej 14, 8000 Aarhus C, Denmark, <sup>d</sup>Carbon Dioxide Activation Center (CADIAC), Department of Biological and Chemical Engineering, Aarhus University, Åbogade 40, 8200 Aarhus N, Denmark, <sup>e</sup>Department of Applied Physics and Applied Mathematics, Columbia University, New York, NY 10027, USA, <sup>f</sup>MAX IV Laboratory, Lund University, Fotongatan 2, 221 00 Lund, Sweden, and <sup>g</sup>Department of Chemistry, Aarhus University, Langelandsgade, 8000 Aarhus, Denmark

Understanding how electrocatalysts behave under working conditions is essential to improving their performance and stability. We present the AUREX (Aarhus University Reactor for Electrochemical studies using X-rays) cell designed as an easy-to-use versatile setup with a minimal background contribution and a uniform flow field to limit concentration polarization and handle gas formation. To demonstrate its capabilities, we performed *operando* X-ray total scattering, diffraction, and absorption spectroscopy experiments on a commercial Ag electrocatalyst. These measurements capture short-, medium-, and long-range structural changes during electrochemical operation. Data analysis using non-negative matrix factorization, linear combination analysis, the Pearson correlation coefficient, and real/reciprocal space refinement revealed a reversible transformation pathway: under oxidative potential in Ar-saturated 0.1 M KHCO<sub>3</sub>/K<sub>2</sub>CO<sub>3</sub>, fcc Ag converts to trigonal and then monoclinic Ag<sub>2</sub>CO<sub>3</sub>, reverting to fcc Ag under reducing conditions.

This work demonstrates the importance of monitoring electrochemical phase transitions in real time and demonstrates the AUREX cell as a robust tool for studying the structure-property relationships of electrocatalysts. [1]

[1] S. Frank et al., *Journal of Applied Crystallography*, **2024**, 57, 1489-1502

# Key Points of Compound Semiconductor Material Evaluation by High resolution XRD

\*S. Ibrahimkutty,<sup>1</sup>

<sup>1</sup>Rigaku Europe SE, Hugenotten alle 167, 63263 Neu-Isenburg, Germany

\*E-mail: shyju.ibrahimkutty@rigaku.com

For the fabrication of microelectronics and optoelectronics devices the crystalline quality of semiconductor layers is a key factor. High resolution X-ray diffraction is a versatile and powerful tool for the characterization of compound semiconductor materials and devices. Quick and non-destructive characterization of thickness, composition, quality, orientation, Curvature, lattice strain, etc. are feasible by X-ray diffraction measurements.

This presentation will cover different XRD based approaches, the basic and sophisticated characterization of epitaxial layers by means of a Rigaku SmartLab diffractometer [1]. The thickness and composition of epitaxially grown layers are evaluated from high resolution 2theta-omega scans (Figure 1). Rocking curve measurements can be used for the determination of crystal quality, curvature, and offset angles of semiconductor layers [2]. Further, the possibility to extract the correct in-plane and out of plane lattice parameter and strain involved in the system by appropriate reciprocal space map (RSM) measurements will be shown. Figure 1 shows the high resolution XRD measured on GaN/InGaN multiple quantum well super lattice structure and the asymmetric RSM (01-15) (Figure 2) showing completely strained growth.

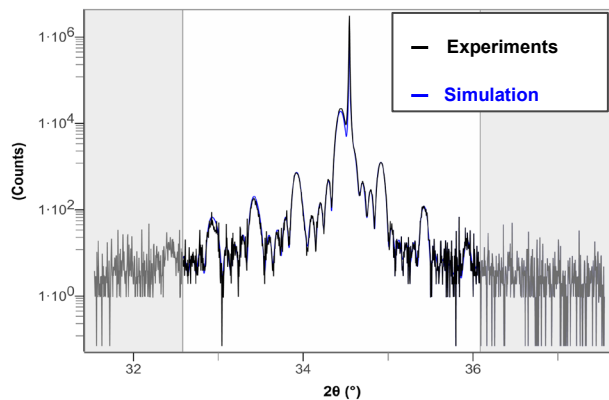


Fig 1: High resolution 2theta-Omega scan of GaN/InGaN MQW Super lattice.

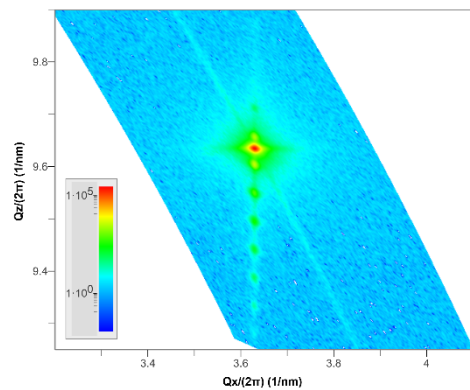


Fig 2: RSM measured at asymmetric (01-15) peak of GaN/InGaN MQW super-lattice.

[1] T. Konya, The Rigaku Journal 25 -2 (2009).

[2] S. Kobayashi, K. Inaba, The Rigaku Journal 28- 2 (2012).



## **Poster abstract - Signe Brummerstedt**

*Ravnsbæk Group, Aarhus University*

Understanding structural disorder in crystalline battery electrode materials and how this changes with battery cycling is essential to improve battery performance. To obtain structural insights with high accuracy, there is a desire to utilize single crystal scattering measurements. However, as single crystals are difficult to grow, and most batteries are based on powdered materials, not a lot of research is done on single crystal structures during electrochemical (dis)charging.

This study is a showcase using interesting sustainable materials, namely  $(\text{NH}_4)_2\text{Mo}_x\text{S}_y$  ( $x=1, 3, y=4, 13$ ), which has been investigated in literature in the powder state. As it is simple to grow single crystals of these materials, they are ideal to showcase the ideas behind elucidating structural changes and/or disorder in single crystal battery materials.

# Virtual Experiments on the BIFROST Spectrometer at ESS

*Kristine M. L. Krighaar<sup>1</sup>, **Silas Schack**<sup>1</sup>, Niels Bech Christensen<sup>2</sup>, Rasmus Toft-Petersen<sup>2,3</sup>, & Kim Lefmann<sup>1</sup>*

<sup>1</sup> Niels Bohr Institute, University of Copenhagen, Denmark.

<sup>2</sup> Technical University of Denmark, Lyngby, Denmark.

<sup>3</sup> European Spallation Source (ESS), Lund, Sweden.

The applicability of inelastic neutron scattering is limited by inherently weak signals. Mapping significant portions of  $(Q, \omega)$ -space can take days, making parametric studies as a function of temperature, pressure, and magnetic field essentially impossible. The triple-axis community has addressed this limitation by improving the efficiency of triple-axis spectrometers through the construction of multiplexing analyzer arrays, which cover large intervals of scattering angles in the horizontal plane. Examples include CAMEA (PSI) and MACS (NIST). In contrast, direct spectrometers provide large coverage but suffer from even lower flux.

BIFROST, currently under construction at ESS, employs a CAMEA-like multiplexing backend on an indirect geometry time-of-flight (ToF) front end. The primary spectrometer enables an unprecedented polychromatic sample flux of  $6 \cdot 10^9$  n/s/cm<sup>2</sup> at 2 MW accelerator power, with a bandwidth of 1.7 Å, whilst retaining a primary spectrometer resolution  $\Delta E_i/E_i$  of 4 %, common in cold neutron spectroscopy. The multiplexing backend consists of 9 Q-channels, each covering 5.2° and containing 5 fixed analyzers probing a scattered neutron energy range of 2.7 to 5.0 meV. The analyzers utilize the graphite crystal mosaicity combined with position sensitive neutron detectors, resulting in a back-end resolution considerably better than on a classical TAS setup.

We here present extensive McStas simulations of BIFROST and its energy resolution in different operation modes. We show that it is possible to obtain excellent energy resolution even in deep inelastic scattering where we at 10 meV energy transfer find a resolution of approx. 30 µeV and we illustrate this by a complete virtual phonon experiment.

ICT-K&G-ENEDSKI-ICT-J&I: ?-E; -K-E; LKPL-LJ-E-  
E<LKFE-E; -OPI8P-J: @E: <

To reach its climate neutrality goals Europe needs to rely heavily on Power-to-X (PtX) technology to replace the many applications of fossil fuels that are not easily electrified. Many PtX technologies are still immature or not ready for deployments yet, highlighting the need for a sustained R&D effort in the field. Neutron- and synchrotron sources can play a crucial role in this effort, however lack of key instrumentation is limiting the current possibilities. For this reason, the European Union has funded the ACTNXT project under the HORIZON-INFRA-2024-TECH call with a total budget of € 9,229,258 = 68.913.115 DKK.

ACTNXT will upgrade the instrumentation at current neutron- and synchrotron sources (ESRF, ILL, and PSI) by development of:

- Operando measurements of processes and flow inside PtX components
- Materials behavior under hydrogen exposure
- Reliable and high throughput investigation novel materials
- Operando measurements of hazardous chemical reactions

The new instrumentation will be designed for broad adaptation as upgrades for many existing research instruments across Europe. Prototypes of all 4 instrumentation types will be constructed at leading research infrastructures and their capabilities tested and demonstrated.

These efforts are supplemented by a common knowledge platform addressing common challenges such safety and planning of complicated experiments. During the project the consortium will have a very strong dialogue with the user communities to ensure that the developed instrumentation matches its needs and that it is ready to take full advantage of the instrumentation also after the end of the project.

The project had a kick-off meeting in March 2025, and will continue for four years. Danish Technological Institute leads the project, and we hope to engage the DanScatt community to develop the best possible sample environments.



# Fuel cell catalyst degradation mechanisms – an operando electrocatalyst study

S. Punke<sup>1</sup>, R. K. Pittkowski<sup>1</sup>, J. J. K. Kirkensgaard<sup>2</sup>, K. M. Ø. Jensen,<sup>1</sup> M. Arenz<sup>3</sup>

<sup>1</sup>Department of Chemistry, University of Copenhagen, Universitetsparken 5, 2100 Copenhagen Ø, <sup>2</sup>Niels Bohr Institute, University of Copenhagen, Blegdamsvej 17, 2100 Copenhagen Ø, <sup>3</sup>Department of Chemistry, Biochemistry and Pharmaceutical Sciences, University of Bern, Freiestrasse 3, 3012 Bern

*spu@chem.ku.dk*

We here use operando X-ray scattering to investigate the stability of fuel-cell Pt catalyst during operating conditions. Our investigation focuses on bimodal benchmark Pt catalysts and their corresponding monomodal counterparts, aiming to elucidate the degradation mechanisms observed during Accelerated Stress Tests (AST). ASTs involve subjecting the catalyst to start-stop conditions to expedite degradation processes for observation. Bimodal size distributions refer to catalyst particles exhibiting two distinct size populations, whereas monomodal distributions consist of particles of one size population.

Our primary objective is to gain deeper insight into degradation phenomena, such as electrochemical or classical Oswald ripening, nanoparticle agglomeration, nanoparticle desorption from the support, and coalescence. This research builds upon prior work on Pt catalyst degradation, encompassing both monomodal and bimodal catalysts [1,2].

The experimental approach employed a combination of Small and Wide Angle Scattering (SAXS and WAXS) along with Pair Distribution Function (PDF) analysis of Total Scattering. By integrating these diverse X-ray scattering techniques, we could track the degradation across various length scales, see Fig. 1.

SAXS enabled the observation of nanometer-scale degradation, specifically capturing the morphological and size evolution, aided by a Monte-Carlo analysis [3] approach for assessing the size distribution changes during degradation. Furthermore, SAXS provided insights into the volume fraction of scatterers, facilitating the monitoring of relative changes in Pt nanoparticle abundance pre-, during, and post-AST. Whereas WAXS and the PDF analysis furnished information on the crystallite size and strain within the catalyst, enabling a closer examination of degradation phenomena, such as Pt catalyst coalescence.

The measurements were conducted at ID31, European Synchrotron Radiation Facility (ESRF), using an operando Gas Diffusion Electrode (GDE) in ambient air. The small beam size at the beamline allowed for tracking of degradation at different depths within the catalyst layer. We found out that agglomeration and subsequent coalescence of the nanoparticles appear to be the main driving factor of the degradation.

This study contributes to our understanding of fuel cell catalyst degradation, laying the groundwork for the development of robust and resilient fuel cell catalysts.

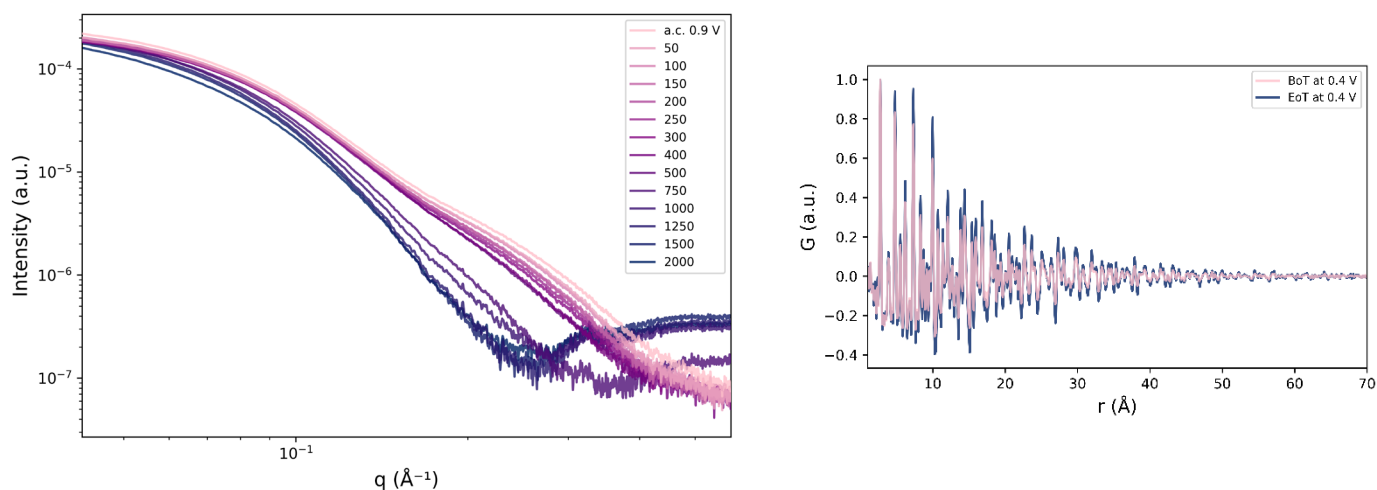


**Figure 1.** Left side: Following the change of the bimodal size distributions with SAXS. Right side: The difference of the coherent scattering domain of the bimodal catalyst at the Beginning of Test (BoT) and End of Test (EoT) is visible in the PDF.

[1] R. Chattot, M. Mirolo, I. Martens, et al. (2023), Journal of Power Sources **555**, 232345.

[2] J. Schröder, R. K. Pittkowski, I. Martens, et al. (2022), ACS Catalysis **12**(3), 2077-2085.

[3] I. Bressler, B. R. Pauw and A. F. Thünemann (2015), Journal of Applied Crystallography **48**(3), 962-969.

# ESS data reduction software overview

---

As European Spallation Source(ESS) was built in Lund, data reduction software for ESS was developed at DMSC in Copenhagen. In this presentation, we would like to illustrate an overview of our open-source data reduction software stack.

Data reduction team(scipp) has built application-like Python packages to support various instruments at ESS. Those packages are composed of various lower level packages, that can be useful for certain techniques, or arbitrary data reduction for neutron experiments or even general data manipulation. We hope this presentation can help readers to navigate among our packages for their right purposes.

For example, if you want a low level interface to process data directly, our core package called `scipp` will be useful as it has data structure similar to `numpy` but with physical properties taken into account to the computation. And if you want a workflow that can reduce time-of-flight neutron data, `essreduce` can help you. If you want to load `NXevent` dataset from a `nexus` file, `scippnexus` can do the job.

There will be demonstration of data reduction routines using our software stack along with the poster.

## **NMX Macromolecular Diffractometer at the European Spallation Source**

Swati Aggarwal (1,2), Justin Bergmann (1), Aaron Finke (1), Daniel Lundström (1), Giuseppe Aprigliano (1), Esko Oksanen (1,2)

(1) European Spallation Source ESS ERIC (2) Division of Computational Chemistry, Lund University

The NMX Macromolecular Diffractometer is a time-of-flight (TOF) quasi-Laue diffractometer at the European Spallation Source (ESS) in Lund, Sweden. The ESS long pulse source is well suited for structural biology techniques such as macromolecular crystallography. NMX is optimised for small samples and large unit cells in order to locate the hydrogen atoms relevant for the function of biological macromolecules. We estimate that at full ESS source power NMX could be used to collect data from crystals of  $\sim 200\text{ }\mu\text{m}$  dimension in a few days, which represent an order of magnitude improvement in both crystal size and data collection time over currently available sources. The robotic detector positioning system also overcomes present limitations in unit cell size can resolve cell edges up to  $300\text{ }\text{\AA}$ . This would broaden the range of systems that can be investigated by neutrons to many biologically very interesting molecules, including membrane proteins such as proton pumps and would transform neutron crystallography into a technique that could answer a significantly larger number of hydrogen related questions in biomolecular science than before. The instrument is under construction and is expected to be available for first science in 2026.

# Phosphate Recovery from As-laden Groundwater Treatment Sludge

Tinatin Tkesheliadze<sup>1,2</sup>, Kaifeng Wang<sup>1</sup>, Knud Dideriksen<sup>1</sup>, Shima Kadkhodazadeh<sup>3</sup>, Peter E. Holm<sup>1</sup>, Case van Genuchten<sup>2\*</sup>

Groundwater treatment produces sludge rich in phosphate (P), a critical resource needed for global agriculture. Nevertheless, this waste stream has been overlooked for its potential for resource recovery due to coexisting toxic components, particularly arsenic (As). Our group has developed a novel two-stage process including alkali extraction and subsequent selective As reduction to convert toxic As from groundwater treatment sludge into chemically pure As(0) nanoparticles which leaves an alkali solution rich in aqueous extracted P that can be recovered as calcium phosphate (Ca-P). However, the P-rich solution also contains low concentrations of residual aqueous As, posing a potential challenge for P recovery via precipitation as solid Ca-P due to the similar reactivity of P and As(V) and thus possible co-uptake of As into the Ca-P solids. Knowledge of the factors that control P and As uptake during Ca-P precipitation is thus critical to design resource recovery systems for groundwater treatment sludge that minimize As content in the end-products.

In this study, we dosed calcium chloride (CaCl<sub>2</sub>) at a range of Ca:P ratios and pH settings to synthetic and field P-rich solutions containing low As concentrations to optimize the valorization of the extracted P and minimize As accumulation in the Ca-P solids. Aqueous concentration of P and As were measured by ICP-OES to determine P recovery and As uptake in the Ca-P solids. To obtain structural information of the Ca-P solids, the valorized materials were characterized by pair distribution function (PDF) analysis of high-energy X-ray scattering data (DESY, Hamburg, DE) and scanning transmission electron microscopy (STEM). Our results suggest an optimal dosed Ca:P ratio between 1 and 1.6 that can remove a high fraction (>60%) of P from solution, while minimizing As uptake into the solid (Figure 1A). Importantly, nearly complete P recovery (>95%) can be achieved by the combination of adjusting pH to 8 and dosing Ca:P at a 1.6 ratio, but at the cost of disproportionately increased As uptake into the solid. PDF analysis revealed that all solids consisted of hydroxyapatite, though significant differences in crystallite size were observed (Figure 1B). By fitting the experimental PDFs using hydroxyapatite as the starting structure, we were able to resolve an increase in unit cell parameters due to the presence of As, suggesting As incorporation into the Ca-P solids which was consistent with the homogeneous spatial distribution of As in the particles revealed by STEM. These results can be used to inform the design and operation of P recovery systems for groundwater treatment sludge, thus helping to shift the paradigm in how this waste stream is managed.

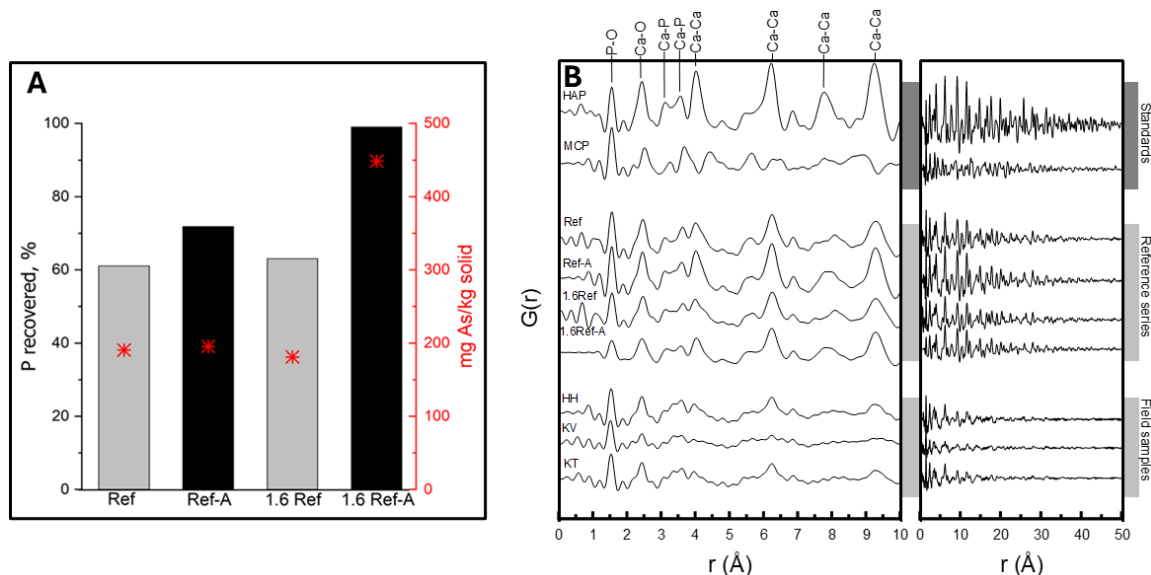


Figure 1. (A) Phosphate recovery (bars) and As uptake in the solid (secondary axis). (B) PDFs of standards, samples from synthetic solutions and field samples. The Ref samples represent reference conditions of 30 mM P, initial pH of 10, 3 mg/L As(V) and 30 mM dosed Ca. Ref samples with 1.6 and A included in the sample name indicated pH adjustment to 8 and a dosed Ca:P ratio of 1.6 mol:mol. The field samples were obtained from Holmehave (HH), Kvaerndrup (KV) and Kerte (KT) water works.

<sup>1</sup>Department of Geochemistry, Geological Survey of Denmark and Greenland (GEUS), Øster Voldgade 10, Copenhagen 1350, Denmark

<sup>2</sup>Department of Plant and Environmental Sciences, University of Copenhagen, Thorvaldsensvej 40, 1871 Frederiksberg C, Denmark

<sup>3</sup>DTU Nanolab – National Centre for Nano Fabrication and Characterization, Technical University of Denmark, Kongens Lyngby, 2800, Denmark

# Whole-nanoparticle-ensemble refinements of compositionally complex systems from X-ray pair distribution function data *via* the Reverse Monte Carlo method

Tobias Mølgaard Nielsen<sup>1</sup>, Kirsten M. Ø. Jensen<sup>1</sup>, Lewis R. Owen<sup>2</sup>

<sup>1</sup>Department of Chemistry, University of Copenhagen, Universitetsparken 5, Denmark

<sup>2</sup>School of Chemical, Materials and Biological Engineering, University of Sheffield, Sir Robert Hadfield Building, Mappin Street, Sheffield, United Kingdom  
[tmn@chem.ku.dk](mailto:tmn@chem.ku.dk)

Compositionally complex nanomaterials such as High-Entropy Alloys (HEAs), which consist of five or more elements randomly mixed in a solid solution structure, have continued to attract interest as promising catalyst materials in recent years<sup>1</sup>. While their multi-element nature makes HEAs promising catalyst materials, it also complicates comprehensive structural analysis through conventional methods such as powder X-ray diffraction and X-ray absorption spectroscopy. This is further hindered as particle sizes decrease into the nano regime where the Bragg scattering starts to diminish. Total scattering and pair distribution function (PDF) analysis has proven an excellent tool for structural characterisation of compositionally complex and nano-sized materials<sup>2,3</sup>. However, the identification of chemical short-range ordering and elemental inhomogeneities in compositionally complex nanoparticle systems through PDF analysis remains largely unexplored. Such structural features are not easily describable through commonly employed small-box modelling methods, and large-box modelling for nanoparticle systems are only just starting to emerge<sup>4</sup>.

In this work, we present an approach for the investigation of chemical short-range order and elemental inhomogeneities in multimetallic nanoparticle systems through large-box modelling of X-ray PDF data. Specifically, we develop a methodology for atomistic whole-nanoparticle-ensemble refinements of compositionally complex nanoparticle systems through the Reverse Monte Carlo method. PDF refinements are carried out against nanoparticle-ensembles of different compositional orderings, including core@shell, compositional gradients and fully random structures, to determine the best description of the particles. By introducing atom-type swapping in the refinement algorithm, we further investigate the compositional ordering of the atomic configuration providing the best fit to the PDF data. Our work presents a new approach to the identification of chemical short-range ordering and compositional inhomogeneities in nanoparticle systems, and emphasises the challenge of comprehensive structural characterisation of compositionally complex nanomaterials.

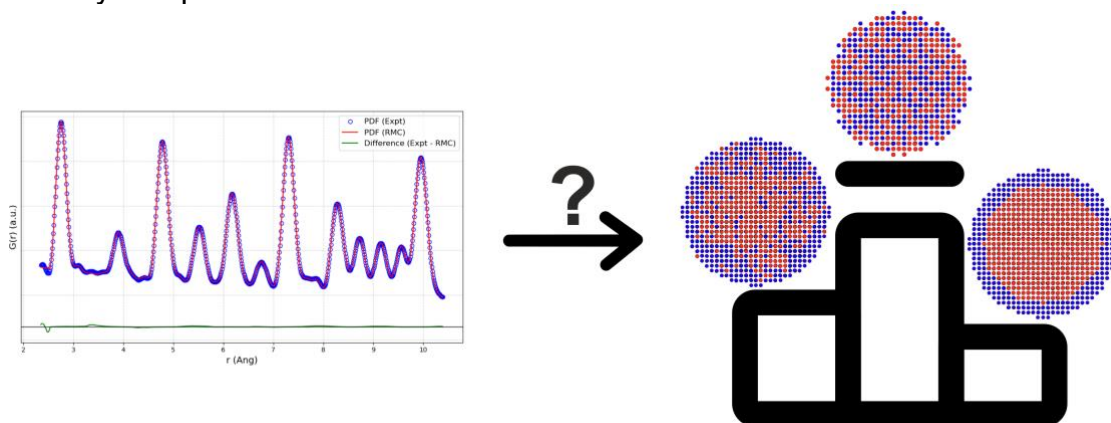


**Figure 1.** Nanoparticle configurations of different elemental orderings are refined against X-ray PDF data.

[1] T. Löffler, A. Ludwig, J. Rossmeisl and W. Schuhmann, *Angew. Chem. Int. Ed.*, 2021, **60**, 26894-26903.

[2] B. Jiang, C. A. Bridges, R. R. Unocic, K. C. Pitike, V. R. Cooper, Y. Zhang, D.-Y. Lin and K. Page, *J. Am. Chem. Soc.*, 2021, **143**, 4193-4204.

[3] L. R. Owen, E. J. Pickering, H. Y. Playford, H. J. Stone, M. G. Tucker and N. G. Jones, *Acta Mater.*, 2017, **122**, 11-18.

[4] Y. Zhang, M. McDonnell, W. Liu and M. G. Tucker, *J. Appl. Cryst.*, 2019, **52**, 1035-1042.



## **MicroMAX – a beamline with time-resolved macromolecular crystallography capabilities at the MAX IV Laboratory**

J. Nan, M. Milas, M. Chenchiliyan, C.M. Casadei, D. Lang, M. Bjelčić, O. Aurelius, I. Gorgisyan, E. Jagudin, M. Eguiraun, A. Nardella, E. Panepucci, A. Gonzalez, M. Malmgren, S. Kapetanaki, and T. Ursby

MAX IV Laboratory, Lund University, Fotongatan 2, 224 84 Lund, Sweden

The rise of 4<sup>th</sup> generation sources, including the MAX IV Laboratory 3 GeV ring, has enabled new possibilities to study dynamics using crystallography. The MicroMAX beamline is focussed on providing optimal X-ray characteristics for serial and time-resolved crystallography. The beamline offers a flexible sample environment for bespoke experimental setups and supports also high-throughput single crystal data collections.

MicroMAX recently started user operations and has performed experiments with SPINE-based fixed targets, flow injectors (high viscosity extrusion, capillary), and customized microfluidics mounted to an MD3-up diffractometer. Time-resolved SSX measurements have also been performed using a nanosecond pump laser (210-2600 nm). An X-ray chopper (0,8-70% duty cycle) in conjunction with a Jungfrau 9M Si integrating hybrid pixel detector also enables 2 kHz data collections at 10  $\mu$ s resolution. Data can also be collected with an Eiger2 X 9M CdTe photon counting hybrid pixel detector, with automatic changes between both detectors in under a minute. The end station is equipped with an automatic sample changer (ISARA2) that can be used in cryogenic conditions housing up to 29 unipucks but can also exchange crystallisation plates and room-temperature spine-based sample holders. Experiments are controlled by MXCuBE with ISPyB used for data management. Automated fast feedback is implemented as well as data processing using CrystFEL.

The second experimental hutch at MicroMAX can be used for other activities while the first hutch is in X-ray operation. The second hutch is currently used as an off-line laser and spectroscopy laboratory for sample pre-characterization studies but will later be available for X-ray experiments.

The beamline has two monochromators, a crystal monochromator giving a narrow bandwidth beam with up to  $10^{13}$  photons/s and a multilayer monochromator giving a wider bandwidth (up to 1%) with more than  $10^{14}$  photons/s. The X-ray beam is initially focused by beryllium X-ray lenses down to around 10  $\mu$ m. With further focussing using a mirror system that will be installed in 2026 the beam focus will be a few  $\mu$ m.

MicroMAX is funded by the Novo Nordisk Foundation under the grant number NNF17CC0030666.

## Imaging Orientation of Hydroxyapatite Crystallites Across Full Mouse Femora

Thorbjørn Erik Køppen Christensen<sup>a,b</sup>, Takeshi Moriishi<sup>c</sup>, Toshihisa Komori<sup>c</sup>

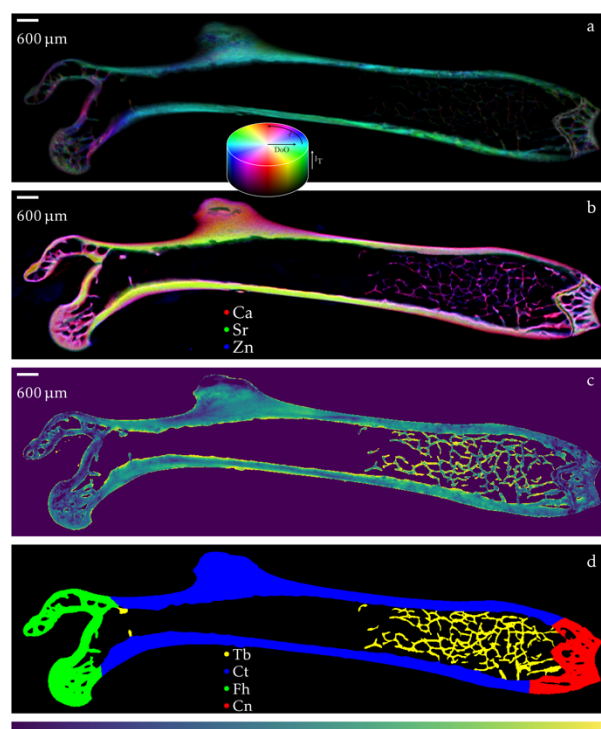
a: DanMAX, MAX IV, Sweden.

b: DTU Compute, DTU, Denmark.

c: Graduate School of Biomedical Sciences, Nagasaki University, Japan.

X-ray diffraction (XRD) and fluorescence (XRF) mapping are great tools for characterization of biomineralized materials. As they can be used to show variation in both structure and composition of materials, both of which are present throughout many different types of biomaterials[1–3]. These techniques are time consuming, as every point in the picture need a long enough exposure, to create high quality data, and they have hence traditionally been limited to either individual samples[3], or small regions of interest across multiple samples [4]. Such studies can bring tremendous value for the understanding of biomineralization. However, they cannot map biological variance larger areas and sets of samples. However, combining the advent of fourth generation synchrotrons, with the advent in detector development over the last decades, it is now possible to scan much larger regions across more samples than previously, and thus map large biological variation[1].

In the present study[5], 16 full mouse femora have been scanned with a step size of 15  $\mu\text{m}$ , for a total of 5 million diffraction patterns and XRF spectra. This makes it possible to map out statistical variations of composition and structure across different regions (figure 1(d)).



Different parameters were mapped out: The orientation as shown in figure 1(a); Elemental composition, figure 1(b); unit cell *c*-axis (figure 1(c)); and apparent crystallite size. Comparing these parameters, across the different regions shown, show that the crystallites in the trabeculae and cortical bone is more highly oriented, than that in the condyle and the femoral head. It is also seen that the more oriented crystallites are more well aligned.

While XRF data from the trabeculae cannot be used, due the variation in thickness, there is a clear increase in Sr content in the long bone compared to the other regions, combined with an increased unit cell *c*-axis in the cortical bone, it is shown that the Sr is indeed substituted into the hydroxyapatite crystal lattice.

Figure 1 (a) Orientation plot: Hue angle, Saturation: Degree of Orientation, Value: amount of crystallites. (b) XRF. (c) unit cell *c*-axis. (d) segmentation: Yellow: Trabeculae (Tb), Blue: Cortical (Ct), Green: Femoral head (Fh), Red: Condyle (Cn).

[1] Christensen et al 2023, IUCrJ.

[2] Chua et al 2023, Acta Biomaterialia.

[3] Wittig et al 2019 ACS, Nano.

[4] Schenz-Spasic et al 2025, Materalia.

[5] Christensen et al 2025, Faraday Discussions.

# autoXAS: Automated Analysis of X-ray Absorption Spectroscopy Data

Ulrik Friis-Jensen<sup>\*ab</sup>, Kirsten M. Ø. Jensen<sup>a</sup> and Rebecca Pittkowski<sup>a</sup>

*a. Department of Chemistry and Nano-Science Center, University of Copenhagen*

*b. Department of Computer Science, University of Copenhagen*

\* [ufj@chem.ku.dk](mailto:ufj@chem.ku.dk)

Designing new functional materials is essential to develop the catalysts and batteries needed for a greener and more sustainable future. An extensive understanding of the synthesis-structure-property relationships is important for an efficient and fruitful design process. A popular technique for probing the structure of materials is X-ray absorption spectroscopy (XAS), which can give element-specific information about oxidation states and the local atomic structure [1]. XAS is primarily a synchrotron technique, as it requires an energy-tunable X-ray source to scan across the element-specific absorption edges [2]. Over the last 30 years, the proportion of published XAS papers using in-situ or operando methods has steadily increased from 6 % to 36 % [3]. As a result, having user-friendly analysis software that can efficiently process substantial amounts of time-resolved data would be highly beneficial to the XAS community.

A variety of sophisticated XAS analysis programs already exist. These include Athena [4] and Larch [5] which each have their own graphical user interfaces (GUIs) and/or programming packages. These programs are designed for and excel at in-depth analysis of XAS data but are complex and require a lot of user input. Often there are also rigid formatting requirements for input files and the GUIs struggle with handling more than a handful of ex-situ measurements at a time.

We propose autoXAS, a powerful and user-friendly Python package for automating the analysis of in-situ and operando XAS data. The design philosophy behind autoXAS is to empower scientists to analyze large XAS datasets at home or the synchrotron beamline without expert knowledge in programming and/or existing GUI programs. Using a Jupyter Notebook, autoXAS can rapidly read, clean up, and normalize data from time-resolved experiments in a matter of seconds with minimal setup required. The processed data can be exported or analyzed further with autoXAS using techniques such as linear combination analysis (LCA), principal component analysis (PCA), or non-negative matrix factorization (NMF). All processed data and analysis results can be explored using interactive plots or exported in standard image formats.

## References

- [1] S. Calvin, *XAFS for Everyone*, CRC Press, 2013.
- [2] [xafs.xrayabsorption.org](https://xafs.xrayabsorption.org), <https://xafs.xrayabsorption.org/>
- [3] Web of Science<sup>†</sup>, <https://www.webofscience.com/>
- [4] ATHENA: XAS Data Processing, <https://bruceravel.github.io/demeter/documents/Athena/index.html>
- [5] Larch: Data Analysis Tools for X-ray Spectroscopy, <https://xraypy.github.io/xraylarch/index.html>

---

<sup>†</sup> Queries used: "ALL=("X-ray Absorption Spectroscopy")" and "ALL=("X-ray Absorption Spectroscopy" "In situ") OR ALL=("X-ray Absorption Spectroscopy" "Operando")"

# Investigating electrochemical phenomena in PEM water electrolyzers using operando neutron imaging techniques

**Authors:** Vahid Karimi<sup>1</sup>, Cedric Qvistgaard<sup>2</sup>, Ron Hajrizaj<sup>1</sup>, Domenico Battaglia<sup>2</sup>, Anna Fedrigo<sup>3</sup>, Alessandro Tengattini<sup>3</sup>, Pavel Trtik<sup>4</sup>, Pierre Boillat<sup>4</sup>, Jongmin Lee<sup>4</sup>, Raghunandan Sharma<sup>1</sup>, Luise Thein Kuhn<sup>2</sup>, Shuang Ma Andersen<sup>1</sup>

<sup>1</sup> Department of Green Technology (IGT), Southern University of Denmark, Denmark

<sup>2</sup> DTU Energy, Technical University of Denmark (DTU), Denmark

<sup>3</sup> Institute Laue Langevin (ILL), Grenoble, France

<sup>4</sup> Paul Scherrer Institut (PSI), 5232 Villigen, Switzerland

Neutron imaging is a powerful operando tool for characterizing state-of-the-art electrochemical devices such as proton exchange membrane water electrolyzer (PEMWE). As the performance and stability of these energy devices has yet to be improved for rapid commercialization, a better understanding of loss mechanisms such as mass and charge transfer obtained by neutron imaging is highly valuable for the advancement of the PEMWE.

In this research, we suggested an operando neutron radiography experiment (NeXT beamline, ILL), in which two porous transport layers (PTLs) with or without Pt coating were placed side by side and the oxygen distribution inside the cell was measured for these two PTLs (Fig. 1a), while the results were immediately compared with current distribution inside the cell. This was done to grasp an understanding regarding the Ti passivation (forming  $\text{TiO}_2$  during electrolysis) of PTL inside the PEMWE.

Also, a neutron radiography was performed at NEUTRA beamline, PSI, where the water distribution inside the PEMWE was evaluated for various ratios of  $\text{D}_2\text{O}/\text{H}_2\text{O}$  (Fig. 1b-c), highlighting the kinetic and mass transport differences between the normal and heavy water while the imaging results backed by in-situ and ex-situ electrochemical data. The data confirmed a clear advantage of  $\text{H}_2\text{O}$  due to its both lower activation energy for catalysts, and faster ion exchange rate inside the membrane. Furthermore, the PEMWE were tested for various PTL layers, correlating the efficient charge and mass transport to the high-performance PEMWE.

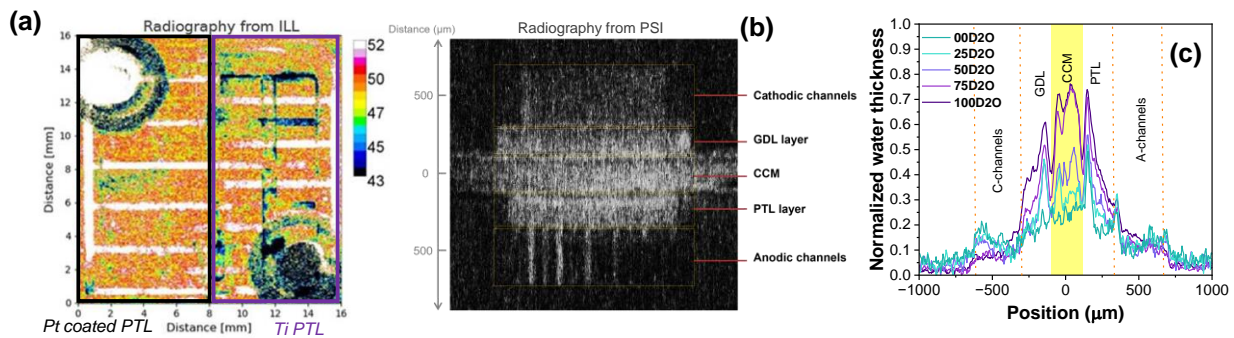


Figure 1a) shows the results for radiography for two types of PTL b) demonstrates the resulted radiography for the PEMWE c) is the water profile inside the PEMWE with different  $\text{D}_2\text{O}$  ratios

# In situ X-ray scattering study of VO<sub>2</sub> formation from VOSO<sub>4</sub> precursor under solvothermal conditions

V. A. Kaznelson<sup>1\*</sup>, A. B. Borup<sup>1</sup>, A. D. Bertelsen<sup>1</sup>, M. K. Kjær<sup>1</sup>, B. B. Iversen<sup>1</sup>

<sup>1</sup>Center for Integrated Materials Research, Department of Chemistry, Aarhus University, Langelandsgade 140, Aarhus 8000, Denmark

\*Contact: vak@chem.au.dk

**Keywords:** *In situ* PXRD, VO<sub>2</sub>, Insulator-to-Metal transition, *in situ* PDF

Vanadium dioxide (VO<sub>2</sub>) is a correlated electron material known for its reversible insulator-to-metal transition (IMT) near room temperature [1]. In the ground state VO<sub>2</sub> exists in the monoclinic insulating phase VO<sub>2</sub>(M) and transitions to a metallic rutile phase upon thermal- or photoexcitation [2,3]. This IMT has been studied widely within the field of ultrafast science [3,4], and for different smart material applications [5,6,7]. However, the synthesis of phase-pure VO<sub>2</sub> is a challenge due to the many polymorphs of vanadium oxide, and the sensitivity of the VO<sub>2</sub>(M) phase formation to the synthesis conditions [7,8].

In this study, a synthesis route inspired by the TiO<sub>2</sub> synthesis from TiOSO<sub>4</sub> is explored [9]. This approach avoids toxic oxidizing agents such as hydrazine, often used during synthesis [7], by using a VOSO<sub>4</sub>-based precursor that avoids the need for a redox step during formation. Using a flow cell under hydrothermal conditions, a monoclinic VO<sub>2</sub>(B) phase is synthesized. *In situ* powder X-ray diffraction (PXRD) reveals that this metastable VO<sub>2</sub>(B) phase irreversibly transforms to the thermodynamically stable VO<sub>2</sub>(R) phase above 300 °C. The lifetime of the VO<sub>2</sub>(B) phase decreases with increasing temperature, indicating a kinetically activated solid-state transition mechanism. This is elucidated through Pair distribution function (PDF) analysis, to explore why the VO<sub>2</sub>(B) phase is formed initially. Based on these findings a synthesis is proposed for a safe and scalable methods for VO<sub>2</sub>-based materials.

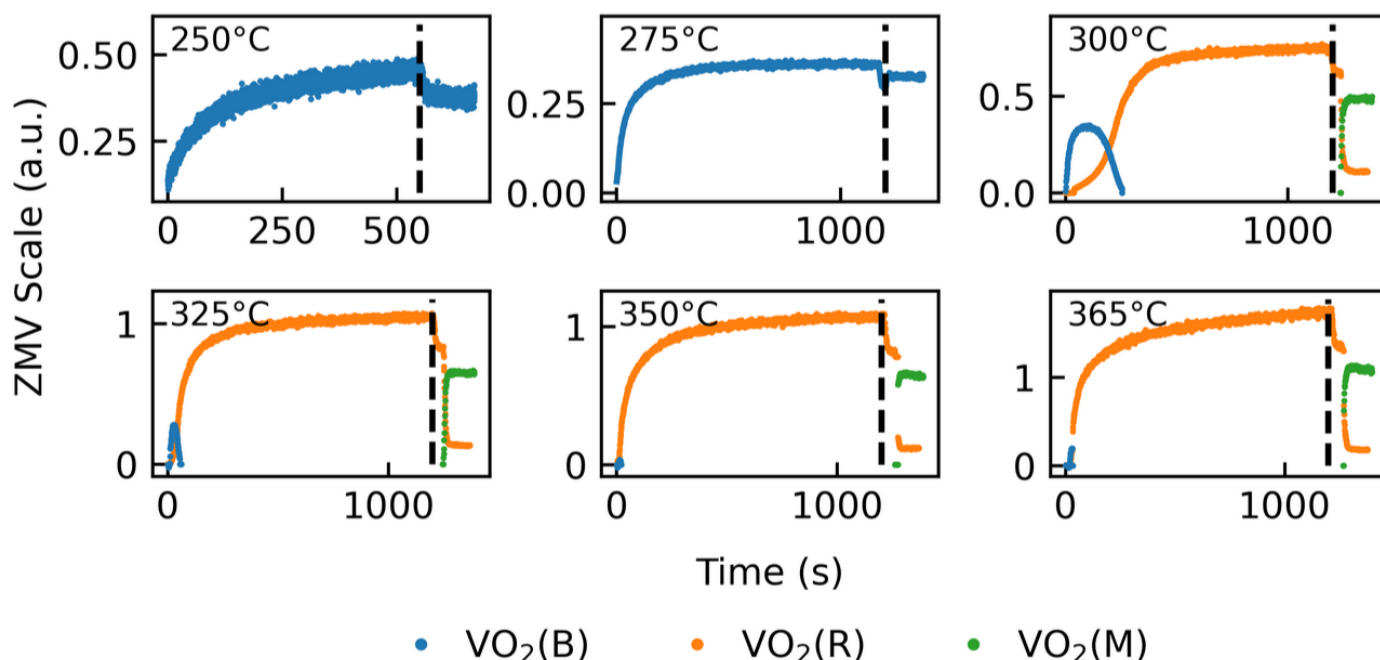


**Figure 1.** In Situ PXRD data collected at DanMAX. The scale parameter extracted by Rietveld refinement indicating the amount of crystallite formed during reaction. Cooling second indicated with dashed lines. The phases are indicated by blue, orange and green dots for the VO<sub>2</sub>(B), VO<sub>2</sub>(R) and VO<sub>2</sub>(M) phases respectively.

[1] S. Zewei, C. Xun, L. Hongjie, and J. Ping. Recent Progress in the Phase-Transition Mechanism and Modulation of Vanadium

Acta Cryst. (2025). A81, e1 (ÆNDRE?)

Dioxide Materials. *NPG Asia Materials*, 10(7):581–605, 2018.

[2] N. Tamai and H. Miyasaka. Ultrafast Dynamics of Photochromic Systems. *Chem. Rev.*, 100(5):1875–1890, 2000.

[3] A. Johnson, E. Pastor, and S. Battle-Porro et al.. All-Optical Seeding of a Light-Induced Phase Transition with Correlated Disorder. *Nature Physics*, pages 1–6, 2024

[4] S. Wall, S. Yang, and L. Vidas et al.. Ultrafast Disordering of Vanadium Dimers in Photoexcited VO<sub>2</sub>. *Science*, 362(6414): 572–576, 2018.

[5] W. Li, S. Ji, and Y. Li et al.. Synthesis of VO<sub>2</sub> Nanoparticles by a Hydrothermal-Assisted Homogeneous Precipitation Approach for Thermochromic Applications. *RSC Adv.*, 4(25):13026–13033, 2014.

[6] Y. Liao, Y. Fan, and D. Lei. Thermally Tunable Binary-Phase VO<sub>2</sub> Metasurfaces for Switchable Holography and Digital Encryption. *Nanophotonics*, 13(7):1109–1117, 2024.

[7] A. Mamakhel, F. Gjørup, and M. Kløve et al.. Synthesis of Phase-Pure Thermochromic VO<sub>2</sub> (M1). *Inorg. Chem.*, 61(23): 8760–8766, 2022.

[8] J. Nag and R. Haglund. Synthesis of Vanadium Dioxide Thin Films and Nanoparticles. *Journal of Physics: Condensed Matter*, 20(26):264016, 2008.

[9] Beyer, J., Mamakhel, A., Søndergaard-Pedersen, F., Yu, J., & Iversen, B. B. (2020). Continuous flow hydrothermal synthesis of phase pure rutile TiO<sub>2</sub> nanoparticles with a rod-like morphology. *Nanoscale*, 12(4), 2695-2702

# Systematic investigation of His protonation states in high resolution X-ray crystallography structures in the PDB

Zimeng Liu<sup>1\*</sup>, Zhiyu Huang<sup>1</sup>, Leila Lo Leggio<sup>1§</sup>

*<sup>1</sup>Dept. of Chemistry, University of Copenhagen, Universitetsparken 5, DK-2100, Denmark.*

*[\\*zimeng@chem.ku.dk](mailto:*zimeng@chem.ku.dk) , [\\$leila@chem.ku.dk](mailto:$leila@chem.ku.dk)*

Histidine residues play a crucial role in biochemical reactions, especially in proton transfer processes within enzymes. Although high-resolution X-ray crystallography provides detailed structural information, accurately determining the protonation states of histidine remains challenging due to limitations in electron density maps. To address this, we have developed a fully automated analysis pipeline that employs partially unrestrained refinement and geometric parameter calculations using existing methods<sup>[1],[2]</sup> to assess the protonation states of histidine residues.

We first selected high-quality crystal structures from the PDB database based on strict quality criteria. For these structures, we applied criteria such as average B-factors and alternative conformations to select histidine residues suitable for analysis. To correct potential histidine flipping errors, we used the MolProbity tool for detection and developed scripts to automatically correct these errors in the PDB files.

To validate the predictions, several well-characterized protein groups were analyzed. During this evaluation, limitations of the linear discriminant analysis (LDA) method<sup>[2]</sup> we were using became evident, prompting the development of an alternative classifier based on the random forest algorithm<sup>[3]</sup>. The results from both geometry-based methods were then compared with experimentally derived protonation states<sup>[4],[5]</sup> obtained from ultra-high resolution X-ray crystallography, neutron crystallography and from estimates based on correlating crystallization pH with residue-specific pKa values determined by NMR spectroscopy. Despite strong overall concordance, certain discrepancies were observed. We also investigated further if these discrepancies could come from inaccuracies in PDB-reported crystallization pH values.

Our research provides a foundation for the automated assessment of histidine protonation states and reveals the applicability and limitations of existing methods across different proteins. This lays the groundwork for developing more precise prediction methods, which is of great significance for deepening the understanding of protein function.

## Reference:

- [1]Banerjee, S., Muderspach, S. J., Tandrup, T., Frandsen, K. E. H., Singh, R. K., Ipsen, J. Ø., Hernández-Rollán, C., Nørholm, M. H. H., Bjerrum, M. J., Johansen, K. S., & Lo Leggio, L. (2022). *Biomolecules*, 12(2), 194.
- [2]Malinska, M., Dauter, M., Kowiel, M., Jaskolski, M., & Dauter, Z. (2015). *Acta Crystallogr D Biol Crystallogr*, 71(Pt 7), 1444-1454.
- [3]Breiman, L. (2001). *Random Forests. Machine Learning*, 45(1), 5-32.
- [4]Liebschner, D., Dauter, M., Brzuszkiewicz, A., & Dauter, Z. (2013). *Acta Crystallographica Section D*, 69(8), 1447-1462.
- [5]Zoë Fisher, S., Raum, H. N., & Weininger, U. (2025). Proton Occupancies in Histidine Side Chains of Carbonic Anhydrase II by Neutron Crystallography and NMR - Differences, Similarities and Opportunities. *Chembiochem*, 26(5), e202400930.

# ***In situ* GIWAXS during tensile testing of vacuum deposited thin organic films**

K. A. Janik<sup>a</sup>, C. Fynbo<sup>a</sup>, M. K. Huss-Hansen<sup>a</sup>, O. Bikondoa<sup>b</sup>, A. Chumakov<sup>c</sup>, M. Schwartzkopf<sup>c</sup>, S. V. Roth<sup>c</sup>, O. Albrektsen<sup>a</sup>, M. Knaapila<sup>d</sup>, and J. Kjelstrup-Hansen<sup>a</sup>

<sup>a</sup> NanoSYD, Mads Clausen Institute, University of Southern Denmark, 6400 Sønderborg, Denmark

<sup>b</sup> XMaS UK CRG Beamline, European Synchrotron Radiation Facility, 38043 Grenoble, France; Department of Physics, University of Warwick, CV4 7AL Coventry, U.K.

<sup>c</sup> Photon Science, Deutsches Elektronen-Synchrotron (DESY), 22607 Hamburg, Germany

<sup>d</sup> Department of Physics, Norwegian University of Science and Technology, 7491 Trondheim, Norway

Stretchable electronics have the potential to revolutionize many industries by enabling technologies that are more adaptable, durable, and closely integrated with the human body. Realizing such devices requires, on the one hand, the appropriate choice of conformable materials which can replace brittle inorganic components with small organic molecules or polymers, and, on the other hand, a clear understanding of the relationship between microstructure, charge transport, and mechanically induced strain. As a first step toward explaining the microstructure-strain relationship in thin organic films on stretchable substrates, we introduce a robust method that couples tensile testing with *in situ* grazing-incidence wide-angle X-ray scattering (GIWAXS). We demonstrate the applicability of a Deben tensile rig integrated into the XMaS beamline BM28 at ESRF and the P03 beamline at PETRA III (DESY). The method is validated using a ~70 nm thick C8-BTBT film deposited on a PDMS substrate. GIWAXS patterns are collected under uniaxial strain of up to 30 %, and their preliminary analysis indicates microstructural evolution in the film.